

## Evaluating of daylighting in selected office room: Case of Study

**Dolnikova Erika**

Technical University of Košice, Slovakia  
Civil Engineering Faculty, Institute of Architectural Engineering  
e-mail: erika.dolnikova@tuke.sk

### Abstract

On average, we spend 90% of our time indoor particularly at work and a healthy work space is essential to that feeling of wellbeing. In a typical building, lighting accounts for up to 40% of energy consumption. Allowing more natural light to penetrate the building and controlling both the light and heat components of power consumption, will result in significant reductions. However, using natural light doesn't come without some issues. Glare, overheating, variability and privacy issues can all cause problems. Daylight is a basic human need, which is highlighted by the provision of transparent and translucent surfaces to all occupied spaces that we see around us. In many cases, the drive to create healthier, more occupant-conscious buildings works hand in hand with the requirement for greater energy efficiency. This article presents illumination of indoor workspace using daylight lighting. Measured values were compared with values calculated by simulation program Velux Daylight Visualizer 3.

**Key words:** daylighting, glare, daylight factor, workspaces, illuminance, simulation

### 1 Introduction

Daylighting means simply to introduce natural light into a building. To maximize the positive benefits natural light can provide, it is vital that we expand the interpretation of what daylighting is. Rather than being a question of weather to include daylighting measure or not, it should always be considered as part of a buildings holistic energy strategy to produce interiors that truly work for owners and occupiers. If unmanaged direct sunlight can cause disruptive or disabling glare or may lead to an overreliance on air cooling systems. Increasing energy use and running costs as well as causing low humidity and uncomfortable air quality. Quality of daylighting and the correct selection of daylighting materials to provide controlled natural daylighting is therefore essential [1].

Daylighting is the practice of allowing a controlled amount of natural light into a building to reduce electric lighting costs. A daylighting system includes skylights and windows along with a daylight-responsive lighting control system. Such a system can reduce energy costs by

as a much as 33%. Through the passage of light through the atmosphere, some wavelengths are absorbed by oxygen, ozone, water vapor and carbon dioxide [9].

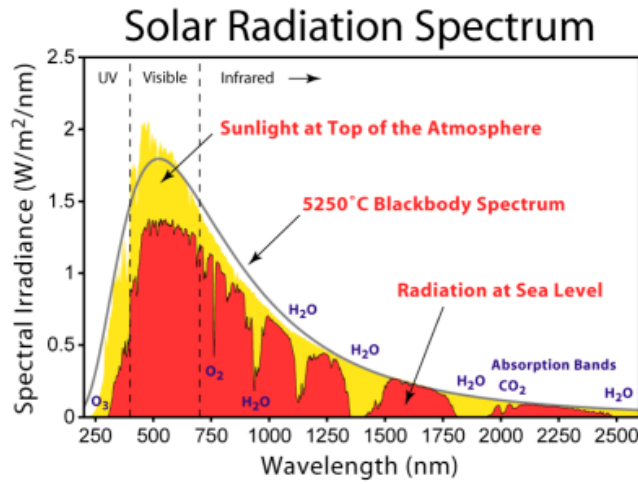


Figure 1: Spectrum of solar radiation [9].

## 2 Daylight requirements in internal spaces

The quantitative aspect of daylight illumination is enough daylight for securing the visual activity. The quantitative level of daylight is expressed by the daylight factor. Daylight factor is the ratio of the internal light level to the external light level

$$DF = (E_i / E_0) \times 100 \quad (\%) \quad (1)$$

where

$E_i$  - illuminance due to daylight at a point on the indoors working plane

$E_0$  - simultaneous outdoor illuminance on a horizontal plane from an unobstructed hemisphere of overcast sky

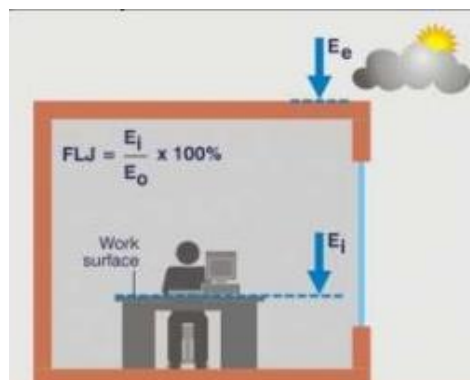


Figure 2: Room – Daylight factor [4].

Lighting technical requirements for daylight are specified by the standard STN 73 0580-1 Daylighting of buildings. Part 1: Essential requirements. The daylight-light requirements required for different occupational activity are determined using daylight-light values based on the inclusion of work activity in the room in the visual activity class [6, 7].

### 3 Experimental Setting

Measurements were realized in a typical office room in Košice. The selected room was facing south and located on the third floor. Interior dimensions of room are 3.5m x 5 m x 2.7 m. In the room there is sidelighting. Sidelighting is created by the window with dimensions 1200 mm x 2100 mm. The height of parapet is 900 mm. The fenestration systems are created by double plastic glass. In the calculation the following coefficients were considered (transmittance coefficient 0.8, maintenance factor of glazing on exterior surface 0.9, maintenance factor of glazing on interior surface 0.85, reflectance factor of ground 0.15 - dark ground). The surface of walls is white color with reflectance factor 0.7, white ceiling by reflectance factor 0.7. The floor has reflectance factor 0.2. Light loss coefficient due to window construction was  $\tau = 0,63$ . The height of the assessed point, where the daylight was measured was 0.75 m. The room is used for medium-precision production with work of various kinds and therefore the room is classified in III. - IV. light – technical class. With the given lighting system in the critical point of functional place on horizontal plane these values are required: minimum standard value of daylight factor  $D_{\min} = 1.5 - 2 \%$ , average daylight factor  $D_{\text{average}} = 5 - 6 \%$  [5]. We recommend levels of minimum 300 lx for most of the room area by meeting of target climate-based daylight factor and 500 lx for areas where productive work is performed. In the calculation exterior horizontal illumination of 5000 lx was considered. On the selected days, the value of the outside light ranged from 6.500-7.000 lx in the first day, 6.500-8.000 lx on the second day and 6.500-8.500 lx on the third day.

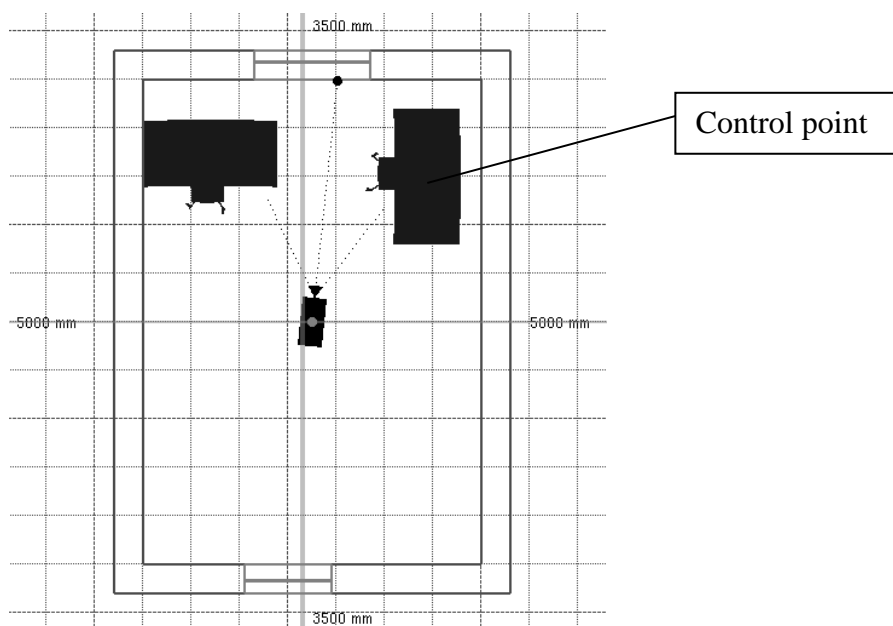


Figure 3: Plan of the test office room

## 4 Results

The article presents the results of measurements for control point for three days in January (shown in Figure 4-6). Illuminance levels of work-surface ranged between 100 and 600 lux averaging 350 lux. The results of the measurement values can be seen in Table 1. Temperature of room varied about 24°C and humidity varied about 40%. The results of DF lighting and illumination and luminance calculated can be seen in Figure 7-11.

Table 1. The calculated DF values from the measured values.

1 <sup>st</sup> day		
$D_{min}$	$D_{max}$	$D_{average}$
0.37	3,35	1.08
2 <sup>nd</sup> day		
$D_{min}$	$D_{max}$	$D_{average}$
0.36	4.65	1.38
3 <sup>rd</sup> day		
$D_{min}$	$D_{max}$	$D_{average}$
0.81	6.02	1.42

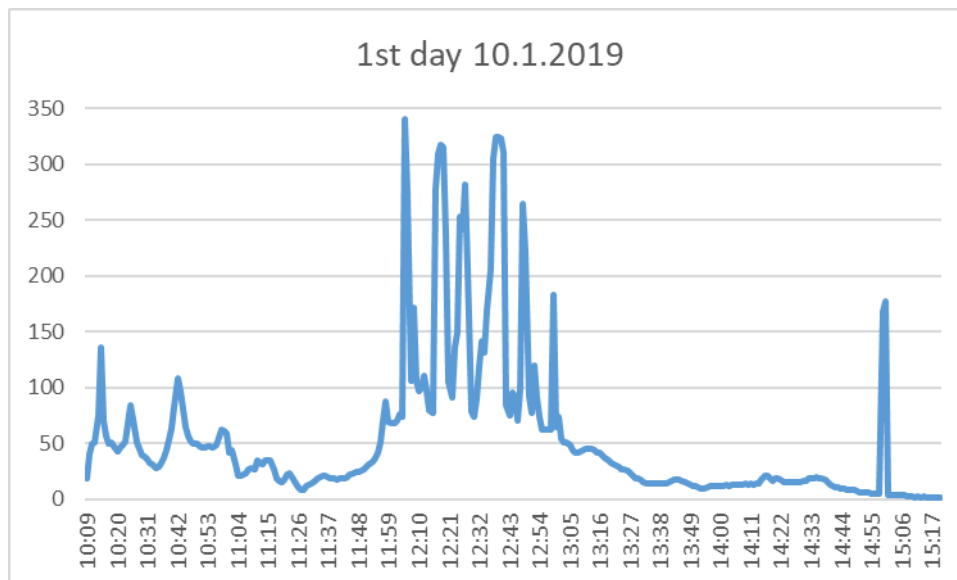


Figure 4: Measured values-1<sup>st</sup> day

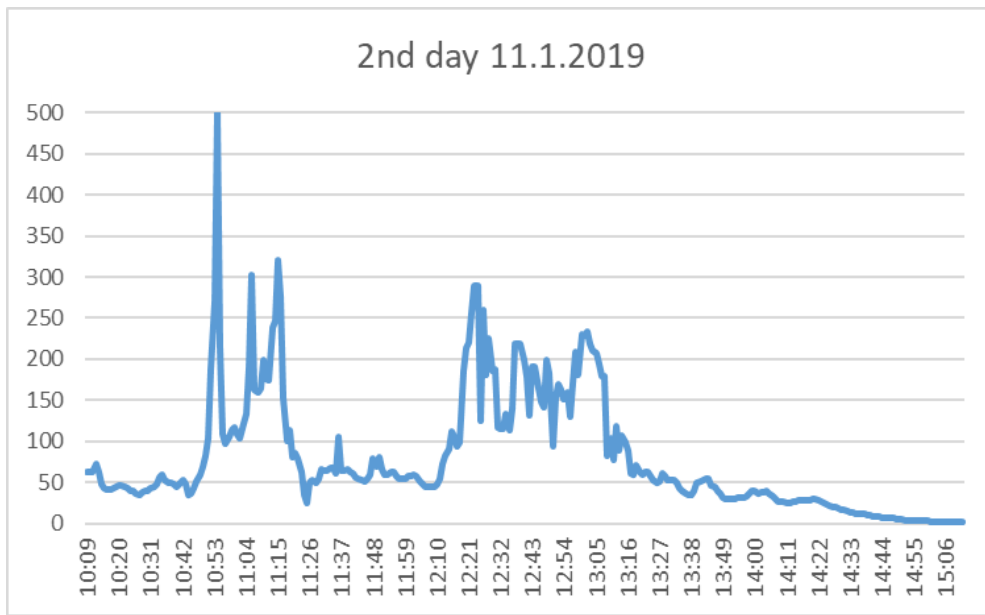


Figure 5: Measured values-2<sup>nd</sup> day

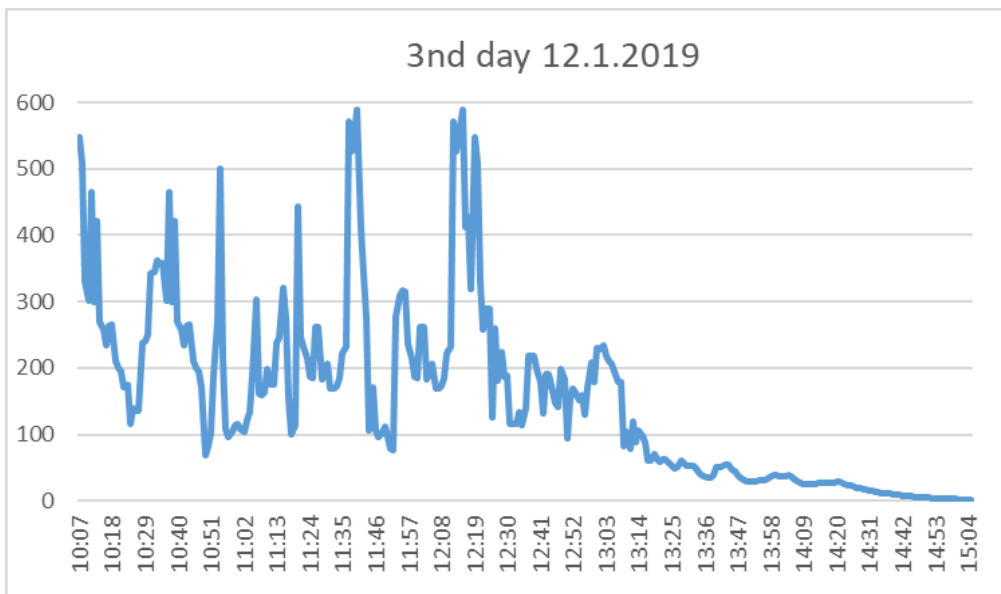


Figure 6: Measured values-3<sup>rd</sup> day

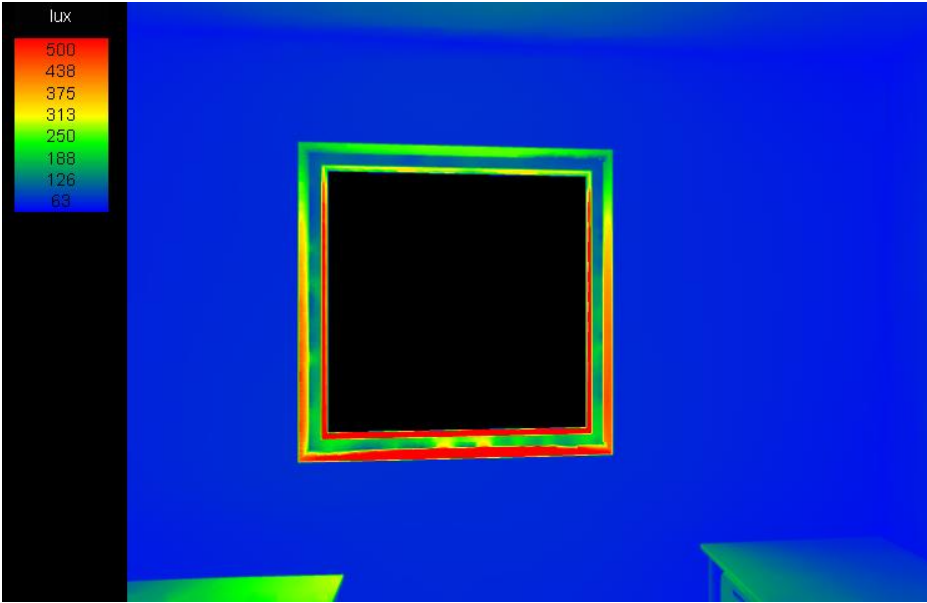


Figure 7: Results of illumination (lx) - overcast sky

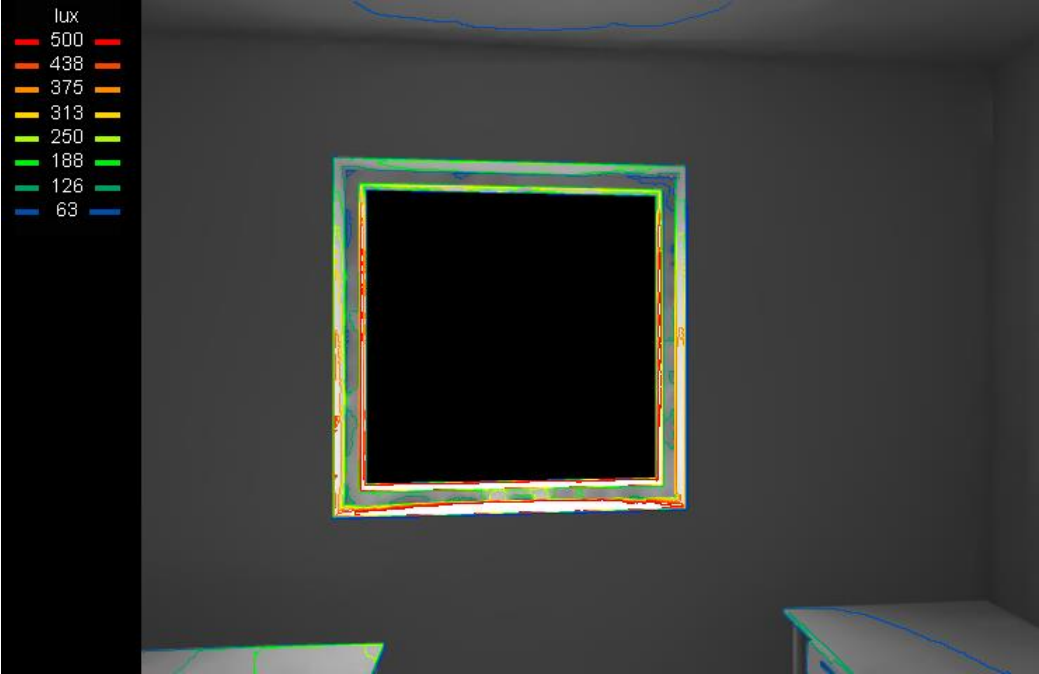


Figure 8: Results of illumination (lx) - overcast sky

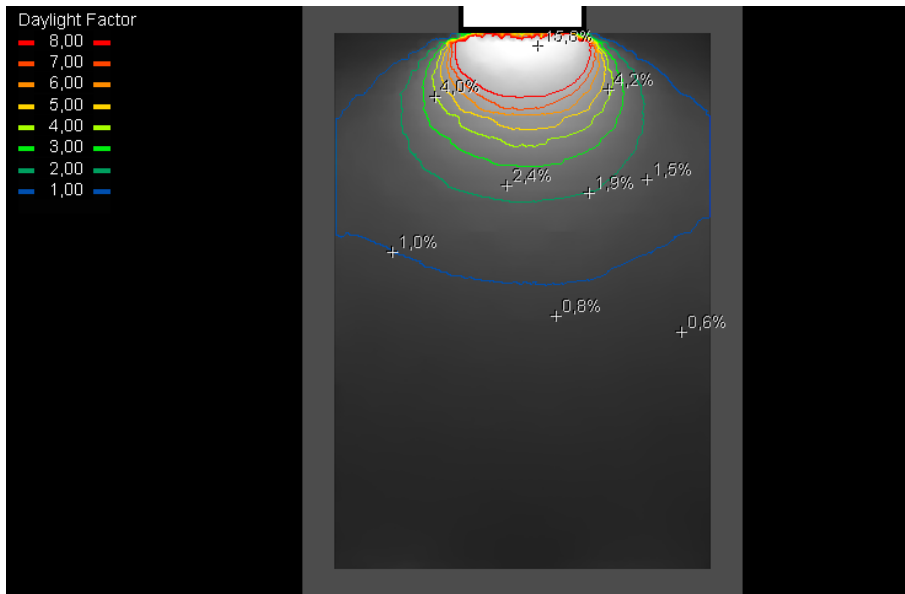


Figure 9: Results of daylight factor DF (%) - overcast sky

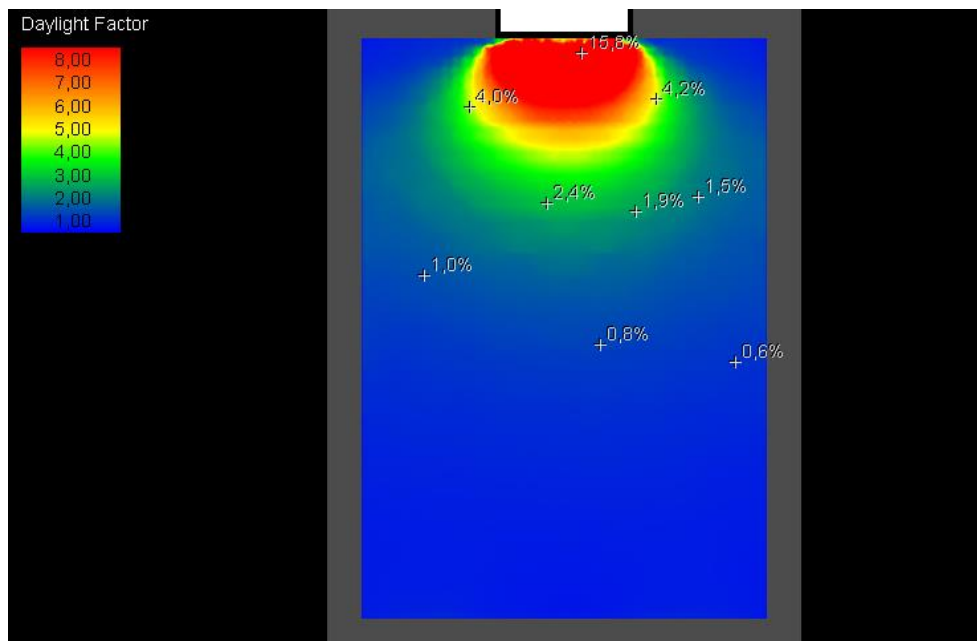


Figure 10: Results of daylight factor DF (%) - overcast sky

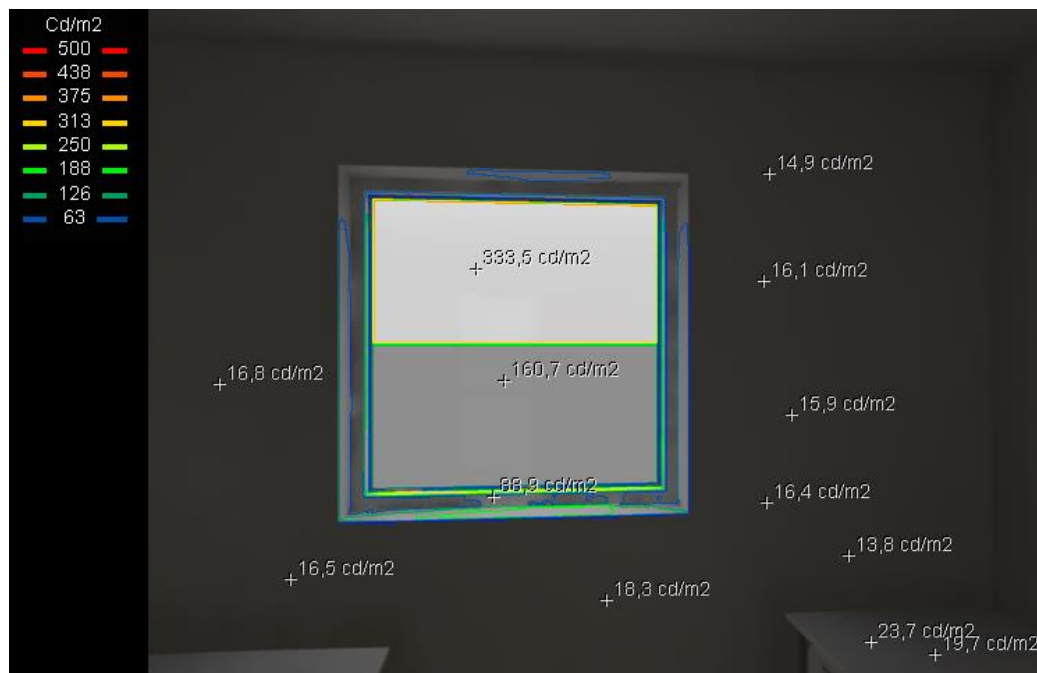


Figure 11: Results of luminance ( $\text{cd.m}^{-2}$ ) – overcast sky

## 5 Conclusion

The provision of natural daylight within the built environment can deliver genuine, positive benefits to the finished construction; benefits that can enhance the financial and environmental performance of the building in service, benefits that can improve the internal environment and make it a better, more pleasant place to be. When our mind needs to be stimulated and concentrated, it's important to have the area or office brightly lit. Unfortunately offices tend to turn to fluorescent light, but even the slightest bit of natural light can make a big difference in productivity [11].

The zone with sufficient daylight is only about 1/3 of the room depth where work is located. In the test room window is about 15% floor area. The pictures (Figure 4-6) show that the most light is around lunch. Then there is also glare. Morning is not enough light levels, so you need to use artificial lighting. Then, after about 15.00 p.m., the level of illumination decreases again. From the calculated values by simulation program it shows that in the middle of the room is a daylight factor 1% (Figure 9-10). Daylight factor at a point on the indoors working plane is 2% (Figure 9-10). Minimum standard value of daylight factor  $D_{\min} = 1.5 - 2 \%$  is met. However, protection against glare is required, especially in the afternoon (Figure 11).

From the calculated value from measured values is shows that minimum standard value of daylight factor (requested value  $D_{\min} = 1.5 - 2 \%$ ) is not fulfilled in several hours. The requirement is met between 12 am and 13 pm on each day and also on the third day when the sky was less cloudy.



The difference between the measured values and the calculated values by simulation program is that the external horizontal illumination has changed and in simulation is constant (5.000 lx-requirement by standard).

### Acknowledgements

This paper was elaborated with the financial support of the research project VEGA 1/0674/18 of the Scientific Grant Agency, the Ministry of Education, Science, Research, and Sport of the Slovak Republic and the Slovak Academy of Sciences.

### References

- [1] Konis, K. 2013. Evaluating daylighting effectiveness and occupant visual comfort in a side-lit open-plan office building in San Francisco, California. *Build. Environ.* 59, 662–677.
- [2] Bellia, L.; Bisegna, F.; Spada, G. 2011. Lighting indoor environment: Visual and non-visual light sources with different spectral power distribution. *Build. Environ.* 46, 1984–1992.
- [3] Gonzalez, J.; Fiorito, F. 2015. Daylight design of office buildings: Optimisation of external solar shadings by using combined simulation methods. *Buildings* 5, 560–580.
- [4] Lee, J.H.; Moon, J.W.; Kim, S. 2014. Analysis of occupants' visual perception to refine indoor lighting environment for office tasks. *Energies* 7, 4116–4139.
- [5] Integral Lighting. 2015. ČSN 360020; Czech Office of Standards, Metrology and Testing: Prague, Czech Republic.
- [6] EN 12464-1:2012. 2012. Light and Lighting-Lighting of Work Places-Part 1: Indoor Work Places; Slovak Republic Office of Standards, Metrology and Testing: Bratislava, Slovakia.
- [7] STN 730580; Daylighting in buildings, – 1 Basic requirements, 1986 – 2; Daylighting of residential buildings, 2000, Slovak Republic Office of Standards, Metrology and Testing: Bratislava, Slovakia; 2000
- [8] CEN/TC 169 07/2017 2017. Daylight in buildings (TC 169 WI 00169068) CEN/TC 169.
- [9] Gou, Z.; Lau, S.S.; Qian, F. 2015. Comparison of mood and task performance in naturally-lit and artificially-lit environments. *Indoor Built Environ.* 24, 27–36.
- [10] Shishegar, N.; Boubekri, M. 2016. Natural light and productivity: Analyzing the impacts of daylighting on students' and workers' health and alertness. In Proceedings of the International Conference on "Health, Biological and Life Science" (HBLIS-16), Istanbul, Turkey.
- [11] Ferencikova, M.; Darula, S. 2017. Availability of daylighting in school operating time, *Light and Engineering.* 25 (2), 71-78.

## Light Pipe Comparative Study

**Ayodeji Omishore, Petr Mohelník, Denis Míček**

Brno University of Technology, Czech Republic  
Faculty of Civil Engineering, Institute of Building Structures  
e-mail: ayodejiomi@gmail.com, mohelnik.p@fce.vutbr.cz, denis.micek@gmail.com

### Abstract

Results of daylight illuminance measurements of the field testing of two light guides with different roof installations is presented in the article. The first one is a common tubular system with a glass roof dome and the second one is a new light guide prototype with a concentrator head. The daylight illuminance was measured in a test chamber with the light guides installation. The measurements were carried out at the end of a summer season from August to September 2017. The measured data show differences in the daylight illuminance of the two tested light guides. The measured data were compared with simulation outputs in software Holigilm. In summary, it was found that the common light guide is about 37 percentage more efficient in light transmittance compared to the new light guide prototype. In temperate climate with dominant cloudy and partly cloudy daylight conditions the common light guide transmitted more light than the device with the concentrator head which reduced light transmission much more.

**Key words:** light guide, light measurements, daylight evaluations

## 1 Introduction

Light guide are tubular devices that transmit daylight into internal parts of buildings. They are usually installed in roofs constructions [1]. Common light guides consist of roof domes, tubes with mirrored surface and diffusers. Daylight is transmitted through the roof dome into the tube and it is scattered in the interior due to the diffuser [2,3]. Optical properties of light guide components and their installation are key factors influencing the light guide efficiency [3,4]. Most research projects have been focused on the solution of light guiding systems recently. Evaluations and studies of light guides were mostly focused on the influence of tubes and their dimensions as well as reflectance on the daylighting inside of building interiors [6-11]. Theoretical studies were pointed on the light transmittance of tubes with high reflective surfaces [12,13]. Analytic descriptions, physical models as well as algorithms and computer simulations of various types of light pipes were published [14,15]. A physical model for interior illuminance calculation applied to cylindrical guiding systems was developed [16]. Ray-tracing models [17-19] were used for developing of the light guide models and progressive photon mapping and stochastic progressive photon mapping were tested [20]. The

simulations were used for the modelling of the real building and light guide design [21-24]. Achieved and predicted installation performances were studied [25] and good design practices of the light guides installations were published [26,27].

Light reflectance of the light guides influences light transmittance through the light guiding systems. Installations of roof transparent covers play also important role in the light guiding design and their applications. Transparent covers at the top of light guides in roof installations are usually completed by domes or collector heads. Domes are made of glass or transparent plastics like PMMA. Collector heads have glass cover over a system consisting of mirrors and/or parabolic concentrators focusing light rays into the light tube [28,29]. The light focusing elements and reflecting parabolic head are used for enhancement of the light guiding systems efficiency. Efficiency of the light guiding systems is important for both the indoor visual comfort and energy savings [30-32].

Applications of the light focusing and redirecting reflective elements for light guides should be considered in the context of the light guide geometry and its installation in the building constructions. Otherwise the very efficient light guide system but installed in less favourable position in the roof could decrease its efficiency as it is presented in the article. The article demonstrates main results of field testing of two light guides with different roof installations. Presented study is focused on the light guide transmittance has been involved into the university research project orientated on research of advanced materials, structures and technologies.

A comparative study was carried out for two light guides with different roof dome installations. The study was carried out for the testing of the new light guide prototype and potentials its applications compared to the common light guide systems in temperate climatic conditions. The light guide prototype has a special light concentrator head. The head consists of two parabolic mirrors which concentrate and redirect sunlight into the tube. The prototype is compared with the commercially available light guide with transparent roof dome without any concentrator mirrors. The comparative study was completed in the field test chamber under real sky conditions. The purpose of the testing is to find advantages and possible drawbacks of the prototype light guiding system and suggest some improvements for its applications in buildings.



Figure 1: Concentrator head of the light guide prototype

- a) schematic section of the light guide with the concentrator head (PM-primary mirror, SM-secondary mirror),  
 b) side view, c) view into the parabolic concentrator.

## 2 Method

Two light guides with identical tubes of length 0.6 m and diameter 0.52 m were installed into a roof of a test chamber, Figure 2. Light guides have different roof domes – the first one has a mirror parabolic head with a flat glass cover (light guide LP1) and the second one is with a glass cupola (light guide LP2), Figure 1 and Figure 2. Both of the light guides were equipped by internal transparent plastic cover – diffuser. The diffusers scattered light into the chamber. The chamber internal room is separated by curtain into two identical parts. Each light guide is installed over its own part. Daylight illuminance chambers was monitored simultaneously. Internal surfaces of the chamber were faced with black cloth. It means that only sky component of daylight transmitted through the light guide influences indoor illuminance levels. External horizontal illuminance on roof of the test chamber was also monitored. A set of calibrated illuminance meters Lutron LX-1128SD were used for the experiment. Achieved measured illuminance were completed in one-minute monitoring intervals for one month period between 22<sup>nd</sup> August and 23<sup>rd</sup> September 2017. The monitoring time period is characteristic with number of days with clear sky conditions and higher external illuminance levels of the end of the summer period. These conditions are more convenient for the intended comparative study. Illuminance meters were positioned in the axes of the light guide and in the distance 2.8 m from the light guide diffuser. The testing was completed in the temperate climatic region of city Brno in the Czech Republic, latitude 49°12', longitude 16°37', altitude 237 m.

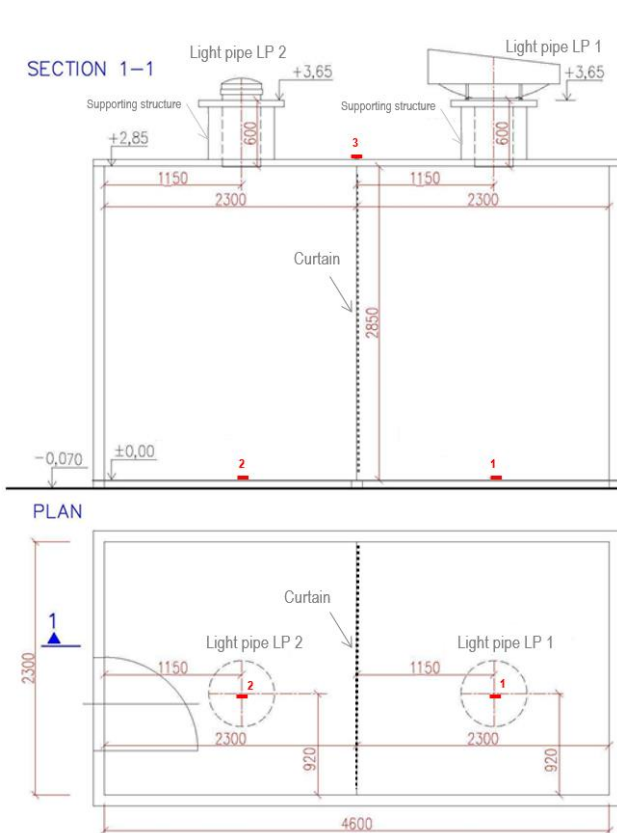


Figure 2: Scheme of installation of light guides LP1 and LP2

1 (resp. 2) – illuminance meters for LP1 (resp. LP2) light measurements,  
 3 – illuminance meter for external horizontal illuminance measurement

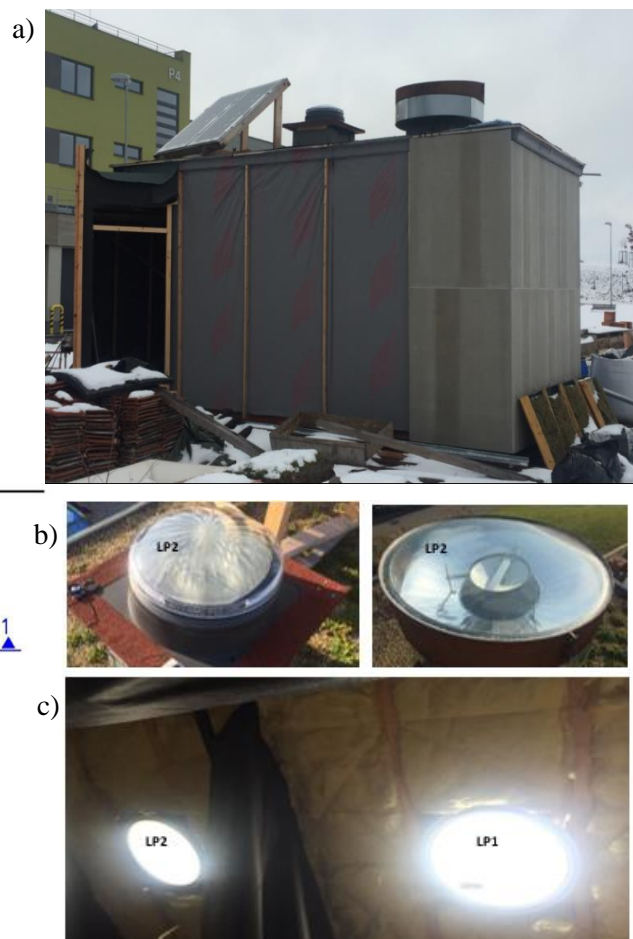


Fig. 3 Photographs of light guides LP1 and LP2 installation

- a) the test chamber
- b) light concentrator head of LP1 and roof dome of LP2
- c) view from the test chamber to the diffusers of LP1 and LP2

The light measurements were completed between August and September 2017. The illuminance measurement results give overview about the light transmittance of the tested light guides. Examples of the illuminance under LP1 and LP2 compared to the simultaneously measured external horizontal illuminance are shown in Figure 4. It is obvious that the illuminance under LP2 is higher compared to the daylight level under the LP1. This can be noticed in daily illuminance profiles of characteristic days shown in Figures 5 a 6. Measurements for partly cloudy sky gives more correlated data (Fig. 5) compared to the illuminance under sky with dynamic illuminance variations (Fig. 6). Values of mean, median, maximum and minimum values over the monitored period are summarized in Figure 7. In summary, the percentage of the difference of mean illuminance values from the illuminance measurements under LP1 and LP2 is shown in the graph of Figure 8. Results from the presented measurements gives information that the LP1 transmitted all the time more daylight compared to the LP2. On an average, the light transmittance is reduced about 37 percent as shown in Figure 8. It means that the concentrator head of the LP1 prototype is obstructive for daylighting during partly cloudy and cloudy sky conditions.



Figure 4: Examples of the internal and external horizontal illuminance profiles

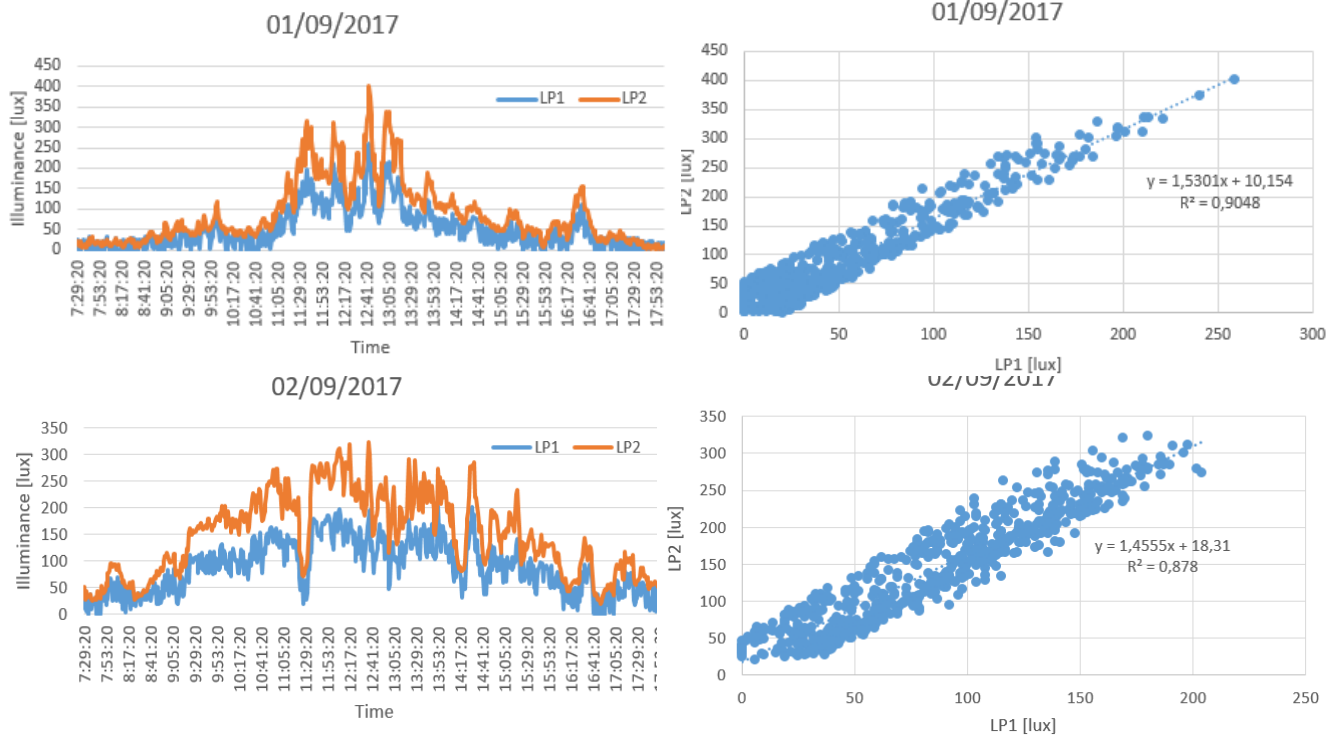


Figure 5: Daily illuminance profiles and correlation graphs for illuminances of LP1 and LP2 (partly cloudy sky conditions, on the 1<sup>st</sup> September and 2<sup>nd</sup> September 2017)

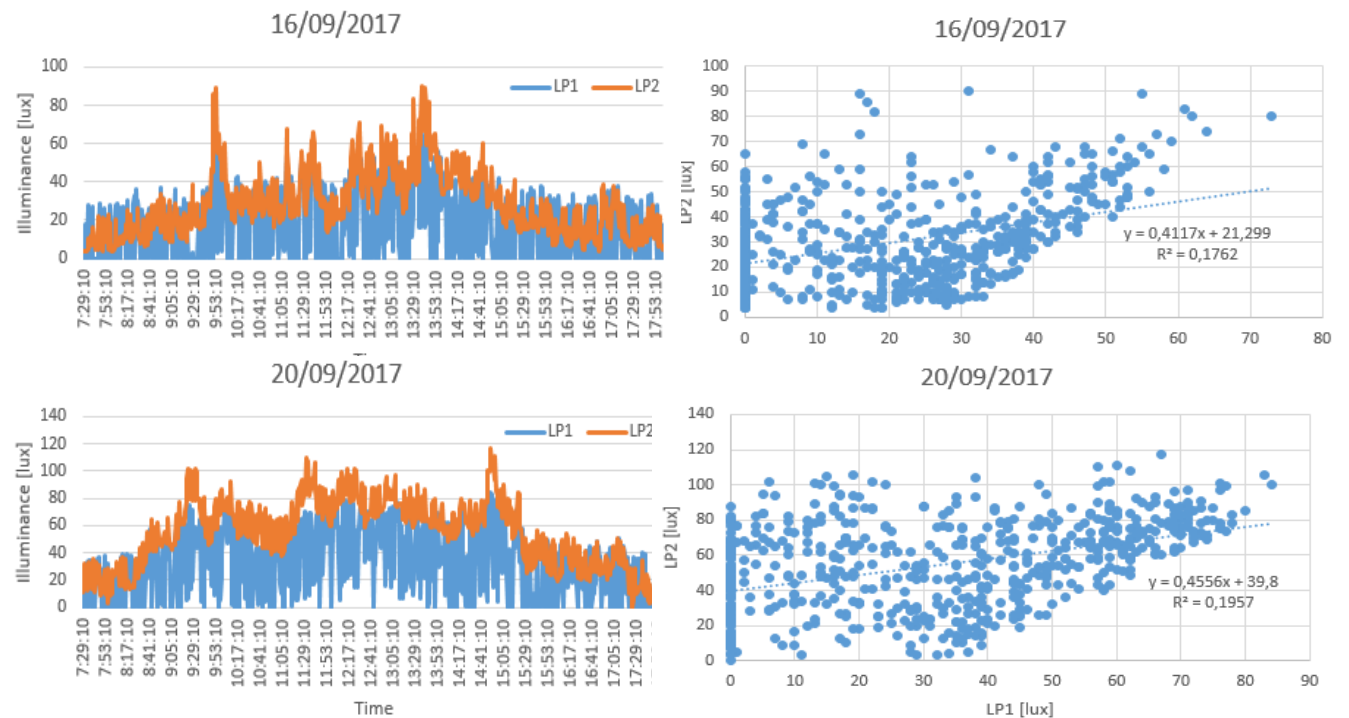


Figure 6: Daily illuminance profiles and correlation graphs for illuminances of LP1 and LP2 (dynamic changes of cloudy sky, on the 16<sup>th</sup> September and 20<sup>th</sup> September 2017)

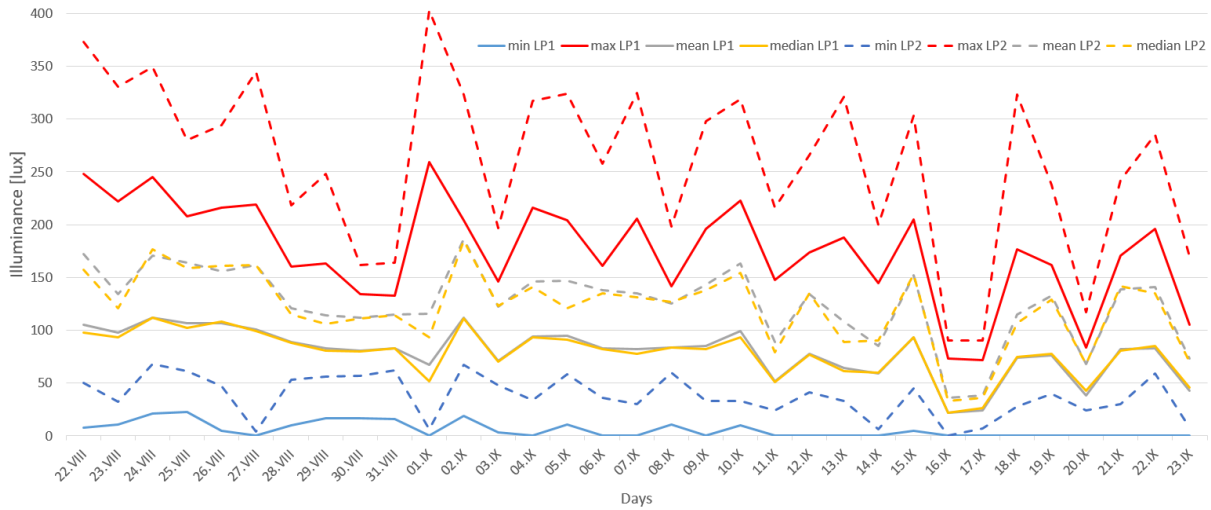


Figure 7: Daily illuminance min, max, mean and median values (from 22/08 to 23/09/2017)

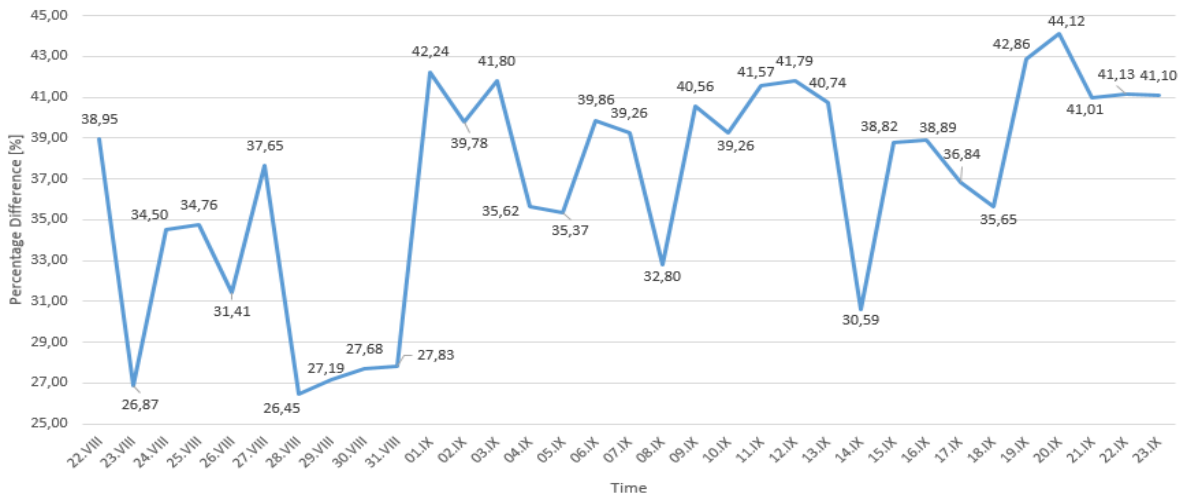


Figure 8: Percentage of the difference between mean values of LP1 and LP2 illuminance

### 3 Daylight simulations

Daylight simulations of the tested light guides LP1 and LP2 were run in software Holigilm [16]. Simulations were carried out for the 1st September, overcast sky [33] to be compared with data from measurements at daytime 12:00. Parameters selected for the simulations are:

- 1) dimensions of light types LP1 and LP2 are: length 0.6 m, diameter 0.52 m,
- 2) light reflectance of internal surface of the both tubes is  $\rho = 0.97$ .
- 3) light transmittance of ceiling diffusers of LP1 and LP2 is  $\tau = 0.75$ .
- 4) light transmittance  $\tau$  [-] of roof transparent covers of LP1 and LP2 are:
  - parabolic concentrator head of LP1:  $\tau_1 = 0.53$ , - roof cupola of LP2:  $\tau_2 = 0.9$ .

The light transmittance of the LP1 concentrator head was determined from light transmittance of glass dome 0.9 decreased for the reduction determined from the illuminance measurements in the test chamber which is in average 37 percentage. The simulation outputs of internal horizontal illuminance at level 2.8 m under the ceiling diffusers (the test chamber floor level) were evaluated. Positions of the light guides LP1 and LP2 are in accordance with Figure 2, it means  $x = 0.92$  m,  $y = 1.15$ ,  $z = 2.8$  m for coordinate system with 0.0 in the left hand side lower corner of the schemes in Figure 9.

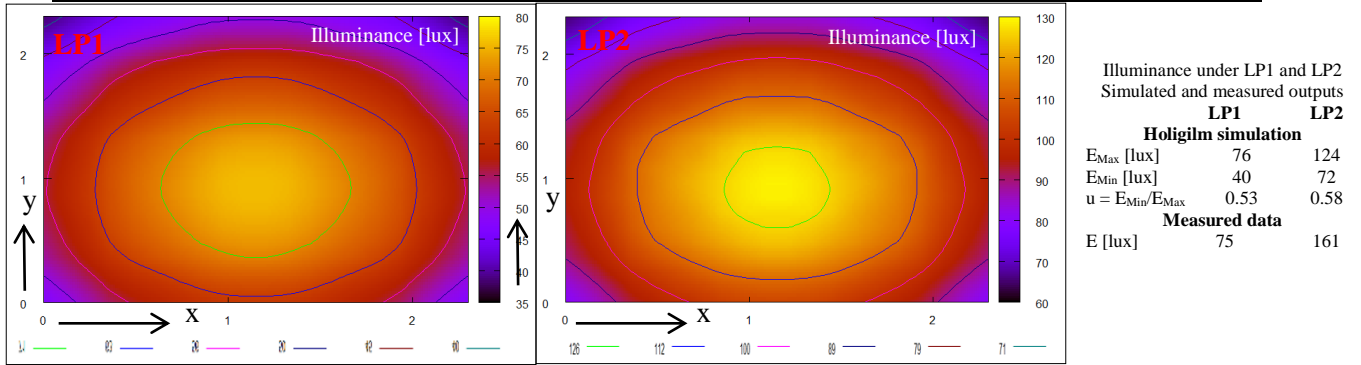


Figure 9: Illuminance  $E$  [lux] under light pipes LP1 and LP2, on 1st September, 12:00

Simulation output are in conformity with the measured data. The illuminance simulations also confirm that in this case the light guide LP1 with the concentrator head is less efficient system that gives lower illuminance level on the working plane indoors compared to light guide LP2. The concentrator head in static horizontal position represents an obstruction for daylight transmittance. Especially for overcast and partly cloudy sky conditions the system with the concentrator head in static position is less efficient. Also the secondary concave mirror of the head appears to be less convenient than the convex one. If light rays affect the concentrator head at low solar altitude they are reflected outside of the focus mirror. Then light transport is due to multi-reflections inside of the light tube and the effect of the concentrator head is not fully used. It is recommended to complete the concentrator head with a sun tracking system for activation of the head direction towards the solar radiation in case of the clear sky. Example of the light reflection and redirection on the parabolic head on the 1st September at 9:00 and 12:00 is shown in Figure 10 in parabolic head position  $0^\circ$  (horizontal),  $25^\circ$  a between  $40^\circ$ - $55^\circ$ . Dependence of the rotation on the solar altitude is shown in Figure 11.

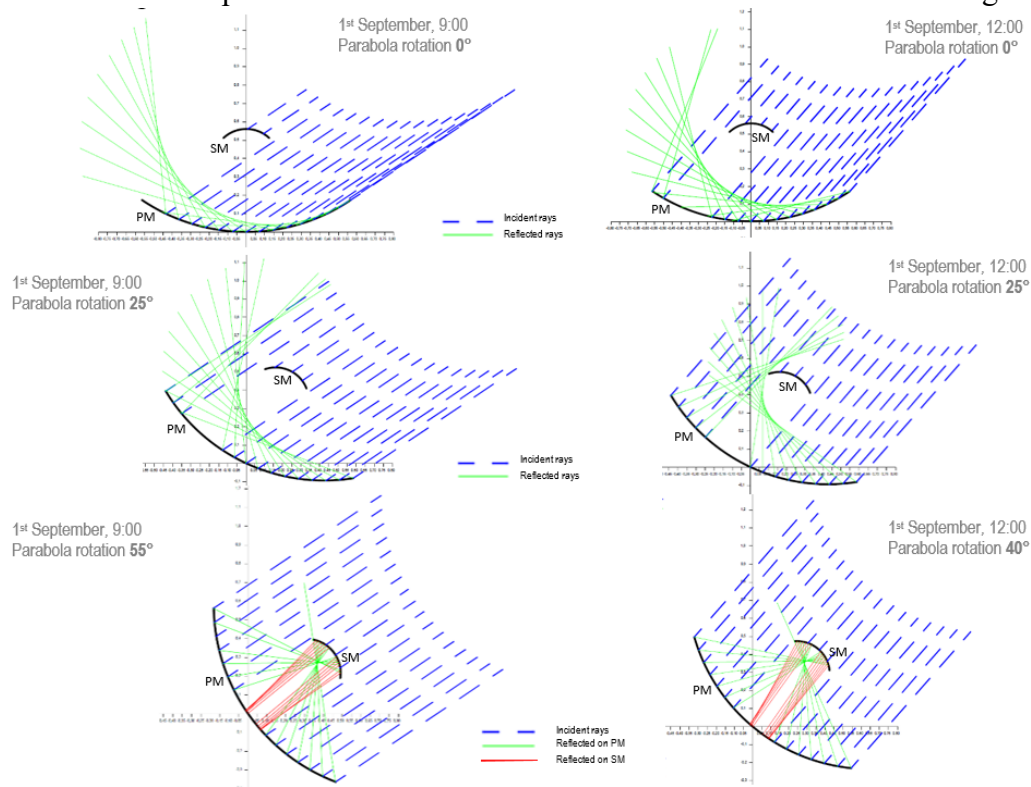


Figure 10: Examples of the light reflection and redirection on the parabolic head  
 PM-primary mirror, SM-secondary mirror



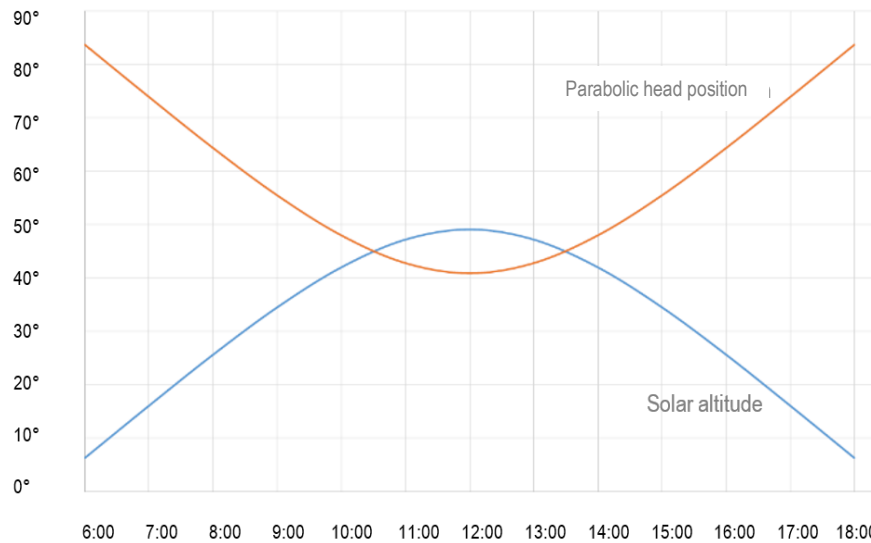


Figure 11: Dependence of the parabolic head position and orientation on solar altitude

## 4 Conclusion

Two comparable light guides with different roof installations were investigated. The case study was focused on evaluation of the common light guide with the glass roof dome and the new prototype with the roof concentrator head. The measured daylight illuminance data show light efficiency differences between two tested light guide systems. It was proven that the roof installation with the glass dome (LP2) is more efficient than the prototype with the light concentrator head (LP1). The concentrator head of the LP1 creates obstruction for daylight penetration in case of its static horizontal position. Daylight illuminance levels in the part of the test chamber illuminated by the LP1 are reduced about 37 percentage compared to that achieved the chamber illuminated by the LP2 system. The evaluation was done for conditions representing the region with temperate climatic with dominance of overcast and partly cloudy skies. Daylight simulations using software Hologilm give overview of daylight illuminance for tested light guides and comparison of measurements. Simulation outputs are in conformity with the measured data. The simulations also confirm that in this case the light guide with the concentrator head LP1 is less efficient system because gives lower illuminance level on the working plane indoors compared to the light guide LP2. The light guide prototype with the concentrator head LP1 was tested within the frame of the dissertation research. The further investigations of the light guide prototype is aimed at its installation in real buildings with different roof structures, slopes and orientations towards cardinal points. Some improvements of the light guide are recommended for its application in temperate climates as the system with movable concentrator heads completed with roof heliostats directing solar radiation inside of the light tube.

The installation of the concentrator head should be more efficient in sloped roofs oriented towards the south. The most efficient the light guide system LP1 would be in case when the light concentrator is equipped with a sun tracking system. This solution is more expensive compared to common light guides with glassed cupola. The sun-tracking light guide system is suitable for hot climates in installations exposed to intensive solar radiation.

## Acknowledgements

This article has been worked out under the project No. LO1408 "AdMaS UP - Advanced Materials, Structures and Technologies", supported by Ministry of Education of the Czech Republic, Youth and Sports under the „National Sustainability Programme I". Authors acknowledge company Lightway for the light guides for measurements and testing.

## References

- [1] Phillips, D. Daylighting: Natural Light in Architecture. Oxford: Architectural Press, Elsevier, 2004.
- [2] Carter J., Developments in tubular daylight guidance systems, *Building Research Information*, 32 (2004), No. 3, 220–34.
- [3] Rosemann, A., Kaase, H., Light pipe applications for daylighting systems. *Solar Energy*, 78 (2005), p. 772-780.
- [4] Oakley G. et al., Daylight performance of light pipes. *Solar Energy*, 69 (2000), No. 2, 89–98.
- [5] CIE 173. Tubular daylight guidance systems. Technical report, CIE, Vienna 2012.
- [6] Carter, D.J., The measured and predicted performance of passive solar light pipe systems. *Lighting Research and Technology*, 34 (2002), No. 1, 39-51.
- [7] Paroncini M., Calcagni, B., Corvaro, F., Monitoring of a light-pipe system, *Solar Energy*, 81 (2007), No. 9, 1180–1186.
- [8] Li, D.H.W. Tsang, E.K.W., Tam, C.C.O., An analysis of light-pipe system via full-scale measurements. *Applied Energy*, 87 (2010), No. 3, 799–805.
- [9] Marwaee A, Carter D., A field study of tubular daylight guidance installations, *Lighting Research and Technology*, 38 (2006), No. 3, 241–58.
- [10] Su, Y, Khan, N. Riffat, S.B., Gareth, O., Comparative monitoring and data regression of various sized commercial light pipes. *Energy and Buildings* 50 (2012), 308-314.
- [11] Mohelníková J. Evaluation of indoor illuminance from light guides. *Light and Visual Environment*, 32/1 (2008), No. 1, 20-26.
- [12] Jenkins D., Muneer T., Modelling light-pipe performances - a natural daylighting solution. *Building and Environment*, 38 (2003), 965-972.
- [13] Dobre, O., Achard, G., Optical simulation of lighting by hollow light pipes. Ninth Intern. IBPSA Conference, Building Simulation Montréal, 2005, 263-270.
- [14] van Derlofske, J.F., Hough, T.A., Analytical model of flux propagation in light-pipe systems. *Optical Engineering*, 43, (2004), No. 7, 1503–1510.
- [15] Samuhatananon, S., Chirarattananon, S., Chirarattananon, P., An Experimental and Analytical Study of Transmission of Daylight through Circular Light pipes, *Leukos*, 7 (2011), No. 4, 203-219.
- [16] Kocifaj M., Darula, S., Kittler, R., HOLIGILM: Hollow Light Guide Interior Illumination Method - An Analytic Calculation Approach for Cylindrical Light-Tubes, *Solar Energy*, 82 (2008), 247-259.
- [17] Dutton, S., Shao, L., Raytracing simulation for predicting light pipe transmittance. *International Journal of Low-Carbon Technologies*, 2/4 (2007), 339–358.

- [18] Diéguez, A.P., Light Pipes, Forward raytracing as a predictive tool and key design parameters. Thesis: EEED-14/02, Lund University.
- [19] Tejido, M.J.M. Conception and design of illumination light pipes, Thesis, Université de Neuchâtel, 2000.
- [20] Schou, A., Investigation of light pipe simulation algorithms, Thesis, DTU, Kongens Lyngby 2012.
- [21] Pacheco, D.A., Gentile, N., Von Wachenfelt, H., Dubois, M.-C., Daylight Utilization with Light Pipe in Farm Animal Production: A Simulation Approach, *Journal of Daylighting* 3/1 (2016), 1-11.
- [22] Ahmed S., Zain-Ahmed A., Rahman S. A., Sharif M.H., Predictive tools for evaluating daylighting performance of light pipes, *International Journal of Low-Carbon Technologies*, 1 (2006), 315-328.
- [23] Malet-Damour, B., Boyer, H., Fakra, A.H., Bojic, M., Light Pipes Performance Prediction: inter model and experimental confrontation on vertical circular light-guides. *Energy Procedia* (2014), 57, 1977-1986.
- [24] Luz, B., Monteiro, L.M., Alucci, M.P., Empirical and software verification of a simplified predictive model of luminous efficiency of light-pipes. *Proceedings 30th International PLEA Conference 2014*, CEPT University, Ahmedabad.
- [25] Al-Marwae M.B.A.O., Carter D.J., Tubular guidance systems for daylight: Achieved and predicted installation performances, *Applied Energy* 83/7, (2006),774-788.
- [26] Freewan, A. Using tubular daylighting systems to improve illuminance level in double loaded corridors in educational buildings, *Jordan Journal of Civil Engineering*, 10 (2016), 184-196.
- [27] Abd Kadir, A., Ismail, L. H., Kasim, N., Optimization of daylighting system by using light pipe system in a building. In *Proceedings of the 2nd International Conference on Construction and Building Engineering*, Padang, 2015, 1 – 9.
- [28] Swift, P.D., Smith, G.B., Cylindrical mirror light pipes. *Solar Energy Materials and Solar Cells* 36 (1995), 159–168.
- [29] Nair, M.G., Ramamurthy, K., Ganesan, A.R., Classification of indoor daylight enhancement systems, *Lighting Research and Technology*, 46, (2014), No. 3, 245-267.
- [30] von Wachenfelt, H., Vakouli, V., Diéguez, A.P., Gentile , N., Dubois, M-C., Jeppsson, K-H., Lighting Energy Saving with Light Pipe in Farm Animal Production. *Journal of Daylighting* 2/2 (2015), 21-31.
- [31] Bellia L., Fragliasso, F., Pedace, A. Evaluation of daylight availability for energy savings, *Journal of Daylighting*, 2 (2015) 12–20.
- [32] Katunský, D.; Dolníková, E.; Dolník, B. Daytime Lighting Assessment in Textile Factories Using Connected Windows in Slovakia: A Case Study. *Sustainability* 2018, 10, 655.
- [33] ISO 15469:2004(E)/CIE S 011/E:2003 Spatial distribution of daylight - CIE Standard General Sky.

# Utilizing drone technology in the civil engineering

**Matúš Tkáč, Peter Mésároš**

Technical University of Košice, Slovakia  
Civil Engineering Faculty, Institute of Construction Technology and Management  
e-mail: matus.tkac@tuke.sk, peter.mesaros@tuke.sk

## Abstract

An unmanned aerial vehicle (UAVs), also known as drone technology, is used for different types of application in the civil engineering. Drones as a tools that increase communication between construction participants, improves site safety, uses topographic measurements of large areas, with using principles of aerial photogrammetry is possible to create buildings aerial surveying, bridges, roads, highways, saves project time and costs, etc. The use of UAVs in the civil engineering can brings many benefits; creating real-time aerial images from the building objects, overviews reveal assets and challenges, as well as the broad lay of the land, operators can share the imaging with personnel on site, in headquarters and with sub-contractors, planners can meet virtually to discuss project timing, equipment needs and challenges presented by the terrain. The aim of this contribution is to create a general overview of the use of UAVs in the civil engineering. The contribution also contains types of UAVs used for construction purposes, their advantages and also disadvantages.

**Key words:** civil engineering, data capture, unmanned aerial vehicle, drone, aerial mapping

## 1 Introduction

Over the last decades, new digital technologies have appeared to enhance productivity, reduce overall time and cost of construction tasks. The introduction of drones to the construction industry is recent, although their use in other areas of industry (e.g., agriculture, public safety, military purposes, science and research, monitoring security, mining, etc.) has been frequent [1]. In the construction industry, aerial vehicles have been used for numerous purposes; such as, inspection of highways, bridges, roads, cell towers, high mast lighting, wind turbines, power transmission lines, building façade and roof, survey and mapping, construction monitoring, wetland/environmental, drainage and erosion, traffic monitoring, emergency services, etc. [1], [2]. UAVs provide invaluable help and cost savings with wide views of inaccessible and otherwise difficult and tough to navigate locations. UAVs indicate best access with the overhead perspective and 360° panoramas relay a real-time scenario. With this

input, engineering teams can prioritize their approaches. Operators can share the imaging with personnel on site, in company and also with sub-contractors at the distance [3]. The data in terms of drone images from multiple locations and point clouds (from 3D scanning of construction site) can be used to construct a 3D model using the photogrammetry techniques. This so-called "drone model" can be compared to BIM model at various construction stages to monitor the construction progress. Beside construction scheduling and costing, this comparison can be expanded to include real-time recording, reporting, billing, verification and planning [4]. The construction industry is based on the human relationships between project stakeholders. Digital tools and processes cannot replace people, either as individuals or teams, but they are required to increase quality of work, reduce costs and safety risk, improve decisions, reduce time-consuming processes, etc. Drones present increasingly attractive opportunities for achieving these goals, e.g., a team of scientists has demonstrated that UAVs were able to build a rope bridge, assemble items to create a structure, or detect and catch an object in the air. On the present, UAVs offer a high level of automation that allows to reach previously inaccessible areas, while capturing a large amount of data very quickly. However, this is not their only use [5].

## 2 Types of drones used in the construction industry

The use of drones has been one of the most attractive construction trends in recent years. In the construction industry has seen an almost 240% increase in drone usage, higher than any other commercial sector. Drones offer such aviation benefits and capabilities that provide invaluable help in solving construction activities. Although there are a large number of drones on the market, commercial drones are commonly used in the construction industry [6]. Drones can be classified on a different basis, like drones for photography, drones for aerial mapping, drones for military purposes and surveillance, etc. However, the best classification of drones can be made on the basis of aerial platforms. Based on the type of aerial platform used, there are 4 major types of drones; fixed wing drones, multi rotor drones, single rotor drones and fixed wing hybrid VTOL drones [7].

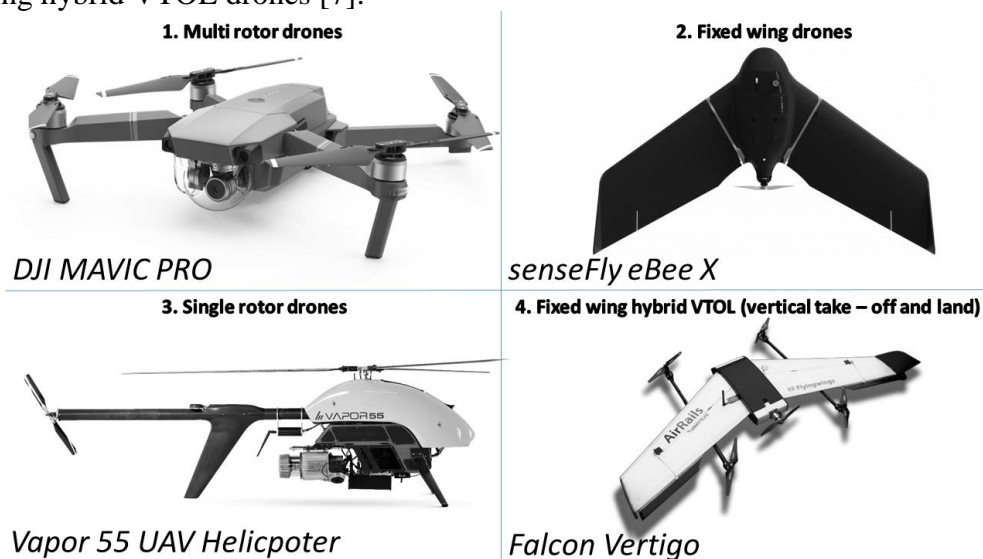


Figure 1: Different types of drones, source: [8], [9], [10], [11]

Multi-rotor drones are the most commonly used types of drones, which are used not only for fun, but also for professional aerial mapping. Common applications of multi rotors are aerial photography, video recording and aerial surveying. These types of drones can be classified according to the number of rotors, e.g., tricopters (3 rotors), quadcopters (4 rotors), hexacopters (6 rotors) and octocopters (8 rotors) [12]. The disadvantage of multi-rotor drones is their limited endurance and speed. Due to these limitations, these types of drones are not suitable for large scale aerial mapping, e.g. pipelines, roads, power lines, highways, etc. Despite the drone technology continues to improve, multi-rotor drones have to do a lot of effort to keep them in the air. Depending on the weight of the drone and camera, multirotor drones currently hold an average of 20-30 minutes or less in the air [13].

Fixed wing drones operate essentially on the same principle as passenger airplanes. These drones do not generate thrust by vertical rotors, but generate lift using fixed wings [12]. These types of drones need energy only to move forward and not to keep them in the air. For this reason, they are a much more efficient variant for topographic mapping of large areas and they are able to cover longer distances than multi-rotor drones. On the other hand, the main disadvantage of the fixed wing drones is the inability to stay in the air in one place, which prevents them from creating detailed aerial mapping, e.g. the as-built buildings. Another disadvantage of this type of drone is its take-off from the ground and landing on the ground. Depending on the size of the drone is necessary to have a runway or catapult launcher to get them into the air and on the other hand is necessary to have a runway to get them to the ground back safely [13]. The fixed wing design allows these drones to reach a higher altitude during flight, making them efficient tool for aerial mapping topography, but on the other hand they can only fly forward. For closer aerial work which requiring more detailed activities, e.g., detailed aerial mapping of buildings, the use of multi-rotor drones is a much better solution because they are easy to work with in the air and their rotor design allows them to hover stable in the air [6].

Multi-rotor drones generate vertical thrust using multiple rotors, but on the other hand a single helicopter drone uses only one rotor. The single helicopters drones can be powered by gasoline engines and thus last much longer in the air than multi-rotor drones. If it is necessary to fly with higher payload, e.g. with the LIDAR scanner, or if it is necessary for aerial mapping to combine a long endurance of the flight with forward flight, in this case a single helicopter drone is a good choice. The disadvantage of this type of drone is the increased complexity, cost, vibration, and they also require more mechanical maintenance due to their increased overall technical complexity [12].

Fixed wing unmanned aircraft is known to be more energy efficient than quadcopters and as a result can cover long distances much faster. But quad-shaped drones do not need that much space for take-off and landing. That is also why some manufacturers have decided to combine these characteristics and have developed unmanned aircraft that can take off vertically and then go into horizontal flight using wings. Their name is very similar to the automobile industry, and it, hybrid drones. The hybrid drone flies on a pre-scheduled flight route at a user-specified height and collects data through its color and multispectral sensors. Upon completion of its mission, the drone will land vertically back to the starting point [12].

### 3 Utilizing drone technology in the construction industry

The drone technology in the construction industry has a very wide range of applications. Drones can be applied in the construction industry in the following ways [14]:

#### Building Surveys

Almost every building survey of the building requires the visibility of the roof of the building in order to assess its technical conditions and to assess any defects or failures. In most cases, the ascent to the roof is complicated, which often requires the use of scaffolding, ladders or other auxiliary structures, which may ultimately pose a danger which are both time consuming and costly. Use of a small drone in these cases can save time, costs, reduce health and safety risks which are connected with the building surveying of the roof structure and with accessing to complex or hard to reach parts of the building's roof. [14].

Looking Fig. 2 it can be seen that for overall aerial mapping of the building it is necessary to create vertical (*left part of the figure*) and oblique (*right part of the figure*) aerial images. Vertical aerial photographic coverage of the roof is normally taken as a series of overlapping flight strips. The overall time for automatic mode was in this case 3 minutes and 100 aerial images were created. The oblique aerial images which were focused on the building's facade were created in the manual mode, it means, that this process is about the pilot's practical and personal experiences. In this mode, 950 aerial images were created in the distance from the building approximately 10 - 15 meters in three altitude levels. The comprehensive data collection time of aerial mapping was 2 hours and 1050 aerial images were created.

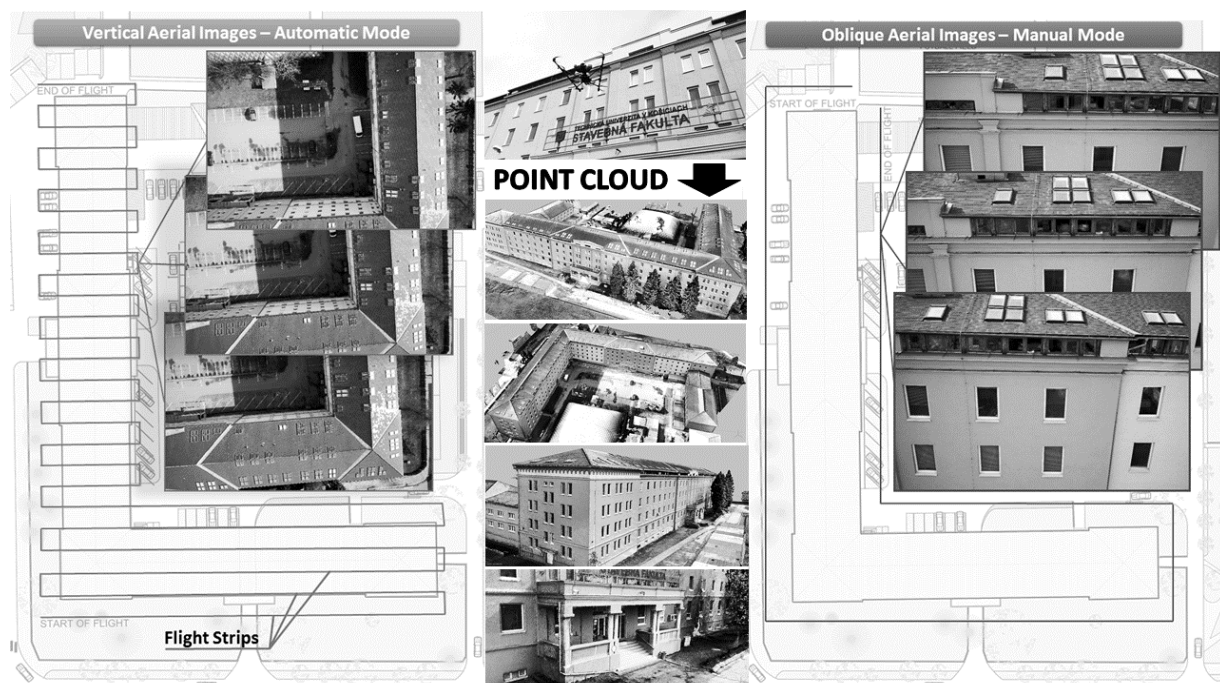


Figure 2: Example of technological process of creating vertical (left) and oblique (right) aerial images of building; source: authors

## Topographic Mapping and Land Surveys

In the case of planning large-scale and complex construction projects, consultation of topographic maps is essential. Topographic maps may reveal construction design errors that are inappropriate for terrain. Although topographic maps are useful for construction projects, their production is often costly and time consuming. The use of drones is very effective in these cases. Due to its ability to capture large amounts of data in a relatively short time, it leads to significant cost savings as well as the project costs required for these activities. Drones, thanks to their capabilities, ensure project time, budget and accuracy. Furthermore, from the high quality aerial images produced by drones can be created 3D models of the surface (DSM-digital surface model) or of the terrain (DTM-digital terrain model) [6].

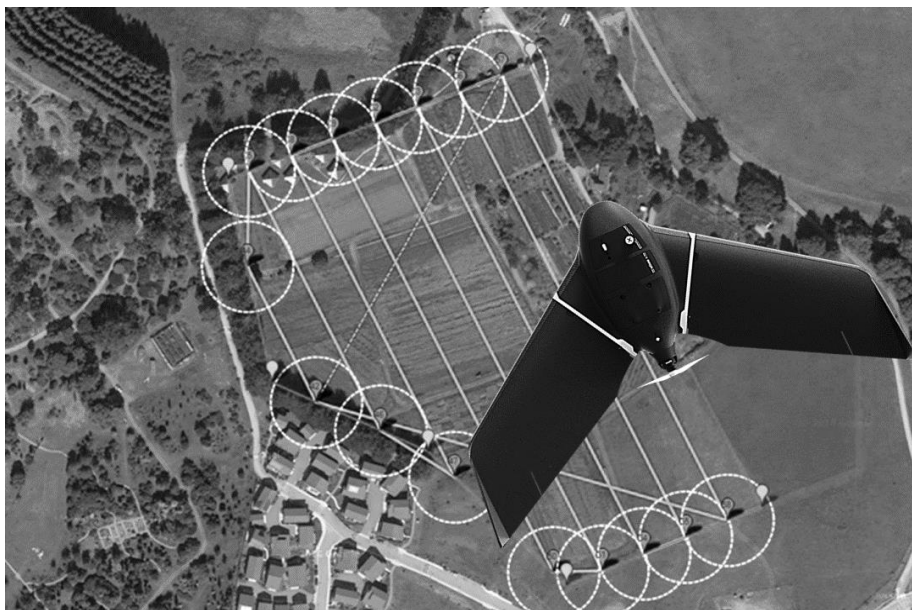


Fig. 3: Aerial mapping of the area of interest using a fixed wing drone; source: [15], [9]

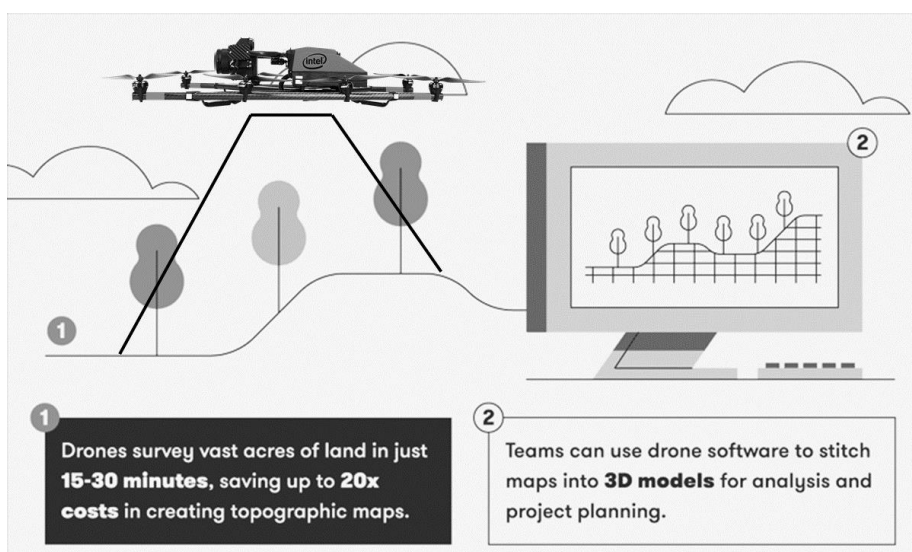


Figure 4: Topographic mapping and land surveys using a drone; source: [6]



## Construction Site Inspections

For builders the data from drones can be collected frequently allowing easy integration into projects and tracking site progress precisely and with hardly any lag time. This allows construction companies to work more effectively in managing their time and resources while minimizing potential issues and delays [16].

Construction site inspection using drones can be a considerable tool for project teams. A pilot with experiences can use the drone to identify any construction or technical problems on the construction site and also using drones for inspection purposes is possible to ensure that the project goals will go according to plan. The use of drones can save thousands of euros in the case of rebuilds and plan changes. Using drones can be much safer as well because it eliminates spaces or areas on the construction site that could potentially be dangerous to assess the damage. With more advanced technology, it is possible also use a drone to fly around a construction site and check out how closely it resembles the construction plan or the model, drones can aid in the creation of detailed 3D models of new construction projects, drones can help to see what things look like on the roof of a skyscraper under construction, etc. [17]. Drone due to its ability to perform visual inspection of high risk areas on the construction site or on the new - exist building can save time, reduce health and safety risks. Aerial photographs can be documented from the safety of the site cabin and then sent to project team in HD quality very quickly and effectively. Site inspections can be undertaken more regularly and cover larger areas more efficiently [14]. There are four main benefits to using drones for construction site inspections: improved safety saves time, less labor-intensive and higher quality data [18].



Figure 5: Construction site inspection by a drone; source [6]

### **Equipment Tracking and Automating**

Equipment tracking and automating is the problem of every project manager on the construction site. This is usually a problem with a large number of different tables and documents, which are often difficult and time-consuming to keep. Using the drone, the same project manager can immediately assess if the equipment is where it should be during the drone flight. It is also possible to quickly assess with a drone if a devices that have already completed its work is still on-site and with this solution is also possible to prevent expensive accidental extension charges [6].

### **Remote Monitoring and Progress Reports**

Probably the biggest advantage of drones in the construction industry they can provide to clients is their visibility from the air, from a great height and from any location [6]. A constant drone flight on the construction site can represents a quick way to map the progress of a project, especially when the clients are not able to be physically present on a site [6], [14]. Thanks to multiple high-resolution aerial images and HD-quality videos, project developers can get a better overview of project progress at daily, weekly or monthly intervals [14]. According to [19] it's recommended to film only those areas of the new construction where the best progress is achieved, unless the client stipulates otherwise.

### **Integration of laser scanning and aerial photogrammetry**

It is often difficult for a surveyor to gain access to a suitable laser scanning location from which would be possible to scan, e.g. roof construction. In this case the final point cloud can be incomplete. The drone technology in integration with the laser scanning can brings solution of this limitation. [14].

Looking Fig. 6 it can be seen the reference building where the technology of terrestrial laser scans and aerial photogrammetry using a drone were used. The measurement of this building was divided into two stages. In the case of terrestrial laser scanning (stage 1), the completely facade of the building was selected for digital surveying, and in the case of aerial photogrammetry (stage 2) the completely roof of the building was selected for digital surveying.

The total data collection time of the first stage was approximately 12 hours and together was created 48 scanner positions which were focused on the exterior part of the building. The total data collection time of the second stage was approximately 30 minutes (flight plan of the drone, aerial photographs in automatic mode, and aerial photographs in manual mode) which were focused on the roof construction of the building. In the second phase, a total of 302 aerial photographs were taken using a DJI MAVIC PRO quadcopter with a 12 Mpx digital camera, and the entire drone flight was performed with one battery.

The phase of data processing in this case consisted from three stages. The first stage was primary focused on creation of two point cloud from two technologies using the appropriate softwares. The second stage was about integration of two local coordinate systems from two

point clouds into common coordinate system. This was very important step for the final connection of two point clouds. The last stage was about final connection of two point clouds based on the common coordinate system (Fig. 6). Data processing time for laser scanning was 3 hours and the Faro Scene and Autodesk Recap software were used. Data processing time for aerial photogrammetry was 31 hours and the “Agisoft Photoscan Professional” was used. The final point cloud includes now all space information about the building and this data can be used for either CAD or BIM modeling like a template for a new as-built project.

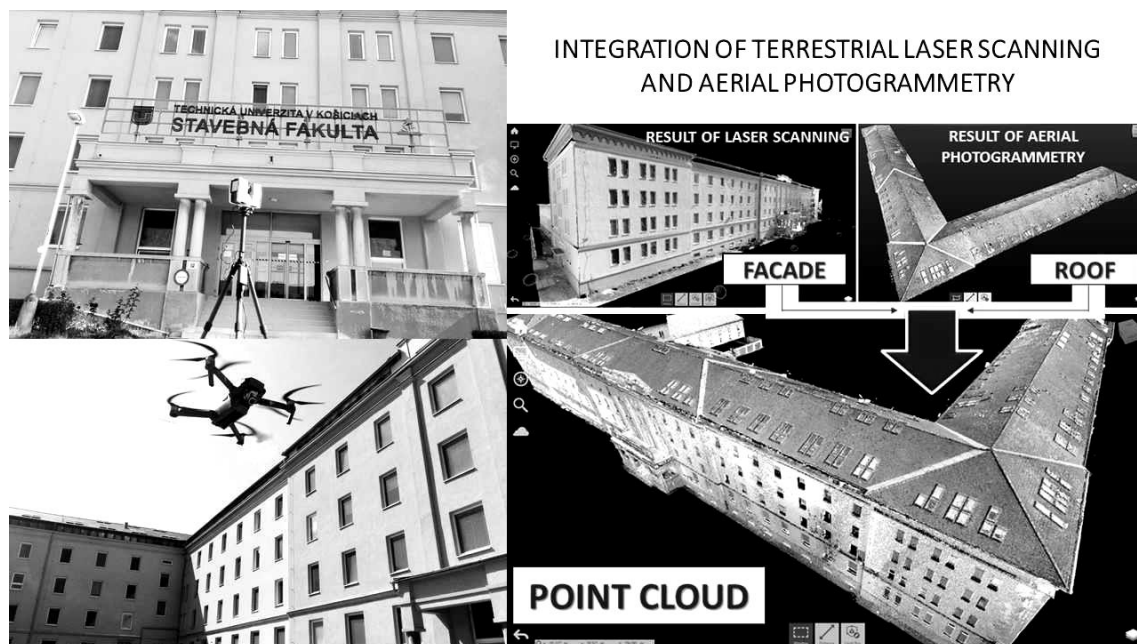


Figure 6: Connection of terrestrial laser scanning and aerial photogrammetry; source: author

### Thermal Imaging recording

Similar to laser scanners, also drones can be used to create aerial thermal images from different parts of buildings which can be used to assess cold spots in buildings. This possibility can bring for engineers, surveyors and contractors necessary information about the building in the case when is essential to identify and rectify building defects, e.g. places where thermal bridges arise and the like [14]. Thermography allows determine thermal technical properties of building envelope and is used to detect hidden building defects. Thermography is able to find these failures with the necessary accuracy and, if evaluated correctly, is the basic step for effective design of the technical solution and consequently also for checking its realization. Combining thermography with drones allows detection of such construction defects that are not visible to the naked eye (Fig. 7) [14].

Thermal imaging of the certain part of the building can also help detect water infiltration, leaks, and areas with mold or rot before they cause serious damage. These cold, damp areas will appear as dark blue on the thermal imaging screen. From the inspector’s standpoint, using the equipment to inspect rooftops, pinpoint leaks and detect heat loss make the process simpler, safer and faster and generally more efficient [20].



Figure 7: Example of drone thermal imaging; source [20]

Other uses of drones in the construction industry can be included security surveillance, personnel safety, health and safety inductions, maintenance inspections, promotional photography, live feed/ virtual walk around, site logistics, monitoring workers, etc. [6], [14], [19].

#### 4 Conclusion

Drones are an important technological asset in the area of civil engineering. Their use in the construction industry will only increase in time because they can efficiently collect data of a high standard, greatly minimizes risk to the safety of a project team. In general, the construction industry is often careful in implementing new progressive technologies into production or in established workflows. The construction industry can be described as a fast-growing industry, and unmanned aerial vehicles technology was quickly adopted as a tool that saves costs, time and increases safety and control. Construction companies receive drones much faster than ever because of their innumerable benefits. Whether drones are used by construction companies for topographic terrain mapping, building surveys, land surveys, construction site inspections, remote monitoring, progress reports, thermal imaging recording or for integration with laser scanners, drones have proved as invaluable tool throughout the life cycle of a construction project. The drone capabilities enable them to save costs, time, risk and labor, which automatically lead engineers, contractors, investors or future customers to more confidence and certainty in working on a construction project.

## Acknowledgements

The paper presents a partial research results of project APVV-17-0549 “Research of knowledge-based and virtual technologies for intelligent designing and realization of building projects with emphasis on economic efficiency and sustainability” and project VEGA 1/0828/17 “Research and application of knowledge-based systems for modelling cost and economic parameters in Building Information Modelling”.

## References

- [1] Motavwa, I., Kardakou, A. (2018). Unmanned Aerial Vehicles (UAVs) for Inspection in Construction and Building Industry. In: Proceedings of the 16th International Operation & Maintenance conference (OMAINTEC 2018), 18-20th November 2018, Cairo, Egypt.
- [2] Cornwell, Ch., Knapp, C. (2017). Civil Engineering Applications of Drones, from [https://static1.squarespace.com/static/5452a33de4b04219d5dae8f8/t/58fe4564beba91c2aca7f/1493058923629/NY2020\\_Civil+Engineering+Applications+of+Drones1.pdf](https://static1.squarespace.com/static/5452a33de4b04219d5dae8f8/t/58fe4564beba91c2aca7f/1493058923629/NY2020_Civil+Engineering+Applications+of+Drones1.pdf)
- [3] Bourque, A. (2017, June). How drones are advancing civil engineering and surveying. Retrieved August 1, 2019, from <https://www.computerworld.com/article/3199631/how-drones-are-advancing-civil-engineering-and-surveying.html>
- [4] Anwar, N., Izhar, A. M., Najam, A. F. (2018). Construction Monitoring and Reporting using Drones and Unmanned Aerial Vehicles (UAVs). In The Tenth International Conference on Construction in the 21st Century (CITC-10), July 2-4, 2018, At Colombo, Srilanka.
- [5] A business approach for the use of drones in the Engineering & Construction industries. (2016). Retrieved August 1, 2019, from [https://www.accenture.com/\\_acnmedia/pdf-24/accenture-drones-construction-service.pdf](https://www.accenture.com/_acnmedia/pdf-24/accenture-drones-construction-service.pdf)
- [6] Zitzman, L. (2018, October). Drones in Construction: How They’re Transforming the Industry. Retrieved August 2, 2019, from <https://www.bigrentz.com/blog/drones-construction>
- [7] (2017, February). Types of Drones – Explore the Different Models of UAV’s. Retrieved August 2, 2019, from <http://www.circuitstoday.com/types-of-drones>
- [8] Download Dji Mavic Pro transparent PNG. Retrieved August 2, 2019, from <https://www.stickpng.com/img/electronics/dji-drones/dji-mavic-pro>
- [9] senseFly. eBee X Fixed-Wing Drone. Retrieved August 2, 2019, from <https://www.sensefly.com/drone/ebee-x-fixed-wing-drone/>
- [10] Skyline UAV. Vapor 55 UAV Helicopter. Retrieved August 2, 2019, from <http://www.skylineuav.com.au/fleet/vapor-55-uav-helicopter/>
- [11] UAS Vision. Affordable Ready-to-Fly Hybrid VTOL Drone. Retrieved August 2, 2019, from <https://www.uasvision.com/2017/02/22/affordable-ready-to-fly-hybrid-vtol-drone/>
- [12] Drone Omega. Types of Drones. Retrieved August 2, 2019, from <https://www.droneomega.com/types-of-drones/>
- [13] Chapman, A. (2016, June). Types of Drones: Multi-Rotor vs Fixed-Wing vs Single Rotor vs Hybrid VTOL. Retrieved August 3, 2019, from <https://www.auav.com.au/articles/drone-types/>
- [14] Ayemba, D. (23, March). Utilizing drone technology in construction. Retrieved August 3, 2019, from <https://constructionreviewonline.com/2018/03/drones-in-construction/>

- [15] Nixon, A. (2019, June). Best Drones For Agriculture 2019: The Ultimate Buyer's Guide. Retrieved August 3, 2019, from <https://bestdroneforthejob.com/drone-buying-guides/agriculture-drone-buyers-guide/>
- [16] Anra Technologies. Construction Site Inspections. Retrieved August 4, 2019, from <http://www.anratechnologies.com/home/construction-site-inspections/>
- [17] Young, J. (2019, July). The Use of Drones in Construction Inspection and General Building. Retrieved August 4, 2019, from <http://www.droneguru.net/the-use-of-drones-in-construction-inspection-and-general-building/>
- [18] Hook, J. (2016, November). Using Drones for Site Inspection. Retrieved August 4, 2019, from <https://www.buildsoft.com.au/blog/using-drones-for-site-inspections>
- [19] Lawson, S. (2018, October). 7 Ways Drones Are Improving The Construction Industry. Retrieved August 4, 2019, from <http://www.droneguru.net/7-ways-drones-are-improving-the-construction-industry/>
- [20] ICA. (2017, February). Drone Thermal Imaging: The Next Wave in UAV Inspection Services. Retrieved August 4, 2019, from <https://icaschool.com/2017/02/13/drone-thermal-imaging-next-wave-uav-inspection-services/>

## The effect of CO<sub>2</sub> on cement composites produced with an admixture of waste sludge water from a concrete plant

Lukas Klus<sup>1,2</sup>, Jakub Svoboda<sup>1,2</sup>, Vojtech Václavík<sup>1,2</sup>, Tomas Dvorský<sup>1</sup>, Jiri Botula<sup>2,3</sup>

<sup>1</sup> Department of Environmental Engineering, VŠB-TU Ostrava, Czech Republic;

<sup>2</sup> Institute of Clean Technologies for Extraction and Utilization of Energy Resources, VŠB-TU Ostrava, Czech Republic;

<sup>3</sup> Department of Mining Engineering and Safety, VŠB-TU Ostrava, Czech Republic  
e-mail: lukas.klus@vsb.cz, vojtech.vaclavik@vsb.cz

### Abstract

This article presents the results of a research dealing with the effect of CO<sub>2</sub> on cement composites prepared on the basis of waste sludge water from the concrete plant. The designed formulas R1 and R3 use waste sludge water from the concrete plant as a partial or complete replacement of mixing water in the production of cement composites. The mixing water was replaced by waste sludge water in the amounts of 25%, 50%, 75% and 100%. Laboratory tests that are defined in ČSN EN 1008 standard were performed in order to determine the effect of partial or complete replacement of mixing water. The test specimens were further subjected to the effect of CO<sub>2</sub> in the Lamart laboratory chamber, where the effect of CO<sub>2</sub> was simulated for the period 50 years. Subsequently, the cement composites were tested for their strength characteristics (tensile flexural strength, compressive strength) and subjected to a mineralogical analysis. The results show that the effect of CO<sub>2</sub> will reduce the strength characteristics of the composite compared to the comparative samples.

**Key words:** accelerated carbonation of composite, replacement of mixing water, waste water from concrete plant, cement composites, tensile flexural strength, compressive strength.

## 1 Introduction

The durability of building materials can be characterized by the time they are able to withstand various effects, such as temperature changes, exposure to sunlight, frost resistance and, last but not least, the effects of aggressive and atmospheric gases. The carbonation of concrete as a result of the effects of carbon dioxide leads to subsequent losses of its ability to withstand external impacts and it contributes to the corrosion of concrete reinforcement. In order to use the maximum potential of waste sludge water from the concrete plant as the mixing water for a concrete mixture, it is necessary to determine the chemical properties and the reactivity with other substances. Testing cement composites by means of accelerated carbonation is quite widespread nowadays. This method was used by Cabral et al. in his research on the Evaluation

of the Effect of Accelerated Carbonation in Cement-Bagasse Panels [1]. The penetration of CO<sub>2</sub> into porous mortar matrix is a diffusion-controlled process. The subsequent chemical reactions between CO<sub>2</sub> and the cement hydration products lead to degradation effects of the hardened cement matrix [2, 3]. A research by Xie et al. focused on the carbonation of concrete with fly ash has reached a conclusion saying that fly ash had positive impact on the resistance of concrete against the effects of CO<sub>2</sub> [4]. The permeability of cement mortars for chloride ions can be reduced by the addition of mineral admixtures, but it can be improved by carbonization curing. The formation of CaCO<sub>3</sub> after curing by means of carbonation has improved the pore structure and has shown higher efficiency for pore filling. That is why carbonation curing provides a good way how to efficiently recycle industrial wastes as mineral additives [5-7]. The samples exposed to the effect of CO<sub>2</sub> show a denser microstructure compared to the samples not exposed to CO<sub>2</sub>. Despite the presence of reactive MgO, the absorption of CO<sub>2</sub> increases with age [8, 9]. Many studies use recycled construction waste to produce composites and concretes [10, 11]. Two formulas marked R1 and R3 were designed on the basis of the already established properties. The designed formulas were exposed to the effect of CO<sub>2</sub> equal to 50 years. Their strength characteristics were examined and their mineralogical analysis was performed after this exposure.

## **2 Materials and Methods**

### **2.1 Sand**

Standardized sand according to ČSN EN 196-1 was used for the production of the test specimens. The amount of sand is presented in Tab. 1.

### **2.2 Cement**

Two types of cement were used for the designed formulas. For formula R1, it was Portland cement CEM 52.5 R, which contained 95% of Portland clinker and 5% of additional components (fly ash), and for formula R3, it was Portland cement CEM II/B-LL 32.5 R, which contained 65% of Portland clinker, 30% of limestone LL and 5% of additional components (fly ash). The amount of cement used is presented in Tab. 1 [12].

### **2.3 Mixing water**

During the production of cement composites, the mixing water was replaced by waste sludge water from the concrete plant in various ratios. This water was tested to the requirements given in ČSN EN 1008 standard [13]. Attention was focused on the adherence to the standard limits (pH, conductivity, alkalinity, concentration of sulphates, nitrates and chlorides, concentration of humus substances, dissolved and undissolved substances). The standard limits defined in ČSN EN 1008 [13] were not exceeded and the used waste sludge water from the concrete plant meets the requirements for mixing water. The replacement of mixing water with waste sludge water from the concrete plant was carried out in the ratios of 1/4 (25%); 1/2 (50%); 3/4 (75%) and 1 (100%). L. Klus, J. Svoboda, V. Václavík, T. Dvorský and J. Botula



## 2.4 Designed formulas

Two formulas marked R1 and R3 were designed. The composition of the individual formulas is presented in Tab. 1.

Table 1: Composition of designed formulas

Formula	R1					R3				
	Comp	1/4	1/2	3/4	1	Comp	1/4	1/2	3/4	1
Mixing water replacem.	450	450	450	450	450	-	-	-	-	-
CEM I 52.5 R [g]	450	450	450	450	450	-	-	-	-	-
CEM II/B-LL 32.5 R [g]	-	-	-	-	-	450	450	450	450	450
Mixing water- pure [g]	225	168.8	112.5	56.3	-	225	168.8	112.5	56.3	-
Sludge water [g]	-	56.25	112.5	168.8	225	-	56.25	112.5	168.8	225
Sand [g]	1350	1350	1350	1350	1350	1350	1350	1350	1350	1350

## 2.5 Mineralogical analysis

Bruker Advance D8 powder diffractometer equipped with a LynxEye linear semiconductor detector and a SOL-XE energy-dispersive detector was used to perform the mineralogical analysis. The samples were dried to a constant weight at 105 °C in a Memmert drier, crushed to a maximum grain size of 8 mm, ground in a BetonTest A 50 vibrating mill, and then sieved through a sieve with a mesh size of 0.063 mm. The sieved material was used as an input for the mineralogical analysis.

## 2.6 Strength characteristics

The tensile flexural strength and compressive strength tests were carried out in compliance with ČSN EN 196-3, ČSN EN 197-1 ed.2. standards [14,15]. Beams with the dimensions of 40x40x160 mm were used as the test specimens. Formtest testing device with a compressive force of 300KN and 100KN was used for the testing.

## 3 Results and discussion

### 3.1 Mineralogical composition of solids obtained from the composite samples

Fig 1. presents the results of the mineralogical analysis of the samples of solids from the tested composites of formula R1, which were exposed to the effects of CO<sub>2</sub> in a CO<sub>2</sub> chamber. Fig. 1 clearly shows that significant mineralogical shares consist of these minerals: Quartz (SiO<sub>2</sub>), Calcite (CaCO<sub>3</sub>), Portlandite (Ca(OH)<sub>2</sub>), Ettringite (Ca<sub>6</sub>Al<sub>2</sub>(SO<sub>4</sub>)<sub>3</sub>(OH)<sub>12</sub>·26H<sub>2</sub>O) and Gypsum (CaSO<sub>4</sub>·2H<sub>2</sub>O). It is obvious from the results of the mineralogical analysis that the type of minerals does not change, but there are differences in the percentage representation.

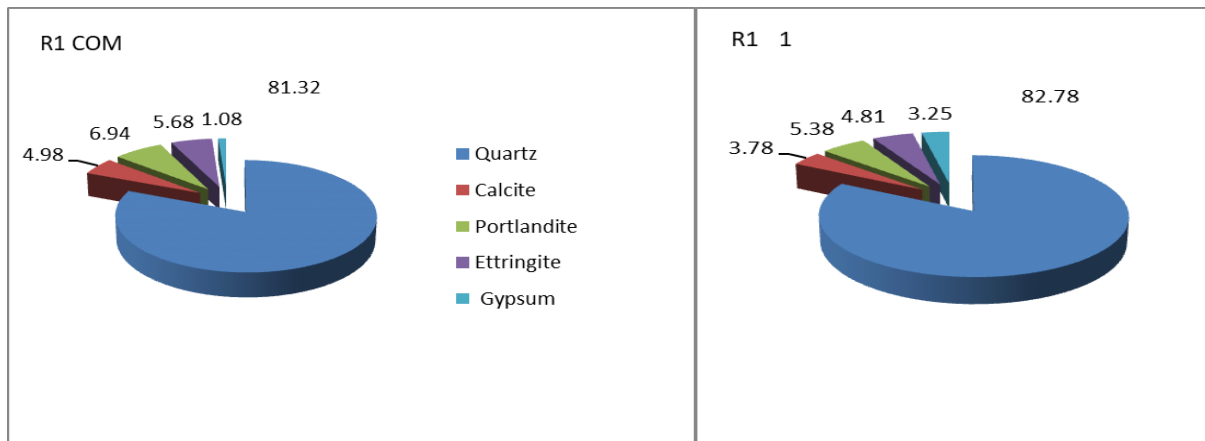


Figure 1: Mineralogical composition of the standardized average of solids obtained from composite samples of R1 Comp formula (0% replacement) and R1 1 (100% replacement) [%].

### 3.2 Surface carbonation

The comparative samples were cured for 90 days in a humid environment and then they were exposed to CO<sub>2</sub> for a period simulating 50 years and broken. A phenolphthalein indicator was applied to the fracture surface of the sample and the area not affected by carbonation turned pink (Fig. 2). An image analysis of the samples after tensile flexural strength test by means of a USB camera was used for the detection of carbonation. The surface of the test specimen was scanned, and the area  $S_w$ , which was affected by the carbonation process, was detected and calculated. See Tab. 2.



Figure. 2: Samples of formula R3 and R1 after the application of phenolphthalein on the fracture surface.

Table 2: Carbonation area

Mixing water replacement	Total sample area [mm <sup>2</sup> ]		Carbonation area S <sub>w</sub> [mm <sup>2</sup> ]	
	Mixture R1	Mixture R3	Mixture R1	Mixture R3
Comp	1626.1	1618.4	643.2	715.5
1/4	1655.6	1621.3	531.7	557.8
1/2	1637.4	1633.2	47.8	255.6
3/4	1614.8	1618.8	412.9	364.3
1	1630.9	1626.9	487.3	534.6

Tab. 2 presents the area affected by carbonation. It shows that the R1 mixture is more resistant to the effects of CO<sub>2</sub> in comparison with the R3 mixture. This is due to the type of cement used in formula R1, which is Portland cement (CEM I 52.5 R), whereas formula R3 uses Portland mixed cement (CEM II/B-LL 32.5 R). When comparing the formulas R1 and R3, all the mixtures with replaced mixing water show better resistance to CO<sub>2</sub> effects compared to the comparative mixture.

The addition of waste sludge water from the concrete plant increases the ability of cement compound to resist the effects of CO<sub>2</sub>, which can be explained by the lower content of calcite (CaCO<sub>3</sub>) in mixture R1-1, as presented by the mineralogical composition in Fig. 1. It shows that the calcite content of R1-1 mixture is lower by 24.1% in comparison with R1-Comp comparison mixture. At the same time, Tab. 2 shows that the carbonated area of R1-1 mixture is 24.2% smaller in comparison with R1-Comp comparison mixture. There is a mutual dependence between the calcite content and the carbonation area.

### 3.3 Strength characteristics

The specimens with the dimensions of 40x40x160 mm were used for the testing of tensile flexural and compressive strengths. The determination of tensile flexural and compressive strength was performed on samples after 90 days of age and on samples exposed to the effects of CO<sub>2</sub> simulating a period of 50 years. The measured values of tensile flexural strengths are presented in Fig. 3.

The results presented in Fig. 3 clearly show that the samples containing waste sludge water from the concrete plant have lower tensile flexural strengths for both formulas (R1, R3) in comparison with the comparative samples. The largest strength difference in case of formula R1 was recorded in the sample with 100% mixing water replacement, with a decrease in strength by 18% in comparison with the comparative sample. The largest strength difference in case of formula R3 was recorded in the sample with 100% mixing water replacement, with a decrease in strength by 19% in comparison with the comparative sample. The results of the compressive strength test are presented in Fig. 4. The figure presents the values of the samples exposed to accelerated carbonation equal to the effect of CO<sub>2</sub> for the period of 50 years.

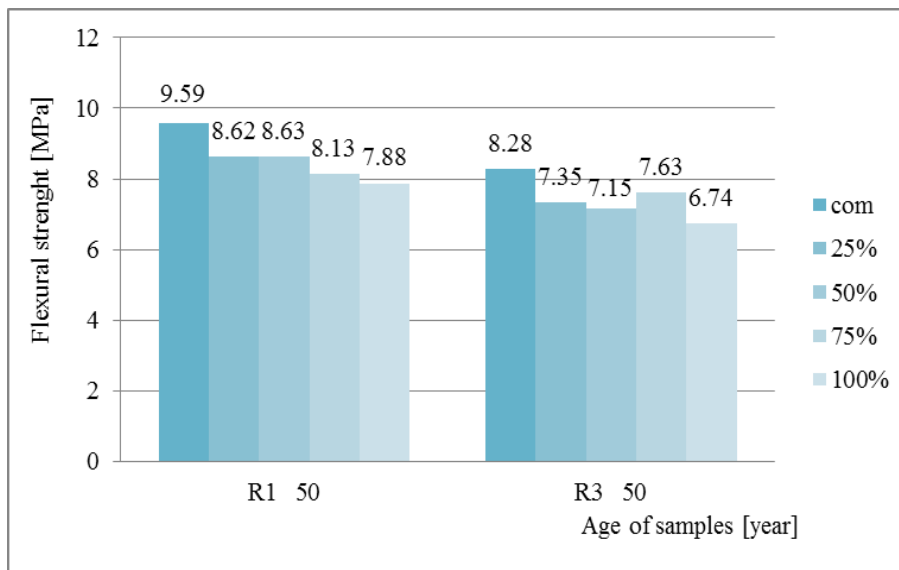


Figure 3: Tensile flexural strength of formula R1 and R3 exposed to the effects of CO<sub>2</sub> for a period simulating 50 years.

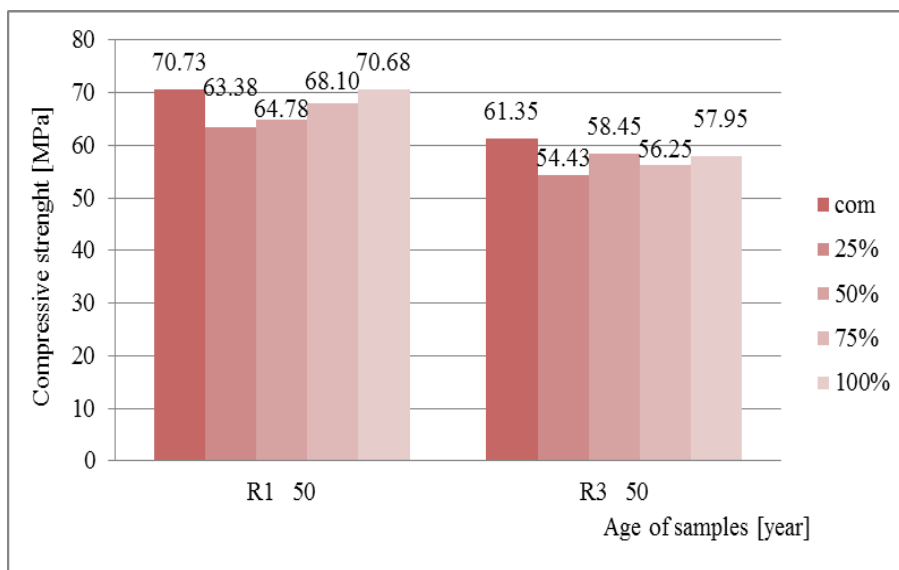


Figure 4: Compressive strengths of formulas R1 and R3 exposed to the effect of CO<sub>2</sub> for the period simulating 50 years.

When comparing the results of the compressive strengths, it is evident that the samples containing waste sludge water from the concrete plant show lower compressive strengths in case of both formulas (R1, R3) in comparison with the comparative samples. The biggest difference in strength for formula R1 was recorded in the sample with a 25% replacement of mixing water, with a decrease in strength by 11% in comparison with the comparative sample. The biggest difference in strength for formula R3 was recorded in the sample with a 25% replacement of mixing water with a 12% decrease in strength in comparison with the comparative sample.

## 4 Conclusion

This article presents the results of the experimental research dealing with the use of waste sludge water from the concrete plant in the production of cement composites. The research was focused on the physical and mechanical properties of cement composites exposed to the effect of CO<sub>2</sub> representing a period of 50 years.

The results of the tensile flexural strength show that the most suitable replacement of mixing water with waste sludge water from the concrete plant for formula R1 is a 25% replacement, and for formula R3, it is a 25% replacement as well. The biggest difference in tensile flexural strength was achieved by samples containing 100% replacement of mixing water. The differences for formula R1 reached 18% and for formula R3, it was 19%. The results of the compressive strength show that the most suitable replacement of mixing water with waste sludge water from the concrete plant in case of formula R1 is a 100% replacement, and in case of formula R3, it is a 100% replacement. The biggest difference in compression strength was achieved by samples containing 25% replacement of mixing water. In formula R1, the difference was 11% and in formula R3, it was a difference of 12%.

The test results of the effect of CO<sub>2</sub> show that the addition of waste sludge water from the concrete plant increases the capability of the cementing compound to resist the effects of CO<sub>2</sub>. This can be explained by the lower content of calcite (CaCO<sub>3</sub>). Calcite content of R1-1 is lower by 24.1% compared to R1-Comp comparative mixture. At the same time, the carbonation area of R1-1 mixture is lower by 24.2% compared to R1-Comp comparison mixture.

## Acknowledgements

- This article was partially supported by Grant of SGS No. SV511889, Faculty of Mining and Geology, VSB – Technical University of Ostrava, Czech Republic.
- This article was written in connection with project Institute of clean technologies for mining and utilization of raw materials for energy use - Sustainability program. Identification code: LO1406. Project is supported by the National Programme for Sustainability I (2013-2020) financed by the state budget of the Czech Republic.
- This article was partially supported by Grant of SGS No. SV511995, Faculty of Mining and Geology, VSB – Technical University of Ostrava, Czech Republic.
- This article has been elaborated in the framework of the grant programme „Support for Science and Research in the Moravia-Silesia Region 2018" (RRC/10/2018), financed from the budget of the Moravian-Silesian Region.

## References

- [1] Cabral M R, Nakanishi E Y and Fiorelli J, 2017. *Evaluation of the Effect of Accelerated Carbonation in Cement–Bagasse Panels after Cycles of Wetting and Drying*, J. Mat. Civ. Eng. 29 doi: 10.1061/(ASCE)MT.1943-5533.0001861
- [2] Marangu J M, Thiong'o J K and Wachira J M, 2019. *Review of Carbonation Resistance in Hydrated Cement Based Materials*, J. Chem. 2019 doi: 10.1155/2019/8489671
- [3] Lazarean H N A, Iliescu M, Ciont N and Abrudan I F, 2019. *Degradation processes of iron-sulfides and calcite containing aggregates from asphaltic mixtures*. Con. Build. Mat. 212, 745-754 doi: 10.1016/j.conbuildmat.2019.04.018

- [4] Xie X, Feng Q, Chen Z, Jiang L and Lu W, 2019. *Diffusion and distribution of chloride ions in carbonated concrete with fly ash*. *Con. Build. Mat.* 218, 119-125 doi: 10.1016/j.conbuildmat.2019.05.041
- [5] Tonoli G H D and kol., 2019. *Influence of the initial moisture content on the carbonation degree and performance of fiber-cement composites*. *Con. Build. Mat.* 215, 22-29 doi: 10.1016/j.conbuildmat.2019.04.159
- [6] Qin L, Gao X and Chen T, 2019. *Influence of mineral admixtures on carbonation curing of cement paste*. *Con. Build. Mat.* 212, 653-662 doi: 10.1016/j.conbuildmat.2019.04.033
- [7] El-Hassan H and Shao Y, 2015. *Early carbonation curing of concrete masonry units with Portland limestone cement*. *Cem. Con. Comp.* 62, 168-177 doi: 10.1016/j.cemconcomp.2015.07.004
- [8] Castellote M, Andrade C, Turrillas X, Campo J and Cuello G J, 2008. *Accelerated carbonation of cement pastes in situ monitored by neutron diffraction*. *Cem. Con. Res* 38(12), 1365-1373 doi: 10.1016/j.cemconres.2008.07.002
- [9] Mo L and Panesar D K, 2013. *Accelerated carbonation – A potential approach to sequester CO<sub>2</sub> in cement paste containing slag and reactive MgO*. *Cem. Con. Comp.* 43, 69-77 doi: 10.1016/j.cemconcomp.2013.07.001
- [10] Li L, Zhan B, Lu J and Poon Ch, 2019. *Systematic evaluation of the effect of replacing river sand by different particle size ranges of fine recycled concrete aggregates (FRCA) in cement mortars*. *Con.* 209, 147-155 doi: 10.1016/j.conbuildmat.2019.03.044
- [11] Juradin S, Goran B and Haparin A, 2012. *Experimental Testing of the Effects of Fine Particles on the Properties of the Self-Compacting Lightweight Concrete*. *Adv. Mat. Sci.* doi: 10.1155/2012/398567
- [12] ČSN EN 196-1. *Methods of testing cement - Part 1: Determination of strength*. Praha: Czech office for standards, metrology and testing, 2016.
- [13] ČSN EN 1008. *Mixing water for concrete—Specification for sampling, testing and assessing the suitability of water, including water recovered from processes in the concrete industry, as mixing water for concrete*. Praha: Czech office for standards, metrology and testing, 2003.
- [14] ČSN EN 196-3. *Methods of testing cement - Part 3: Determination of setting times and soundness*. Praha: Czech office for standards, metrology and testing, 2017.
- [15] ČSN EN 197-1 ed.2. *Cement - Part 1: Composition, specifications and conformity criteria for common cements*. Czech office for standards, metrology and testing, 2012.

## Evaluation of concrete deterioration under simulated acid rain environment

Michaela Smolakova, Adriana Estokova

Technical University of Košice, Slovakia  
Civil Engineering Faculty, Institute of Environmental Engineering  
e-mail: michaela.smolakova@tuke.sk, adriana.estokova@tuke.sk

### Abstract

Acid rain is identified as one of the most serious environmental problems nowadays and it is mainly a mixture of sulfuric and nitric acids. Deterioration of concrete structures exposed to aggressive acid rain attack is a key durability issue that affects the performance and maintenance costs of vital civil infrastructures. The motivation for understanding the acid rain corrosion process is high because of the early age deterioration of many concrete structures exposed to acid rain. The main objective of this study was to investigate the durability of concrete specimens with different supplementary cementitious materials, such as fly ash, zeolite and blast furnace slag against acid rain attack. Experiments of acid rain simulation influence on the composites were carried out for 7 weeks and parameters like visual changes, absorbability and leachability of calcium and silicon ions were evaluated. The increase in absorbability was detected for all samples while the sample with blast furnace slag was identified to be the most durable in this point of view. The most durable sample considering leached-out calcium and silicon ions was found to be sample with fly ash.

**Key words:** concrete, supplementary cementitious materials, deterioration, acid rain

## 1 Introduction

As one of the most used building material, concrete is inevitably exposed to different acidic substances and from this point of view the durability of concrete structures in aggressive environments has become a major concern over the past several decades [1-3]. Suitable compressive strength, large resources of concrete components and cost effectiveness are concrete characteristics that are desirable for various applications [4,5]. When concrete is exposed to acidic environments, deterioration of material occurs, because acidic molecules penetrating the concrete reacts with compounds in concrete matrix [4,6].

British chemist R.A. Smith first observed the pollution of acid rain in 1852, which attracted much attention from researchers, environmentalists and experts from many different fields all over the world [7]. Acid rain attack caused by atmospheric precipitation leads to degradation

of concrete strength and structural stability. With the development of the industry, the acid rain corrosion has become a more serious problem. Studies have showed, that the rainwater of most parts of Europe, the eastern parts of the United States, the southwest parts of China and parts of Japan has been strongly acidified [1].

Acid rain is a corrosive medium containing not only  $H^+$  cations but also other species including  $NH_4^+$ ,  $Mg^{2+}$ , and  $SO_4^{2-}$  ions. Based on its composition, the mechanism of degradation of cement-based materials like concrete by acid rain attack is quite different from and more complicated than the mechanisms of pure acid attack [2].

Value of pH in pore water solution of concrete is typically ranging from 12 to 13.5. Acid rain induces physical and chemical reactions in the matrix, which results in a reduction in the pH. Continued reactions lead the concrete structure to gradually lose its strength and durability characteristics followed by possible structural failure [2,8,9]. Therefore, the mechanism of deterioration of concrete structures under acid rain attack should be studied further to minimize its impact [2].

Under a corrosive environment, concrete properties can be improved by using supplementary cementitious materials either from natural resources like zeolite or in a form of industrial by-products like blast furnace slag and fly ash. Benefits of using supplementary cementitious materials in concrete include increased long-term compressive strength, better workability and reduced permeability [10].

In this paper, the influence of different supplementary cementitious materials (zeolite, blast furnace slag and fly ash) on performance of concrete under acid rain attack has been studied. Parameters like leachability of calcium and silicon ions from concrete matrix, absorbability and visual changes on the surface of 28-day cured composite samples after 7 weeks of their storage in aggressive solution were investigated.

## 2 Materials and methods

### 2.1 Concrete specimens

Four concrete mixtures containing different supplementary cementitious materials were prepared for the acid rain corrosion experiment. Specimen A-0 represents the reference mixture made with Portland cement (CEM I) only, in the mixture A-1 was Portland cement partially replaced by zeolite, in the mixture A-2 with fly ash and in the mixture A-3 with blast furnace slag, respectively.

Concrete samples were prepared according to Slovak standard STN EN 206-1+A1 [11] in a form of prisms of size 100 x 100 x 400 mm. After 24 hours the samples were demoulded and cured for 28 days in tap water. Concrete prisms were cut into small prisms with dimensions of 50 x 50 x 10 mm for the accelerated corrosion experiments. Table 1 shows the mixture designs with appropriate w/c ratio for tested concrete specimens.

Table 1: Concrete mixture design of studied specimens

Component	A-0	A-1	A-2	A-3
Cement ( $kg/m^3$ )	360	331	304.75	54
Natural aggregates, fraction 0/4 mm	845	825	845	825



(kg/m <sup>3</sup> )				
Natural aggregates, fraction 4/8 (kg/m <sup>3</sup> )	405	243	405	235
Natural aggregates, fraction 8/16 (kg/m <sup>3</sup> )	590	752	590	740
Water (L)	190	190	190	162
Fly ash (kg/m <sup>3</sup> )	-	-	41.30	-
Blast furnace slag (kg/m <sup>3</sup> )	-	-	-	306
Zeolite (kg/m <sup>3</sup> )	-	29	-	-
Plasticizer (L)	-	2.65	-	-
w/c	0.53	0.53	0.55	0.45

Before the start of the acid rain corrosion experiments the samples were brushed in order to remove polluting particles and dried at  $105 \pm 5$  °C in the laboratory oven.

The simulated acid rain solution with pH 1.6 was prepared by mixing pure chemical reagents such as H<sub>2</sub>SO<sub>4</sub> and HNO<sub>3</sub> in a ratio 1:1.5, respectively and deionized water.

The volume of the liquid solution was based on the volume ratio of the concrete specimens and liquid phase and was set at 1:10. The ratio was selected according to accelerated short-term corrosion experiments to achieve desired deterioration of concrete samples. The acid rain corrosion tests of concrete samples were carried out in glass beakers during 7 weeks at laboratory temperature of 23 °C.

## 2.2 Absorbability test of concrete specimens

The absorptivity test was performed on concrete specimens according to Slovak Standard STN 73 1316 [12]. Before the corrosion tests, the concrete prisms were dried at  $105 \pm 5$  °C and their weight was determined. The testing of concrete prisms for acid rain solution absorption was performed prior and after the 7 weeks long experiment. At the end of the corrosion tests, the weights of wet specimens were measured and specimens were again dried at  $105 \pm 5$  °C and weights of dry specimens were determined. Absorbability before the experiments and after was calculated using equation (1) [12]:

$$v = \frac{m_W - m_D}{m_D} \cdot 100\% \quad (1)$$

Where  $m_W$  refers to the weight of wet specimen and  $m_D$  is weight of dried specimen.

## 2.3 Leachability of Ca<sup>2+</sup> and Si<sup>4+</sup> ions







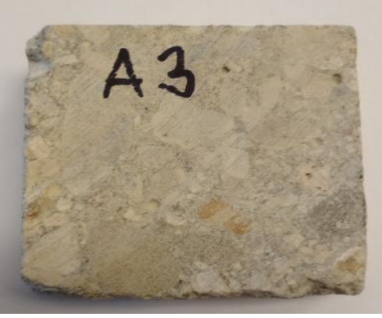

X-ray fluorescence analysis (XRF) was used to analyze the leach-out quantities of Ca<sup>2+</sup> and Si<sup>4+</sup> ions in concrete leachates after 4<sup>th</sup> and 7<sup>th</sup> week of experiment. Spectrometer SPECTRO iQ II (Ametek, Germany) with SDD silicon drift detector with resolution of 145 eV at 10 000 pulses was used. Detailed measurement conditions of the XRF analysis were previously described in [13].

### 3 Results and discussion

#### 3.1 Visual changes

Table 2 shows concrete samples prior and after the exposition to acid rain environment.

Table 2: Visual changes of samples before and after the corrosion experiment

Concrete specimens	Surface prior the experiment	Surface after the experiment
A0	 <p>A rectangular concrete specimen with a light beige, relatively smooth surface. The number 'A0' is handwritten in black on the top surface.</p>	 <p>The same specimen after exposure to acid rain, showing significant surface erosion and a porous, irregular texture with exposed aggregate.</p>
A1	 <p>A rectangular concrete specimen with a greyish, slightly textured surface. There are some small dark spots and a faint label on the top.</p>	 <p>The specimen after exposure to acid rain, showing surface erosion and a porous, irregular texture with exposed aggregate.</p>
A2	 <p>A square concrete specimen with a light blue, porous, and highly textured surface.</p>	 <p>The specimen after exposure to acid rain, showing surface erosion and a porous, irregular texture with exposed aggregate.</p>
A3	 <p>A rectangular concrete specimen with a light beige, slightly textured surface. The number 'A3' is handwritten in black on the top surface.</p>	 <p>The specimen after exposure to acid rain, showing surface erosion and a porous, irregular texture with exposed aggregate.</p>

Due to high concentration of  $H^+$  ions, corrosion due to acid rain solution occurs rapidly on the surface of samples, leading to the failure of cementitious material. Simulated acidic solution severely damaged the samples and the deterioration was significant for all specimens. White crystals identified on the surface of the tested samples A0, A2 and A3 were related to various calcium sulfates. For the sample A1 with zeolite, white to yellow rough-surfaced compounds were detected. Simultaneously, the aggressive solution damaged the cement binder and exposed the coarse aggregates of samples.

### 3.2 Absorbability

Absorbability of concrete specimens before and after the simulated acid rain experiments is given in Fig. 1.

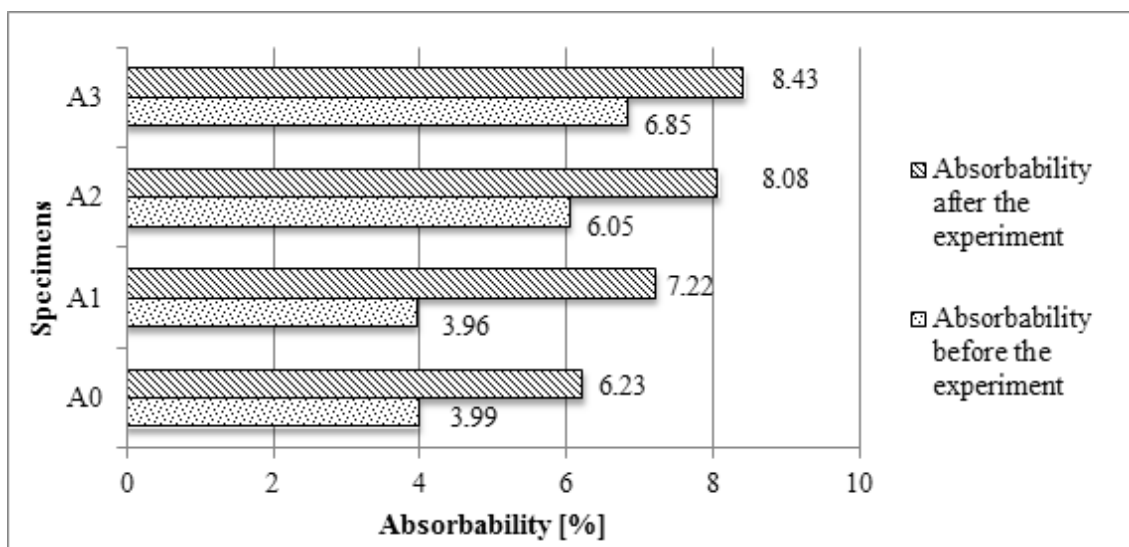


Figure 1: Absorbability of concrete specimens

The absorbability test performed on concretes with different supplementary cementitious materials proved an increase in water absorption for all tested samples after the simulated acid rain exposition. Table 3 shows the percentage increase in absorbabilities of concretes after 7 weeks long corrosion experiment.

Table 3: Change in absorbability after acid rain exposition

Concrete sample	A0	A1	A2	A3
Change in absorbability [%]	2.24	3.26	2.03	1.58

The highest absorbability was observed for sample A3 with blast furnace slag, however the change in absorbability prior and after the acid exposure was the lowest among all the specimens (1.58 %). Sample A1 made with zeolite showed highest change after the corrosion experiment (3.26 %).

### 3.3 Leachability of $\text{Ca}^{2+}$ and $\text{Si}^{4+}$ ions

Fig. 2 presents the leaching trends  $\text{Ca}^{2+}$  ions of concrete samples during the acid rain corrosion experiment.

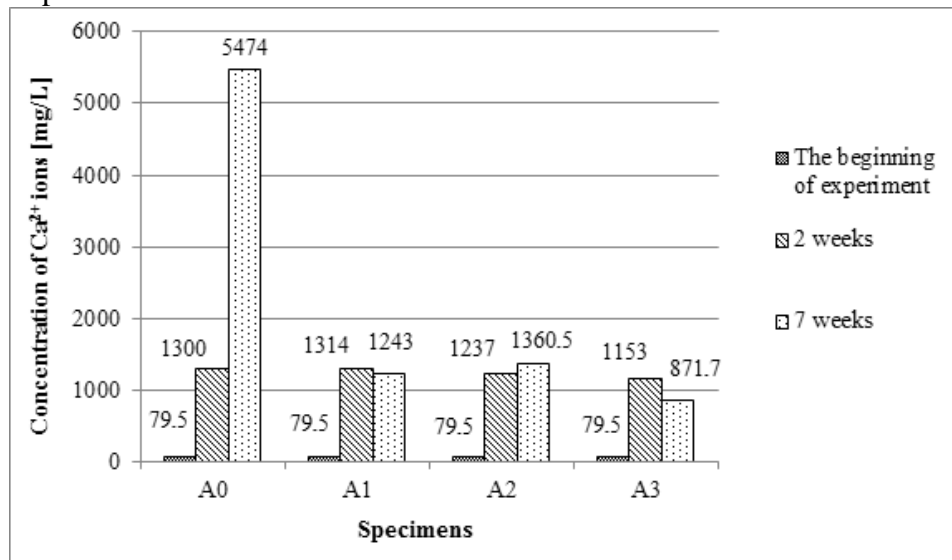


Figure 2: Concentration of dissolved calcium ions of concrete specimens during 7 week long acid rain exposure

The highest amount of leached  $\text{Ca}^{2+}$  ions was observed after 7 weeks of exposure (5474 mg/L) for the reference sample A0 made with ordinary Portland cement. Leaching trends of samples A0 and A2 were similar throughout the corrosion experiment, where the concentration of calcium ions increased with time. However leaching of  $\text{Ca}^{2+}$  ions of samples A1 and A3 had different course, where after 7 weeks the concentration of calcium ions decreased in comparison with the concentration after 2 week long period. The decrease in leached amounts of calcium ions for samples A1 and A3 after 7<sup>th</sup> week could be likely connected with stronger formation of crystal compounds on the surface of concrete samples. Concentration of leached-out  $\text{Si}^{4+}$  ions is presented in the Fig. 3.

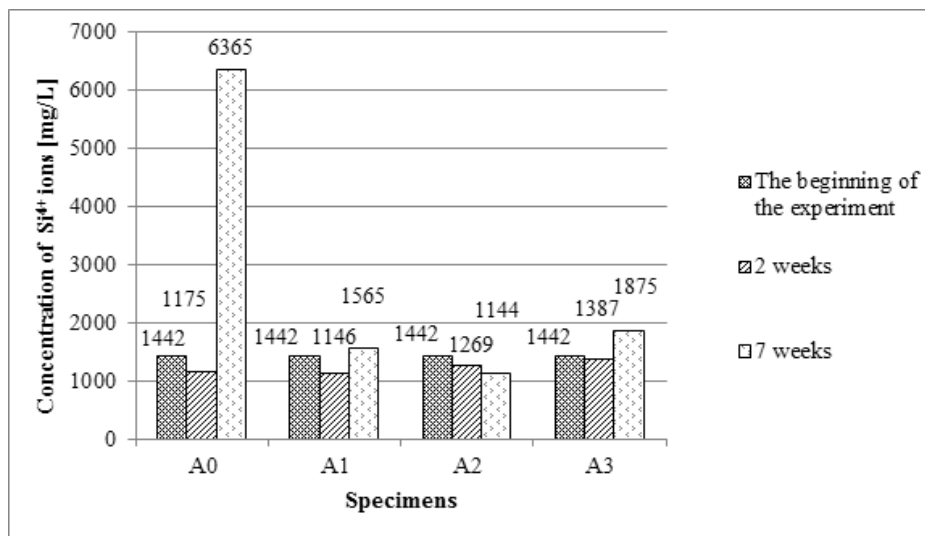


Figure 3: Concentration of dissolved silicon ions of concrete specimens during 7 week long acid rain exposure

Similar to leaching trends of  $\text{Ca}^{2+}$  ions, the leaching of  $\text{Si}^{4+}$  ions was the most intensive for reference sample A0 after the 7<sup>th</sup> week of acid rain corrosion (6365 mg/L). Trends of leached-out silicon ions were the same for samples A0, A1 and A3, where the highest leached-out concentrations of  $\text{Si}^{4+}$  ions were observed after the end of corrosion experiment. Sample A2 with incorporated fly ash had opposite leaching trends of silicon ions, with the maximum leached-out  $\text{Si}^{4+}$  ions at the beginning of experiments.

#### 4 Conclusion

This paper was focused on evaluation of durability of concrete samples with incorporated supplementary cementitious materials (zeolite, fly ash and blast furnace slag) exposed to simulated acid rain environment during a period of 7 weeks. To predict the degradation effect of acid rain on concrete samples, characteristics like absorbability, leaching of basic inorganic elements ( $\text{Ca}^{2+}$  and  $\text{Si}^{4+}$  ions) and visual changes were determined. From the obtained results following conclusions can be drawn:

- The aggressive effect of simulated acid rain environment was confirmed in relation to all studied parameters.
- The concrete specimens show a steady rate of increased absorbability when exposed to the acid rain solution. The increased absorbability goes up gradually with the increase of immersion time, and the most durable sample was the sample with blast furnace slag.
- The leaching trends confirmed the degradation effect on all tested samples. The most durable sample considering leached-out calcium and silicon ions was found to be sample with fly ash.

To give a clear conclusion about the durability of the concrete samples made with different supplementary cementitious materials, more research considering higher substitution of pozzolanic materials and testing mechanical parameters like compressive and flexural strengths or porosity is needed.

## Acknowledgements

This research was funded by VEGA - Scientific Grant Agency of the Ministry of Education, Science, Research and Sport of the Slovak Republic and the Slovak Academy of Sciences, grant number 1/0648/17.

## References

- [1] Zhou, C., Zhu, Z., Wang, Z., & Qiu, H. (2018). Deterioration of concrete fracture toughness and elastic modulus under simulated acid-sulfate environment. *Constr. Build. Mater.* 176, 490-499. DOI: 10.1016/j.conbuildmat.2018.05.049.
- [2] Chen, M. C., Wang, K., & Xie, L. (2013). Deterioration mechanism of cementitious materials under acid rain attack. *Eng. Fail. Anal.* 27, 272-285. DOI: 10.1016/j.engfailanal.2012.08.007.
- [3] Fan, Y. F., & Luan, H. Y. (2013). Pore structure in concrete exposed to acid deposit. *Constr. Build. Mater.* 49, 407-416. DOI: 10.1016/j.conbuildmat.2013.08.075.
- [4] Mahdikhani, M., Bamshad, O., & Shirvani, M. F. (2018). Mechanical properties and durability of concrete specimens containing nano silica in sulfuric acid rain condition. *Constr. Build. Mater.* 167, 929-935. DOI: 10.1016/j.conbuildmat.2018.01.137.
- [5] Zhao, S., & Sun, W. (2014). Nano-mechanical behavior of a green ultra-high performance concrete. *Constr. Build. Mater.* 63, 150-160. DOI: 10.1016/j.conbuildmat.2014.04.029.
- [6] Rozière, E., Loukili, A., El Hachem, R., & Grondin, F. (2009). Durability of concrete exposed to leaching and external sulphate attacks. *Cement Concrete Res.* 39(12), 1188-1198. DOI: 10.1016/j.cemconres.2009.07.021.
- [7] Fan, Y. F., Hu, Z. Q., Zhang, Y. Z., & Liu, J. L. (2010). Deterioration of compressive property of concrete under simulated acid rain environment. *Constr. Build. Mater.* 24(10), 1975-1983. DOI: 10.1016/j.conbuildmat.2010.04.002.
- [8] Okochi, H., Kameda, H., Hasegawa, S. I., Saito, N., Kubota, K., & Igawa, M. (2000). Deterioration of concrete structures by acid deposition—an assessment of the role of rainwater on deterioration by laboratory and field exposure experiments using mortar specimens. *Atmos. Environ.* 34(18), 2937-2945. DOI: 10.1016/S1352-2310(99)00523-3.
- [9] Zivica, V., & Bajza, A. (2001). Acidic attack of cement based materials—a review.: Part 1. Principle of acidic attack. *Constr. Build. Mater.* 15(8), 331-340. DOI: 10.1016/S0950-0618(01)00012-5.
- [10] Paris, J. M., Roessler, J. G., Ferraro, C. C., DeFord, H. D., & Townsend, T. G. (2016). A review of waste products utilized as supplements to Portland cement in concrete. *J. Clean. Prod.* 121, 1-18. DOI: 10.1016/j.jclepro.2016.02.013.
- [11] Slovak Office of Standards, Metrology and Testing. (2017). Concrete. Specification, performance, production and conformity. STN EN 206+A1. Bratislava.
- [12] Slovak Office of Standards, Metrology and Testing. (1989). Determination of moisture content, absorptivity and capillarity of concrete. STN 73 1316. Bratislava.
- [13] Estokova, A., Smolakova, M., & Luptakova, A. (2018). Calcium Extraction from Blast-Furnace-Slag-Based Mortars in Sulphate Bacterial Medium. *Buildings* 8(1), 9. DOI: 10.3390/buildings8010009.

## Verification of building environmental assessment system for houses

Iveta Selecká, Silvia Vilčeková, Andrea Moňoková

Technical University of Košice, Slovakia  
Civil Engineering Faculty, Institute of Environmental Engineering  
e-mail: iveta.selecka23@gmail.com, silvia.vilcekova@tuke.sk, andrea.monokova@tuke.sk

### Abstract

Sustainable construction and its architecture of buildings seeks to minimize the negative environmental impact of buildings by efficiency in the use of materials, energy, and development space and the ecosystem at large. Sustainable buildings use a conscious approach to energy and ecological conservation in the design of the built environment in cities. This article is devoted to the environmental assessment of three family houses which represent three different material and design solutions. The houses were evaluated through the Slovak building environmental assessment system (BEAS), which has been developed for Slovak conditions at the Faculty of Civil Engineering, TUKE. This study shows that the influence of green design, compared to traditional construction, is important and more beneficial for the practice of designing sustainable buildings. It creates the most comprehensive relationship between the building and its environment and significantly affects building sustainability.

**Key words:** House, environmental assessment, BEAS

## 1 Introduction

The high-energy consumption of the construction industry and its associated environmental pollution have become a global challenge. Cities and their buildings result in huge environmental impacts which are critical to reduce. Although the concept of green building (GB) is growing rapidly, the primary emphasis has been on energy-saving design. However, little attention is focused on sustainable post-occupancy operations in buildings. The study [1] presents a developed comprehensive quantitative method which analyzes stakeholder impact during GB post-occupancy evaluation (POE). Results of this study help clients and design teams improve their building designs by integrating the views of stakeholders through the POE for the design of green buildings. However, some of the studies about green buildings focus on either design building requirements or building materials. Those studies use the approach of spatially modeling building stocks and quantifying their embodied environmental requirements. Therefore, this model helps cities quantify and evaluate material and

environmental flows, better manage building stocks, as well as reduce embodied environmental requirements over time [2]. The adoption of the eco-design approach can be a turning point for strategies of the construction sector. The study [3] aims to investigate factors but also drawbacks that drive designers in the implementation of eco-design. Results reveal that designers have also a high environmental sensitivity, but a systematic adoption of the eco-design approach is still far. Therefore, it is necessary to foster the inclusion of energy and environmental criteria in the building design and certification schemes. The promotion of green building needs evaluation standards and technical support. Many countries have issued a series of green building evaluation standards since 1990, and currently there are some representative green building assessment schemes. The study [4] compared the latest evaluation standards for green buildings in China, Britain and United States from five aspects, including energy-saving, water-saving, material-saving, site selection and the outdoor and indoor environmental quality. In order to study the environmental impact of green building development policies, a “Green Building Eco-environment (GBE)” model was constructed and presented in the study [5]. A model is constructed with the method of system dynamics and implemented using Vensim software. The model is used to simulate and evaluate the current state and future trend of variation of the eco-environmental impact of green building development during the years 2008–2050 under current green building development policies. Some policy factors are adjusted in the simulation to determine the optimal green building development policies. Life cycle assessment (LCA) is considered as the most suitable way to assess the environmental impact of buildings. The evaluation needs methodological simplifications of building LCA and the usability of LCA, which are based on EIA software tools during the design process [6]. For life cycle assessment for building energy refurbishment projects, there is a general focus on the operational stage, linked to the main objective of reducing operational energy use. The study [7] evaluates the relevance of each life cycle stage in relation to the overall environmental and economic impact on residential building energy refurbishment projects. Another study [8] once again integrates building information modeling (BIM) with life cycle assessment (LCA) and presents the outcome of multi-storey office building in evaluating environmental impacts of building materials. Most of the negative environmental impacts are occurring during the manufacturing and operation phases. Therefore, this integration encourages reviewing the application of building materials in order to reduce the passive contribution to the environment. As for green buildings, the case study [9] focuses on the analysis of the embodied carbon of building envelopes, especially for aluminum-based curtain wall systems. Standardized methods and databases that better represent the variations in embodied carbon emissions based on the local recycled content, manufacturing process, and energy mix are much needed. The accuracy of environmental performance assessment methods is highly important. However, obtaining accurate results require taking into account the variables that affect the environmental assessment presented in another study [10]. These variables include for example the impact of natural and human changes that occur periodically (the repetition of certain events according to day, month, and year), sequentially (changes over time), and suddenly (disasters and other unexpected events) and are not addressed in current assessment methods. This study proposes an approach for considering the effects of variables with which higher accuracy in evaluation results can be achieved.



This paper aims to present results of a case study which evaluates three family houses designed with various material and construction solutions through the Slovak building environmental assessment system (BEAS).

## 2 Characteristics of low-rise residential family houses and methods

For the environmental evaluation of three new family houses (FH1, FH2 and FH3), the Slovak building environmental assessment system (BEAS) was selected. The houses are located in the north part of the town of Kosice and in the center of Rozhanovce, in the Slovak Republic (Figure 1). The selection of the family houses has taken into account some important requirements. According to the urban zoning plan of the city Kosice, family houses are located in low-rise residential areas. The building locations are not in the floodplain of Kosice [11]. The territories where the family houses are situated are approximately the same quality level of environment. The areas are characterized by mild to severe territorial conditions for construction. The construction sites have different configurations of the terrain.






Figure 1: Location of selected family houses in Slovakia (Google Maps 2019)

Family houses designed as two-storey buildings without basement with flat roof were selected for evaluation. The family houses are designed with various material and construction solutions. The first family house FH1 is designed with bricks, and it has built-up area of 214.5 m<sup>2</sup>; the useful floor area is 339.9 m<sup>2</sup>, and the built-up volume is 1569.2 m<sup>3</sup>. The second family house FH2 is designed as a concrete construction in combination with porous concrete blocks, and it has a built-up area of 106.8 m<sup>2</sup>; the useful floor area is 202.6 m<sup>2</sup>, and the built-up volume is 618.1 m<sup>3</sup>. The third family house FH3 is designed as wooden construction, and it has a built-up area of 145 m<sup>2</sup>; the useful floor area is 127.97 m<sup>2</sup>, and the built-up volume is 441.3 m<sup>3</sup>. The heating systems of the family houses are designed as floor and wall heating or radiators by gas condensing boiler with an additional fireplace or solar system for house FH3. The houses FH1 and FH2 have natural ventilation, and the house FH3 has mechanical ventilation with heat recuperation. The family houses are connected to engineering networks such as electrical, gas, water connection and sewage connection or cesspool for house FH3.

These new family houses are designed according to the requirements of laws and standards of EU and Slovak Republic. These houses have been occupied approximately for 3 years from the end of the construction. Building characteristics and other information about the evaluated family houses are presented in Table 1.

Table 1: Building material solutions of family houses

Family house	Design and construction of evaluated family houses
<p style="text-align: center;"><b>FH1</b></p> 	<p><b>Foundations:</b> reinforced concrete foundation strip; <b>External walls, surface finishes:</b> bricks (300 mm) with exterior silicate plaster, stone facing; <b>Ceiling structures:</b> reinforced concrete slabs (200 mm); <b>Roof construction, roof covering:</b> flat roof, gradient made of polystyrene concrete (60–200 mm), roof cladding — river gravel; <b>Interior walls, surface finishes of walls:</b> bricks (250 mm) and aerated concrete blocks (100–150 mm) with lime-cement plasters and ceramic tiles; <b>Floor and ceiling surface finishes:</b> <i>floors</i> — wooden floor, ceramic tiles, cement screed, composite boards, <i>ceilings</i> — plasterboard; <b>Insulations of ground floor, external walls and roof:</b> <i>ground floor</i> — 2× waterproofing PVC, separating PE foil, mineral wool (80 mm), <i>external walls</i> — mineral wool (100 mm), <i>roof</i> — extruded polystyrene (2×100 mm); <b>Windows:</b> wood windows with triple glazing with horizontal aluminum exterior blinds.</p>
<p style="text-align: center;"><b>FH2</b></p> 	<p><b>Foundations:</b> reinforced concrete foundation strip and reinforced concrete bearing wall (400 mm); <b>External walls, surface finishes:</b> reinforced concrete wall (400 mm); aerated concrete blocks (300 mm) with exterior silicate plaster, stone facing; <b>Ceiling structures:</b> reinforced concrete slabs (200 mm); <b>Roof construction, roof covering:</b> flat roof, roofing foil; <b>Interior walls, surface finishes of walls:</b> porous concrete blocks (250 mm) and blocks (150 mm), lime plasters and ceramic tiles; <b>Floor and ceiling surface finishes:</b> <i>floors</i> — laminate floor, ceramic tiles, <i>ceilings</i> — lime plasters, plasterboard; <b>Insulations of ground floor, external walls and roof:</b> <i>ground floor</i> — 2× waterproofing PVC, separating PE foil, expanded polystyrene (100 mm), <i>external walls</i> — expanded polystyrene (100 mm), <i>roof</i> — expanded polystyrene (150 mm); <b>Windows:</b> plastic windows with triple glazing with horizontal aluminum interior blinds.</p>
<p style="text-align: center;"><b>FH3</b></p> 	<p><b>Foundations:</b> reinforced concrete foundation strip; <b>External walls, surface finishes:</b> wooden construction (400 mm); chipboard (OSB boards), <b>Ceiling structures:</b> reinforced concrete slabs (60 mm) and wooden beams (200 mm); <b>Roof construction, roof covering:</b> flat roof covered with soil (300 mm), counter roof — gravel (50 mm), OSB boards (25 mm); <b>Interior walls, surface finishes of walls</b> — reinforced concrete wall (200 mm), porous concrete walls (150 mm), plasterboard, ceramic tiles; <b>Floor and ceiling surface finishes:</b> <i>floors</i> — wooden floor, ceramic tiles, <i>ceilings</i>—plasterboard; <b>Insulations of ground floor, external walls and roof:</b> <i>ground floor</i> — 2× waterproofing PVC, PE foil, expanded polystyrene (300mm), sand (300 mm), <i>external walls</i> — mineral wool (200 +200 mm), <i>roof</i> — stone wool (100+140 mm), expanded polystyrene (150 mm), mineral wool (100+100+200 mm); <b>Windows:</b> wooden windows with triple glazing with horizontal aluminum and wooden exterior blinds.</p>

The selected family houses were assessed with the building environmental assessment system (BEAS) developed at the Institute of Environmental Engineering at the Technical University of Kosice. The family houses were evaluated in six main fields such as: A-Site Selection and Project Planning; B-Building Construction; C-Indoor Environment; D-Energy Performance; E-Water Management and F-Waste Management. The main fields are divided into individual indicators, where each indicator is assigned a certain weight of significance and is defined by the purpose of evaluation and by a criterion according to which the assessment is made. The methodology and criteria for evaluating the individual indicators in individual fields (A–F) are presented in the studies [12, 13].

### 3 Results and discussion

#### 3.1 Site selection and project planning

Field A is divided into 14 indicators A1–A14. Evaluation of field A takes into account selection of the site for construction in relation to vulnerability to flooding, selection of brownfield areas, for possibilities of connection to engineering networks and exploitation of renewable energy sources. This field assesses site selection in relation to distance to road-traffic infrastructure, city amenities and natural green spaces as well as the occurrence of transport infrastructure in the construction site. The buildings were evaluated for their appropriate architectural design and compatibility of the urban design with local cultural values in given area [13]. In Figure 2, we can see the summary of results of indicators A1–A14.

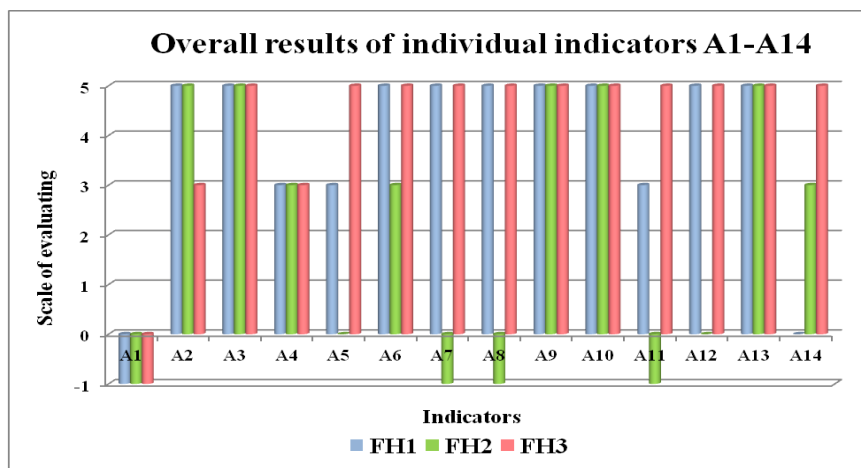


Figure 2: Summary of results of assessing family houses in field A

Indicator A1 reached a negative score (–1) for all three houses. The territories where the family houses are situated are, according to environmental regionalization of Slovakia, strongly disturbed environments (Environmental regionalization of Slovakia, 2018). Indicators A2 and A3 reached a high score because the family houses are not located either in the flood territory or nearby the potential recipient. The family houses are located in a dense built-up area and reached score 3. The houses FH1 and FH3 are located in the center of a built-up area, and this location has city amenities (road-traffic infrastructure, commercial and

cultural facilities, sport and active recreation) and public or natural green space. The distance of the family houses to city amenities and green spaces is between 500 to 800 m, and they reached score from good (3) to best (5). The house FH2 is located in a peripheral part of Kosice city, and its distance is more than 1000 m. This house reached low score (from –1 to 3). Indicators A9, A10 and A13 reached the best score (5) for all houses. The locations of the houses have the possibility of connection to all engineering networks (water and sewage connections, electricity and gas connections), the locations have a possibility to use up to three systems of renewable energy sources (solar panels, photovoltaic panels, heat pumps), and the assessed houses are located near local or tertiary roads. The family houses FH1 and FH3 use passive solar gains by the appropriate orientation of building, and indicator A11 reached high score (from 3 to 5). The percentage area of the glazed surfaces of houses oriented on the southeast, south, southwest, west was ranging from 51 to 81%. The lowest score (–1) was reached by house FH2 because the percentage area of the glazed surfaces is only 41%. The family houses FH1 and FH3 fully respect compatibility with cultural values relating to urban design and architecture in the given locality and reached the highest score (5) for indicator A12. Indicator A14 aims at ensuring minimum percentage of green areas, and it achieved various scores for all houses. The house FH1 ensures minimum percentage of green spaces of the total land area (60%), and therefore it achieves score 0. The houses FH2 and FH3 ensure more as minimum percentage of green spaces of the total land area. The house FH2 (71%) achieves score 3, and the house FH3 (82%) achieves score 5. In this field A, the family houses FH1 and FH3 reached most of the high scores for individual indicators. These houses have better architectural design, better site in relation to their construction, distance of site to road-traffic infrastructure and city amenities, as compared to the house FH2.

### 3.2 Building construction

The field B is focused on environmentally friendly building materials and structures to reduce energy and material flows during the entire building life cycle. This field of assessment system deals with building product environmental labelling, use of local, recycled, natural materials in the building as well as the radioactivity of the building materials. Primary energy embodied in building materials, global warming potential and acidification potential are assessed within the building life cycle [13]. A summary of results of individual indicators B1.1–B2.2 is presented in Figure 3.

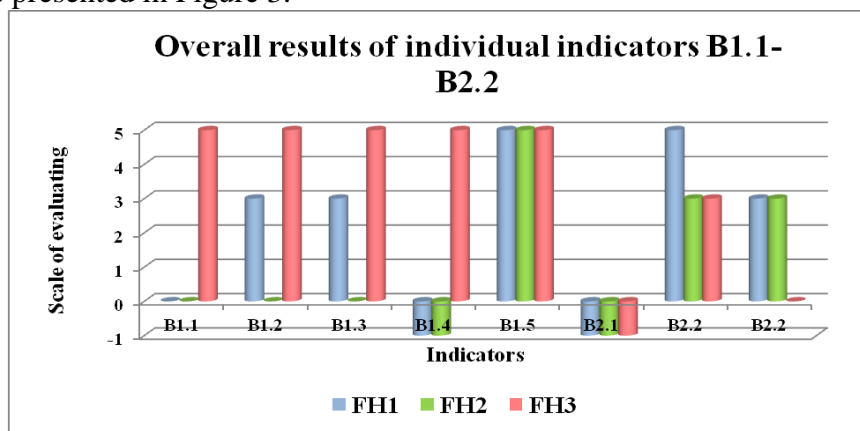


Figure 3: Summary of results of assessing family houses in field B

The family house FH3 reached the highest score (5) for indicator B1.1 because it has more than 50% share of built-in products (wooden parquets, wooden constructions, insulation from mineral wool) with the mark awarded by EPD, European flower, certified wood (FSC) and others. The houses FH1 and FH2 have less than 25% share of built-in environmentally labelled construction products, and they reached score (0). Indicator B1.2 achieves the highest score (5) for the house FH3 because the distance of the location of manufactured building materials to the construction site is up to 200 km. The house FH1 achieves score (3) (distance is 380 km), and the house FH2 achieves score (0) (distance is 520 km). The house FH3 has built-in construction products whose recyclable share in the given building materials is more than 50% (cement chipboard, wood floors, insulation materials), and it reached the highest score (5). The house FH1, with its recyclable share of 38.9% in the given building materials (polystyrene concrete, extruded polystyrene, mineral wool insulations), reached score (3). The house FH2 has the lowest recyclable share (20%) in the given building materials (insulation material underground parts of the external walls), and it reached score (0). The family houses FH1 and FH2 do not use natural materials, and they achieved the lowest score (-1) for indicator B1.4, except house FH3. The house FH3 is designed as a wooden construction with mineral insulation and particle boards, and the percentage share of natural materials is more than the 50%. This house achieved the highest score (5) for this indicator. All three family houses achieved the highest score (5) for the indicator B1.5. The declared mass activity of  $^{226}\text{Ra}$  of the built-in materials and products does not exceed 100 Bq/kg. The indicators B2.1, B2.2 and B2.3 assess the life cycle of building materials. The energy embodied in building materials is more than 2500 MJ/m<sup>2</sup> (3621.33 MJ/m<sup>2</sup> for FH1; 4536.43 MJ/m<sup>2</sup> for FH2; 6742.74 MJ/m<sup>2</sup> for FH3), and therefore this indicator achieved the lowest score (-1) for all assessed family houses. Global warming potential has value of CO<sub>2eq</sub> less than 300 kg/m<sup>2</sup> (240.57 kg/m<sup>2</sup> for FH1), and therefore this indicator achieved the highest score (5) for the family house FH1. The houses FH2 and FH3 have global warming potential value in the range of 301–500 kg/m<sup>2</sup> (338.41 kg/m<sup>2</sup> for FH2; 346.86 kg/m<sup>2</sup> for FH3), and those houses achieved score (3). The acidification potential achieved values of SO<sub>2eq</sub> ranged 0.5–1.5 kg/m<sup>2</sup> (1.038 kg/m<sup>2</sup> for FH1; 1.21 kg/m<sup>2</sup> for FH2). The houses FH1 and FH2 reached score (3) for this indicator. The house FH3 achieved a value for acidification potential in the range of 1.6–2.0 kg/m<sup>2</sup> (1.99 kg/m<sup>2</sup>), and it was assessed with score (0). Based on the overall assessment of the family houses in field B, the best score was reached by the house FH3. This house uses environmentally friendly products and has the highest percentage share of these built-in products, uses products from local sources, and has the most share of built-in recycled building materials and natural products. In terms of life cycle assessment, the house FH1 achieved the best rating.

### 3.3 Indoor environment

For evaluation of field C, the factors concerning IEQ are taken into account. These factors derive from the structural design of the building. This field of the assessment system is divided into 10 subfields in which there are assessed indicators such as thermal comfort during the heating season and cooling season, ventilation, noise attenuation, daylighting and artificial lighting, the materials used in the building and the transfer of pollutants [13]. A summary of the results of individual indicators C1–C10 is presented in Figure 4. The results show that for C1 and C2, the house FH3 meets the requirements according to Slovak standard

STN EN 15251:2007 in all living rooms during heating and cooling seasons. This house reached the highest score (5) for C1 and C2. The houses FH1 and FH2 achieved operative temperature value in range of ( $18 \leq \theta_o < 20 \text{ }^\circ\text{C}$ ) during heating season and achieved minimum requirements of the standard in some living rooms as well as for the cooling season. Those houses reached score (0) for indicators C1 and C2.

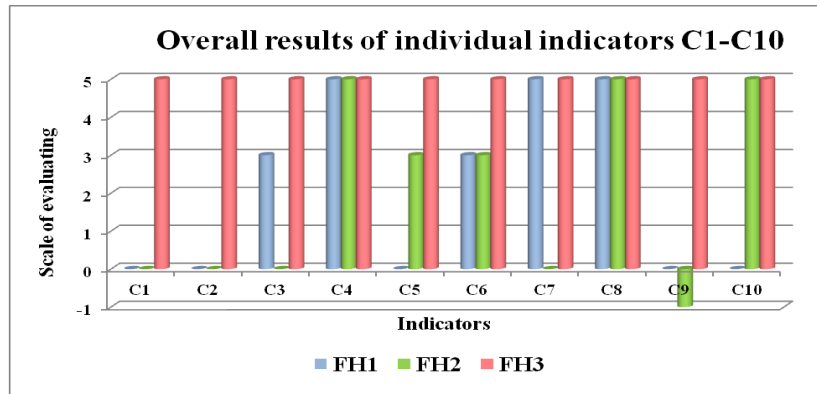


Figure 4: Summary of results of assessing family houses in field C

The houses FH1 and FH2, with natural ventilation, have total area of the openings at least 5% of the total floor area, and more than 50–75% of all the spaces have ventilation from the top down. Those houses reached score from 0 to 3 for indicator C3. In all spaces of house FH3 with mechanical ventilation, the minimum requirements of the standard are exceeded, and this house reached score 5. All family houses reached the highest score (5) for C4. The family houses meet the requirement of noise attenuation through the exterior envelope in residential areas of cities according to standard STN 73 0532 (quality class of sound insulation for windows is  $\geq 4$ ). The design of internal dividing structures in house FH3 exceeds the minimum requirements according to the standard for evaluation of noise attenuation between all rooms of the house, and therefore this house reached score 5. Noise attenuation between some rooms of the house FH2 exceeds the minimum requirements, and the house FH1 fulfills the minimum requirements of the standard. Those houses achieved low score. The design of glazed structures of all houses complies with the daylight requirements defined by STN 73 0532. The total area of windows is 2/10 of the room floor area of the assessed houses, and therefore the family houses reached score 3 for indicator C6. The houses FH1 and FH3 are designed with the most appropriate shielding elements (external wooden slats, external aluminum blinds with automatic control) for optimum indoor brightness, and these houses reached score 5 for indicator C7. The house FH2 is designed with minimum measures, and it achieved score 0. All evaluated family houses ensured a high level and quality of illuminance for the occupancy, and therefore score 5 was assigned for C8. For assessing of interior materials (indicator C9), the house FH3 reached the highest score (5) because all materials are with low or no emissions of TVOC. The houses FH1 and FH2 have more than 75% of materials which are selected as materials with a low release of TVOC emission. Those houses reached the lowest score (from -1 to 0). The family houses FH2 and FH3 achieved the highest score for indicator C10 because those houses have their garage placed out of the building. The house FH1 has a built-in garage which is ventilated but without CO<sub>2</sub> sensor, and it achieved score 0. In this field, the house FH3 meets all requirements for assuring high quality and comfort in an indoor environment.

### 3.4 Energy performance

Field D evaluates strategies of operational energy as energy for heating and domestic hot water, mechanical ventilation and cooling, light intensity control using artificial light sources and further strategies using active systems of renewable energy sources and energy management. These strategies, in connection with smart control of buildings, also reduce a building's energy use [13]. Figure 5 depicts the summary of results of individual indicators D1.1–D3.1.

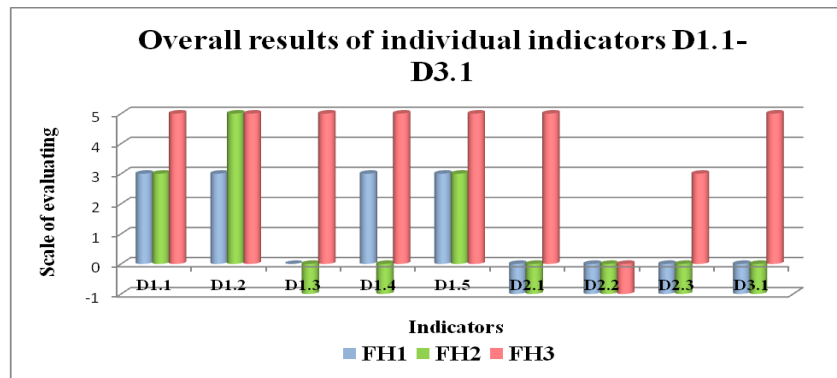


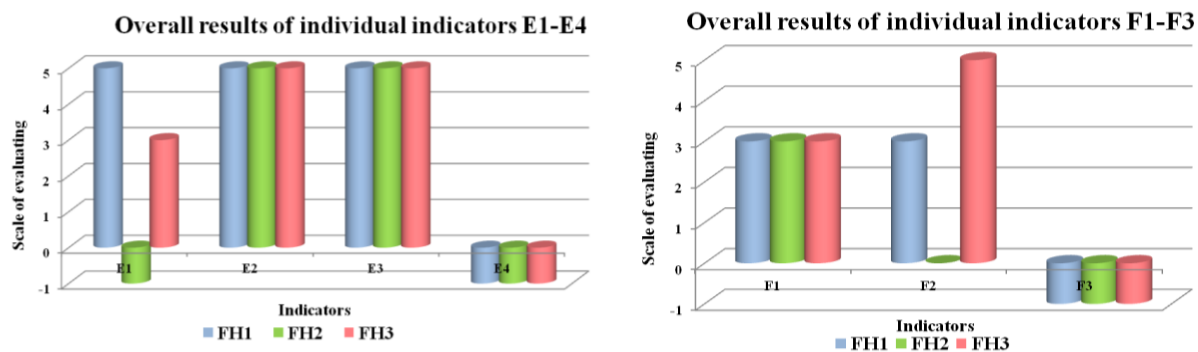
Figure 5: Summary of results of assessing family houses in field D

The family house FH3 achieved the highest score (5) for indicator D1.1 because it belongs to energy class A for heating according to the Law No. 555/2005 of the energy performance of buildings. The houses FH1 and FH2 are classified as energy class B for heating, and therefore they reached score 3. For indicator D1.2 that rates class of energy for domestic hot water according to the Law No. 555/2005 of the energy performance of buildings, the highest score (5) was achieved by the family houses FH2 and FH3 due to their classification to energy class A. The house FH1 belongs to energy class B, and it was evaluated with score 3. The house FH3 achieved the highest score (5) for indicator D1.3 because it uses a mechanical ventilation system with air treatment by recuperation. The lowest score (−1) was reached by the house FH2 because it does not use a mechanical ventilation system or cooling system; the house FH1 uses a cooling system only, and therefore it was evaluated with score 0. Regarding light intensity control (D1.4), the best score was reached for the houses FH3 and FH1 because light intensity control is ensured in the range of 75–100% of the occupancy areas in these houses. The house FH2 has not ensured light intensity control in the building. Indicator D1.5 evaluates the energy consumption by appliances used in houses. The energy class of all appliances in the assessed houses is in energy class A, and 1/3 of appliances are in energy class B. The houses reach scores in the range of 3 to 5. Indicators D2.1, D2.2 and D2.3 evaluate active systems using renewable energy sources. Only the house FH3 uses active solar cells for heating and hot water which covers more than 75% of energy consumption as well as heat recuperation which covers more than 75% of waste heat. This house obtained score in range of 3 to 5. The houses FH1 and FH2 do not use active systems with renewable energy sources, and they reached the lowest score (−1). Only the family house FH3 has a system of energy management into the three components established, and therefore it reached score of 5 for indicator D3.1. Based on the overall assessment of the family houses in field D, the best score was reached by the house FH3. This family house is classified as energy class A for heating and domestic hot water according to the Law No. 555/2005 of the energy

performance of buildings. The house FH3 uses systems with renewable energy sources and has installed control of light intensity in occupancy areas, which lead to a reduction of energy consumption. This house has established a system of energy management.

### 3.5 Water and waste management

The goals of evaluation of field E are to reduce drinking water consumption in buildings and to focused on conserving and reusing storm water. This field is divided into four subfields: regulation of water flow in devices, management of surface runoff, drinking water supply and use of system of grey water [13]. The field F is focused on minimizing the waste generated from construction, during the building occupancy, renovation and demolition of buildings and encouraging better management of waste. The field is divided into three subfields, which evaluate the plan of waste disposal originating in the construction process; measures to minimize wastes resulting from building operation and emissions resulting from air pollution sources [13]. The summary of results of individual indicators E1–E4 and F1–F3 is illustrated in Figure 6.



a) Field E

b) Field F

Figure 6: Summary of results of assessing family houses

The high score (from 3 to 5) for E1 is achieved by the family houses FH3 and FH1, which are those using high-quality equipment to reduce and control the water flow in the armatures and flush toilets. The house FH2 does not use devices for reducing and regulating water flow, and it reached the lowest score. All the family houses were assessed with the highest score for indicators E2 and E3. These houses ensure the capture of water from the surface runoff in a storage tank and use it for irrigation. This criterion E2 was met in all houses. The assessed houses are supplied with a sufficient amount of fresh water of a high quality. Criterion E3 was met in all houses. Indicator E4 reached the lowest level for all houses because the houses do not use a split potable and grey water system. The overall results show that the house FH1 has the best evaluation due to using devices for reducing and regulating water flow in building, ensuring trapped water from the surface runoff and using sufficient amount of drinking water of a high quality. In field F, the family houses have established a detailed waste management plan, and they reached score 3 for indicator F1. All the family houses ensured collection and separation of three to five components of municipal waste (paper, plastic, glass and metal and biodegradable waste). The family houses reached score 0 for FH2, score 3 for FH1 and score 5 for FH3. Indicator F3 was assessed with the lowest score (−1) due to a small source of air pollution (fireplace with solid fuel). The family house FH3 gained the best score due to



measures to minimize the waste generated from construction and during the building occupancy.

## 4 Results

From the overall assessment of family houses, it can be seen that the family houses obtained a total score ranging from 1.59 to 3.87. The lowest total score, with a value of 1.59, was achieved by the family house FH2, and it is certified as BEAS BRONZE. This house obtained the lowest rating in all assessed fields, especially in fields of B (1.28), D (1.03) and F (-0.59). Similarly, the family house FH1 is certified as BEAS BRONZE too, but with higher total score with value of 2.19. Although this house achieved low score in fields such as B (2.21), C (1.80), D (1.38) and F (1.64), the fields A (3.67) and E (3.51) were assessed with higher score. The best total score was achieved by the family house FH3 with a value of 3.87, and it is certified as BEAS GOLD. This house reached the highest rating in fields C (5.00), A (4.16) and D (4.10). A lower rating was obtained in fields such as B, E and F. Results of this study show that family houses (FH1 and FH2) designed from conventional and most commonly used building structures (brick, concrete) and without the use of renewable energy sources have been evaluated with lower scores due to conventional house design. Conversely, the wooden house (FH3) with appropriate architectural design and with built-in environmentally friendly building materials and active systems of renewable energy sources met the majority of sustainability requirements and reached higher score due to integrating an environmentally friendly approach and considering natural resources as part of the design.

## 5 Conclusion

The presented study shows that the influence of green design is important and more beneficial for the practice of designing sustainable buildings. The sustainable design of buildings and the fulfillment of sustainability criteria take into account the interdependence and interaction between the building and its environment. In the current of climate change, green building design is one of the important aspects to reduce the environmental impact of construction. To limit these impacts and to design environmentally and energy efficient buildings, sustainable requirements of green buildings must be understood and subsequently introduced and practiced. While the practices or technologies employed in green buildings are constantly evolving and may differ from region to region, the fundamental principles of sustainability persist. The basis of green building technology is an optimization of one or more of these principles of green design. Also, with the proper synergistic design, individual green building technologies may work together to produce a greater cumulative effect. Sustainable construction reduces the environmental impact of a building over its whole life cycle, while providing healthier and more comfortable living and working environments.

## Acknowledgements

This study was financially supported by Grant Agency of Slovak Republic (No. 1/0307/16).

## References

- [1] Li, H., Ng, S. T., & Skitmore, M. (2018). Stakeholder impact analysis during post-occupancy evaluation of green buildings — A Chinese context. *Building and Environment*. 128, 89–95. <https://doi.org/10.1016/j.buildenv.2017.11.014>.
- [2] Stephan, A. & Athanassiadis, A. (2017). Quantifying and mapping embodied environmental requirements of urban building stocks. *Building and Environment*. 114, 187–202. <https://doi.org/10.1016/j.buildenv.2016.11.043>.
- [3] Annunziata, A., Testa, F., Iraldo, F., & Frey, M. (2016). Environmental responsibility in building design: An Italian regional study. *Journal of Cleaner Production*. 112, 639–648. <https://doi.org/10.1016/j.jclepro.2015.07.137>.
- [4] Zhang, Y., Wang, J., Hu, F., & Wang, Y. (2017). Comparison of evaluation standards for green building in China, Britain, United States. *Renewable and Sustainable Energy Reviews*. 68, 262–271. <https://doi.org/10.1016/j.rser.2016.09.139>.
- [5] Teng, J., Wang, P., Wu, X., & Xua, C. (2016). Decision-making tools for evaluation the impact on the eco-footprint and eco-environmental quality of green building development policy. *Sustainable Cities and Society*. 23, 50–58. <https://doi.org/10.1016/j.scs.2016.02.018>.
- [6] Meex, E., Hollberg, A., Knapen, E., Hildebrand, L., & Verbeeck, G. (2018). Requirements for applying LCA-based environmental impact assessment tools in the early stages of building design. *Building and Environment*. 133, 228–236. <https://doi.org/10.1016/j.buildenv.2018.02.016>.
- [7] Oregi, X., Hernandez, P. & Hernandez, R. (2017). Analysis of life-cycle boundaries for environmental and economic assessment of building energy refurbishment projects. *Energy and Buildings*. 136, 12–25. <https://doi.org/10.1016/j.enbuild.2016.11.057>.
- [8] Najjar, M., Figueiredo, K., Palumbo, M., & Haddad, A. (2017). Integration of BIM and LCA: Evaluating the environmental impacts of building materials at an early stage of designing a typical office building. *Journal of Building Engineering*. 14, 115–126. <https://doi.org/10.1016/j.job.2017.10.005>.
- [9] Meneghelli, A. (2018). Whole-building embodied carbon of a North American LEED-certified library: Sensitivity analysis of the environmental impact of buildings materials. *Building and Environment*. 134, 230–241. <https://doi.org/10.1016/j.buildenv.2018.02.044>.
- [10] Shamseldin, A. K. M. (2017). Evaluate the continuity of meeting items requirements when assessing buildings environmentally. *HBRC Journal*. 13, 233–243. <https://doi.org/10.1016/j.hbrej.2015.05.003>.
- [11] Urban zoning plan city of Kosice. [accessed 2018 Dec 10]. [https://static.kosice.sk/files/manual/uha/up\\_2013\\_V-3.htm](https://static.kosice.sk/files/manual/uha/up_2013_V-3.htm).
- [12] Vilčeková, S., Čuláková, M., Křídlová Burdová, E., & Katunská, J. (2015). Energy and environmental evaluation of non-transparent constructions of building envelope for wooden houses. *Energies*. 8(10), 11047–11075. <https://doi.org/10.3390/en81011047>
- [13] Vilcekova, S., Selecka, I., Křídlova Burdova, E., & Meciariova, L. (2018). Interlinked sustainability aspects of low-rise residential family house development in Slovakia. *Sustainability*. 10(11), 3966–3966. <https://doi.org/10.3390/su10113966>

## Selected problems of thermal insulation of historical buildings

**Jana Katunská, Dušan Katunský, Veronika Labovská**

Technical University of Košice, Slovakia  
Faculty of Civil Engineering, Institute of Architectural Engineering  
e-mail: jana.katunaska@tuke.sk, dusan.katunsky@tuke.sk, veronika.labovska@gmail.com

### Abstract

There are problems with historical buildings when changing the thermal insulation properties of buildings. The Energy Efficiency Act exempted historic buildings from certification. Not all old, historic buildings have monument protection. It is necessary to take into account the above mentioned facts in case of renovation and reconstruction of an old building. Otherwise, a normal building is approached and a building of historical value is treated differently. Methods hidden insulation, which preserves the authenticity of cultural monuments and real estate in the heritage areas, is a current challenge of heritage practice. The sustainability of the operation of historic buildings ultimately means the preservation and appropriate use of the heritage fund. Fortunately, the list of such interventions that do not jeopardize the monumental values or the use of the building is gradually increasing. This is mainly due to modern, increasingly sophisticated materials and technologies. In this paper we offer a basic overview of the most frequently used and practice-tested interventions in historical buildings, but we focus on details.

**Key words:** historical building, thermal insulation, cultural monument, buildings renovation, cultural heritage

## 1 Introduction

An important fact that affects historical buildings after a certain period of their exploitation is their significant renovation. The direction of restoration is divided into research of new materials and the application of simulations, which are considered as a new means to better understand what will happen to the historic building after its repair. Their connection with in situ measurements is seen as an indispensable tool in examining the structure of historic buildings and designing their renovation more effectively [1].

Based on new energy requirements, historic buildings that are undergoing renovation must also show improved thermal insulation properties of packaging structures. Therefore, it must also deal with critical details here. Conformance values can be achieved by a variety of available means, including correct design and evaluation of critical details by simulation, possibly in combination with measurements. However, it is essential to respect the basic rules

on the historical value of a building, while respecting the essential requirements lay down by fundamental renovation procedures and good building research methods and practices [2].

Other key topics in this area are, in particular, research into the indoor environment in historic buildings, damage to historical artifacts due to moisture and heat [3].

Last but not least, the question of the joint spread of moisture and heat across the building and the use of simulation tools is essential [4]. When restoring a historic building, the condition is to use materials that have been verified and are known to affect a particular type of historic building material. Material verification is focused not only on the impact on the building structure, but also on improving its thermo-technical properties while eliminating possible failures. The alternatives and the suitability of the applied thermal insulation layer in terms of the protection of monuments are different [5]. The question of whether thermal insulation and the improvement of the thermo-technical properties of a historical building are needed is addressed by Meier [6].

## **2 Historical building and monument protection**

The term protection of historical monuments appeared in the 19th century. It was introduced in scientific circles by Georg Dehio in 1887. Thus, for the first time, the scientific company began to deal with the protection of historical building structures.

Among the most influential figures in this area was John Ruskin, who created a set of rules of architecture and stood up for preserving, not restoring historic buildings. William Morris also belongs to this category. His idea was that historical monuments and buildings should remain as they were handed over to us, our generation. They are to be a historical object and not a model. The founders of modern protection of historical monuments Alois Riegl, Max Dvořák - caused a shift from purism to more modern methods of care for historical and cultural monuments. The very term historical cultural monument expresses a selection group of movable and immovable things as important evidence of the historical development of society, its way of life and environment from the earliest times to the present. It is a manifestation of human creative work in various fields of human activity. The historical building structure carries a monumental value, which in addition to three-dimensional architectural elements also includes the fourth dimension - time.

Regulations regarding the function of the building, the authenticity of the restoration of architectural elements and the preservation of the original material composition are among the priorities in restoring the historic structure. The authenticity of the construction work is protected and must therefore be preserved. Therefore, the removal and unjustified replacement of historical materials should be excluded during the restoration.

Changes that have occurred over time on the building structure can also take on historical significance. They should therefore serve as an example of development and time layering. As recovery is considered to be a unique process, an individual approach to each monument is needed. The historical and architectural form is considered as the primary value. The content, i.e. the function, must be chosen appropriately, appropriately and largely adapted to the primary value. Otherwise, historical architecture is being rebuilt instead of restored. The decisive criterion is fair value. This includes not only the value of age, but also historical, social, landscape, urban, architectural, scientific, technical, and artistic craft value [6].

The conservation authorities strive to preserve not only architectural but also material substance. However, building materials change over time. Its properties change by changing the weather effects and their intensity. Over the years, the plaster loses the properties that it had or was required to produce and apply to the brick construction. This applies to all materials and therefore the question arises as to whether it is important to give preference to a historical substance or a historical construction. What is more valuable? It is worth considering whether in today's full development and research it is not appropriate to use modern materials and technologies to preserve historical construction [8].

### 3 Issues of thermal insulation in structures of historical buildings

The structure of historic buildings has one basic characteristic. It is a massive wall and also a large storage mass for storing thermal energy (accumulation). It is the value most influencing the thermo technical properties of the building structure. However, this is often neglected in stationary calculations. On the contrary, non-stationary methods can capture this influence (accumulation capabilities) as well as the effect of solar radiation, as well as all factors that affect the structure of the building. Taking them into account would bring some bonus to improving the thermal properties of the envelope structures of historic buildings. However, solar energy is only taken into account when calculating the total solar energy transmittance in the transparent part of the building structure. Taking into account its storage capacity, the building structure could meet the essential requirements even without the use of thermal insulation.

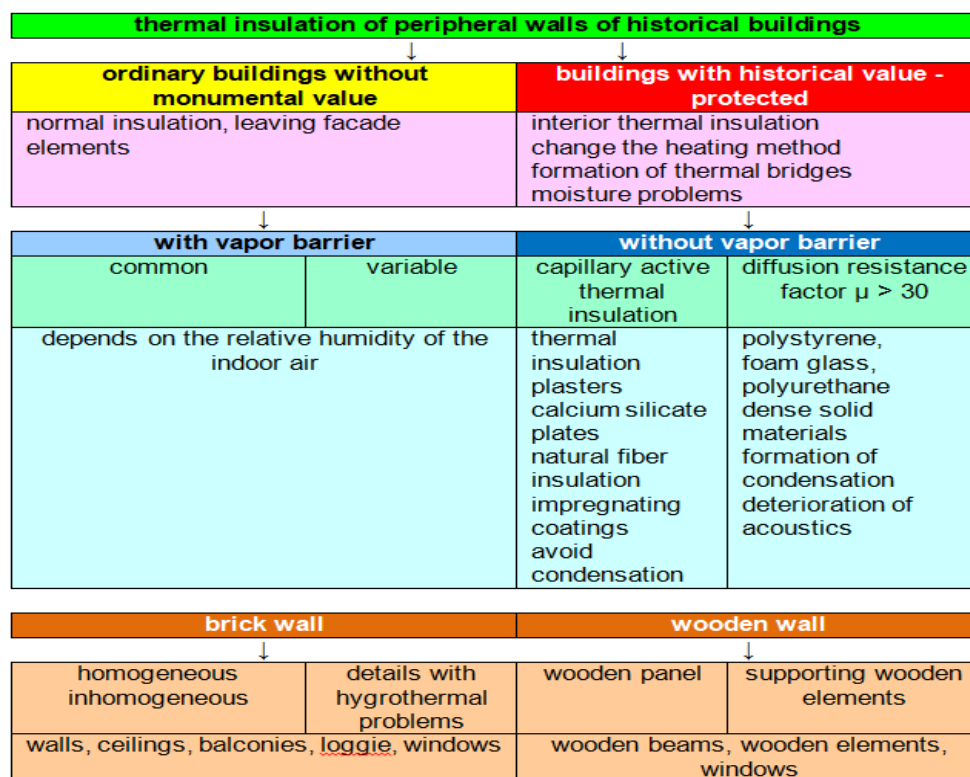


Figure 1: Scheme of building suitability for its renovation (advantages, disadvantages) own source:

At the time of construction of this type of building, people followed the basic rules of construction. They did not solve the problems of building physics; they did not know the term heat protection, energy recovery or high or low heat demand. The basic requirement was protection and durability. Today's requirements are stricter not only for new buildings but also for existing buildings.

Using measurement simulation programs allows us to create a real model using computer simulation. This gives us a better overview of the functioning of the building structure before and after the renovation. This in turn allows for more accurate and better design of measures to improve not only its thermal-moisture behavior, but also the improvement of the indoor climate and, above all, disruption of the centuries-old working environment of the structure.

### 3.1 Thermal bridges in historical building structures

The result of thermal bridges is a change in heat flow and a change in the internal surface temperature. A thermal bridge is defined by the standard STN EN ISO 10211 as part of a building envelope structure, where otherwise the same thermal resistance is changed due to the total or partial penetration of building materials of different thermal conductivity into the envelope structure. The change may also occur when the thickness of the material changes or the difference between the inner and outer surfaces, i.e. the joints of the walls, floors and tracks. Not only the labeling but also the evaluation of thermal bridges has changed in different time periods: "Their current definition is unambiguous, so it should be possible to minimize not only their occurrence, but also to minimize the consequences of their occurrence for existing buildings" (Sternová) [9].

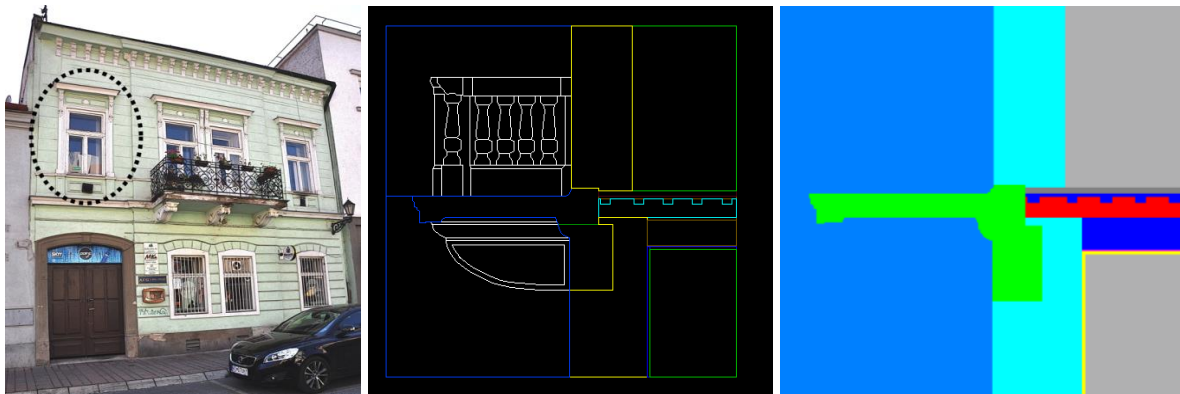


Figure 2: Preparation of bitmap for calculation of thermal bridge, balcony: authors

There are several types of thermal bridges. Thermal bridges can generally be divided into [9]:

- **structural**: changes in the perimeter of the building: balconies, arcades, brackets, etc.
- **material**: change of the thermal conductivity coefficient in one or more layers of the building structure
- **geometric**: change of shape, joints of building structures, more cooled (exterior) surface than heated (interior)
- **environmental-related thermal bridges**: various local surface temperatures or additional heat sources e.g. heaters on the perimeter wall
- **systematic**: design error repeated when building has the same type of others buildings
- **combined**: combination of several types of thermal bridges

The standards STN EN ISO 10211 and STN EN ISO 14683 divide thermal bridges in terms of heat loss and spatial action into:

- **linear thermal bridge:** thermal bridge that has identical cuts in one direction - it can be described by two-dimensional temperature field
- **point thermal bridge:** a concentrated thermal bridge that can be described by a three-dimensional temperature field

Thermal bridges occur at any point in the joint between parts of the building structure or at places where the structure of the building material changes.

### 3.2 Calculations and experimental measurements of thermal properties in situ

In addition to theoretical studies on the effects of non-stationary boundary conditions on the internal surface temperature, it is necessary to verify that the results of the numerical calculations are identical to the experimental measurements.

Experimental measurements in laboratory conditions often lead to completely different hygrothermal conditions in the building structure and do not reflect the actual behavior of the building structure in external and internal environmental conditions. For such types of measurements, it is often not possible to evaluate whether the measured values or structural changes are caused by thermal or moisture effects on the structure or by changes in the properties of building materials [6]. Therefore, we performed measurements of some selected thermal insulation properties of the peripheral wall of a historical building (see Figure 2) and its details.

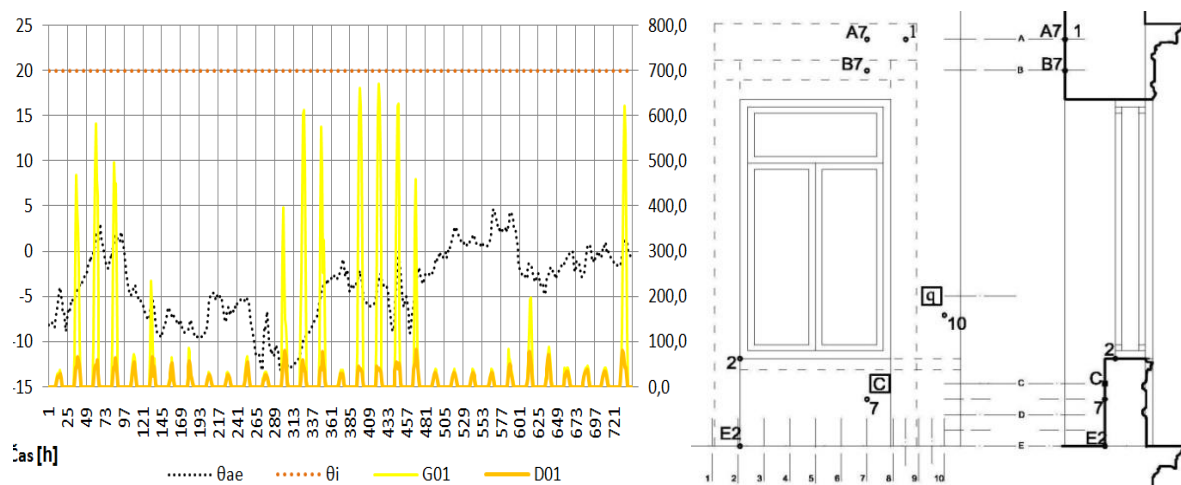


Figure 3: Measured of outside air temperature and intensity of solar radiation in evaluated period, monitored points in fragment of envelope structure – external wall fragment

In situ measurements allow us to record the effects of changes in the external and internal environment on the building structure itself. It reflects the real behavior of the building structure in conditions that are close to physical reality. Uncertainties in situ measurements are due to inaccuracies associated with defining input geometry, shape and material diversity, and defining boundary conditions. The influence of operating and weather conditions also plays an important role. Measurements of outdoor environment (temperature and intensity of solar radiation) were performed in January (see Fig. 3).

The purpose of the experimental measurement was to determine the effect of real non-stationary boundary conditions on the internal surface temperature of selected structures of the historic burgher house [7].

The selected monitoring points (Fig. 3) were deployed to take into account the expected critical points of the building structure. The measurement on the inner surface of the perimeter wall was short-term (7 days) performed in January (see Figure 4, 5). Due to the small number of monitored points, a network of horizontal and vertical axes was used to easily mark them.

The influence of moisture on the thermo-technical properties of building materials in historical buildings is taken into account by the increased value of the thermal conductivity coefficient in the numerical calculation [8].

The measurement itself consisted of recording the internal surface temperature using  $\theta_{si}$  temperature sensors and heat flux density plate's  $q$  ( $\text{W}/\text{m}^2$ ). The COMET sensor ( $\theta_{ai}$ ,  $\varphi_i$ ) was used to record indoor conditions. Data loggers were used to collect the measured data, which recorded the measured data with an hourly step.

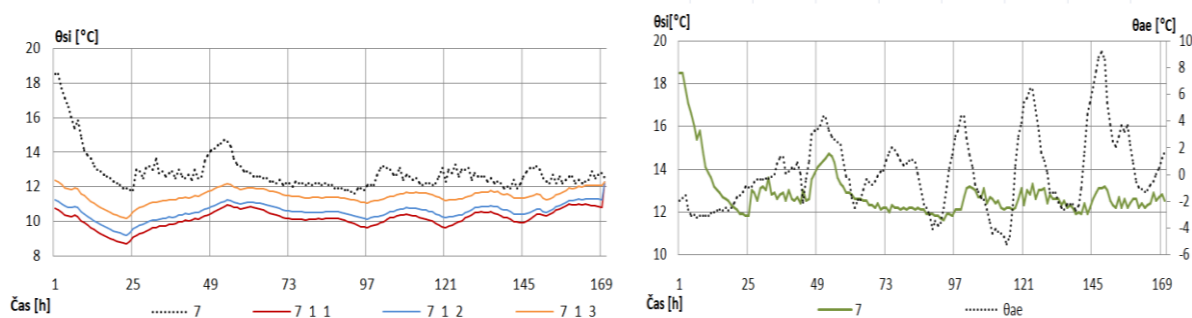


Figure 4: The course of surface temperature in fragment of the peripheral windowsill wall - calculated  
 Figure 5: The course of surface temperature in fragment of the peripheral windowsill wall - measured [7]

The differences in the average measured and calculated surface temperatures at the point of the receding window sill are in the range of 1 to 3 K. The difference is probably due to the hot water distribution system in the radiators. Unevenness of the sheathing is one of the possible causes of a small difference in the calculated and measured surface temperatures (0.2 K). Boundary conditions, especially the outside air temperature used in the simulation, can also significantly contribute to the inaccuracies of the numerical model [10].

The different altitudes and local boundary conditions of the external environment play an important role at ambient air temperature. Neglected sunlight can also affect the internal surface temperature and heat flux density. Numerical calculation of surface temperatures was performed for all details with standard values of resistance to heat transfer (STN EN ISO 10211, 2007). These values take into account the variability of heat transfer resistances and their dependence on many factors. From the calculated surface temperatures at the points evaluated, a difference can be seen using different values of resistance to heat transfer.

Calculations using computer simulations taking into account the non-stationary state at boundary conditions (Fig. 3) were performed for four points 1-4 of the window sill masonry (see Fig. 6). On the basis of the above, it is possible to assess the selected points in terms of thermal protection of a historic building and its hygienic criteria.



The surface temperature, calculated at a lower value of resistance to heat transfer, has fallen below 6 days out of a total of 30 days (period considered) below the hygiene criterion. In the case of higher resistance to heat transfer, the temperature dropped below 12.6 °C (red horizontal line) for almost 12 days. In both cases, window constructions are rated with lower heat transfer resistance. Nevertheless, the heat transfer resistance at the connection point increases to evaluate the opaque portion of the packaging structure.

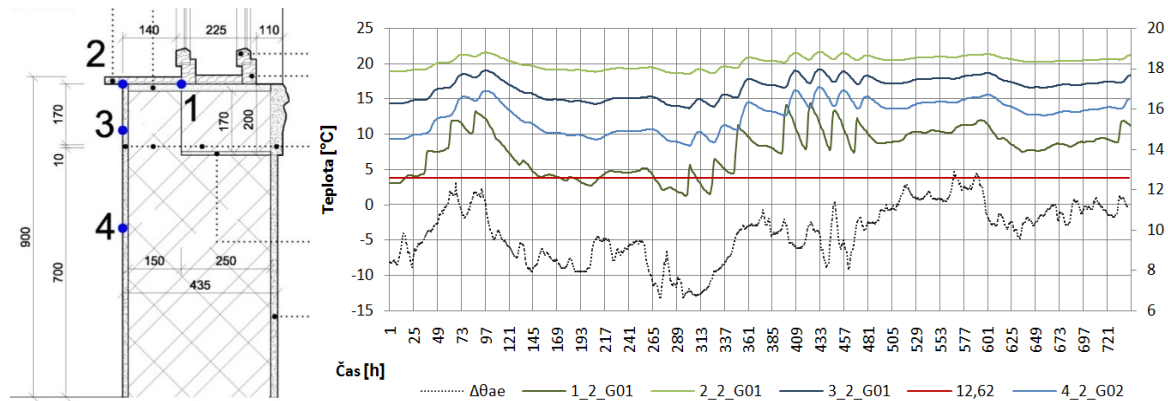


Figure 6: Diagram of building construction - window sill with points for non-stationary calculation 1-4  
Figure 7: Calculated temperatures on the inner window sill at points 1,2,3,4, and outside air temperature

Calculations with the help of computer simulations taking into account the non-stationary state [11] were performed for points on the parapet masonry of the perimeter wall. The masonry is receding.

A more significant increase in the surface temperature occurred under the influence of solar radiation (values higher than  $200\text{W/m}^2$ ). The influence of solar radiation on the building structure ranges from 0.3 to 0.6 K. The most significant effect of solar radiation is at the critical point (connection of the window structure) to the masonry area (point 1).

## 4 Conclusion

In the practice of heritage protection, we can try to prioritize the so-called “hidden forms” of insulation that do not in any way alter the authentic appearance of the historic buildings, their decoration or characteristic details.

Let us try to name at least some basic procedures, which by no means can be understood universally. When we mention the use of a thermal plaster or painting, we mean only places where it is acceptable from the point of view of preservation of historical values. There are a number of authentic structures on which no foreign action is involved: historical paving, gray brickwork, natural plaster colored in mass, textured surfaces, face stone, terrazzo, terracotta elements, natural or grained wood and the like. We have to take into account, that before each thermal insulation procedure, it is required to consult with a monument office employee [12]:

- Before any intervention, it is desirable to submit a thermo-technical assessment to an independent expert who is not interested in the construction supply. Only such an expert can estimate the actual intervention needed in terms of efficiency and cost,
- Give preference to thermal insulation of foundation structures below ground level from the outside,
- thermal insulation of the ground floor above the unheated basement and in contact with the terrain.

- Insulation of the ceiling above the top floor (suitable embankment),
- Removal of thermal bridges, for example by insulating the smooth surface of the lining to a minimum thickness so as not to alter the proportions of the building openings,
- Preservation, implementation of new double-glazed windows with a double frame, or at least the addition of simple windows with internal wooden lining.
- For thermal insulation of vertical external walls, it is preferable to use alternative thin-layer thermal insulations that do not exceed the thickness of the facade coating; today there are thermal insulation coatings on the market, which have been proven to reduce heat losses based on laboratory results. Such a solution is more affordable compared to a contact thermal insulation system when all plumbing products and flashing need to be replaced, which dramatically increase the final cost of the construction intervention,

### Acknowledgements

The paper presents partial research results of project VEGA 1/0674/18 “Theoretical and experimental analysis of architectural-structural shapes and fragments of building envelope structures designed for harsh weather conditions”.

### References

- [1] Zumoberhaus, M. (2009) Die Wärmedämmung von historischen Gebäuden aus bauphysikalischer Sicht, <http://www.heimatschutz.ch/zeitschrift>
- [2] Kastner, R. (2004) *Altbauen Beurteilen, Bewerten*. Stuttgart: Fraunhofer IRB Verlag,
- [3] Williams Portal, N.L. (2011) Evaluation of heat and moisture induced stress and strain of historic building materials and artefacts. Goteborg, Sweden, Master's Thesis.
- [4] Heim, D., (2009) Numerical analysis of heat and moisture transfer in historical ceramic masonry wall. Building Simulation, 11. International IBPSA Conference, Glasgow Scotland.
- [5] Matiašovský, P. Mihálka, P. (2012) Catalog of construction solutions for application of capillary active thermal insulation system on historical objects. Bratislava: Institute of Construction and Architecture of SAV, ISBN 978-80-971077
- [6] Meier, H.R. (2010) *Geschichte und Theorie der Denkmalpflege*: TU Dresden
- [7] Labovska, V. Katunsky, D. (2016) In situ monitoring of internal surface temperature of the historic building envelope. In: *Selected Scientific Papers - Journal of Civil Engineering*. Vol. 11, no. 1 (2016), p. 77-84. –ISSN 1338-9024
- [8] Künzle, H. (2009) *Bauphysik und Denkmalpflege*. 2., Erw. Aufl. Stuttgart: Fraunhofer-IRB-Verlag, ISBN 978-381-6780-472
- [9] Sternová, Z. (2006) *Atlas tepelných mostov*. Bratislava: Jaga, ISBN 80-807-6034-9.
- [10] Katunsky, D.; Zozulak, M.; Kondas, K.; Simicek, J. (2014) Numerical analysis and measurement results of a window sill. *Adv. Mater. Res.*, 899, 147–150.
- [11] Zozulak, M.; Vertal, M.-; Katunsky, D. (2019) The influence of the initial condition in the transient thermal field simulation inside a wall—. In: *Buildings*. Vol 9 (8), p. 1-15 [online]. - ISSN 2075-5309
- [12] Mokriš, R. Zatepl'ovanie historických budov – hádam nie! (2018), In: *Monumentorum tutela – Ochrana pamiatok* 27/2018, Dolis Goen Bratislava ISBN 978-80-89175-88-8

## Green roof in module of climate chamber

**Richard Baláž<sup>1</sup>, Jana Budzáková<sup>2</sup>, Denisa Dorinová<sup>3</sup>**

<sup>1</sup>Technical University of Košice, Slovakia

Faculty of Civil Engineering, Institute of Architectural Engineering

<sup>2</sup>Technical University of Košice, Slovakia, Faculty of Civil Engineering

<sup>3</sup>Cost estimator, COLAS Slovakia, a.s.

e-mail: richard.balaz@tuke.sk

### Abstract

The submitted article is devoted to the research of the green roofs located at Faculty of civil engineering of Technical University of Kosice. The aim of this research work is to improve the quality of integrated research of advanced building constructions with focusing on intelligent buildings and indoor technologies with respect on design and evaluation of design elements for the progressive buildings.

**Key words:** green roof, climate chamber

## 1 Introduction

The mentioned article is elaborated in two main sections. The first section of analysis subsists measurement of roof structure in climate cell, where the only disparity in the roof construction was the addition of a vapor barrier to part of the S2 roof arrangement. We came to the closure after evaluating and examining the result, that the roof construction has to be improved, as a result of summer, the temperatures on the waterproofing layer were high. We modernized the roof structure by installing a green roof layer module on the S2 roof structure (Figure 1). By this specified roof structure model, we are trying to reach elimination of expanding surface temperature on waterproofing layer in summer period, which is mentioned in second section of this article.



Figure 1: Situation of test chambers measure

After evaluating the measurements of the vegetation roof on the S2 roof structure, we have come to the conclusion that the vegetation roof with a 45 ° slope oriented to the south side needs irreparable irrigation during the summer months, which we have taken into account when designing the module of the vegetation roof for the roof structure S1 by adding it to the supporting structure of the vegetation roof gutter for storing water directly in the roof structure. / Figure 3).

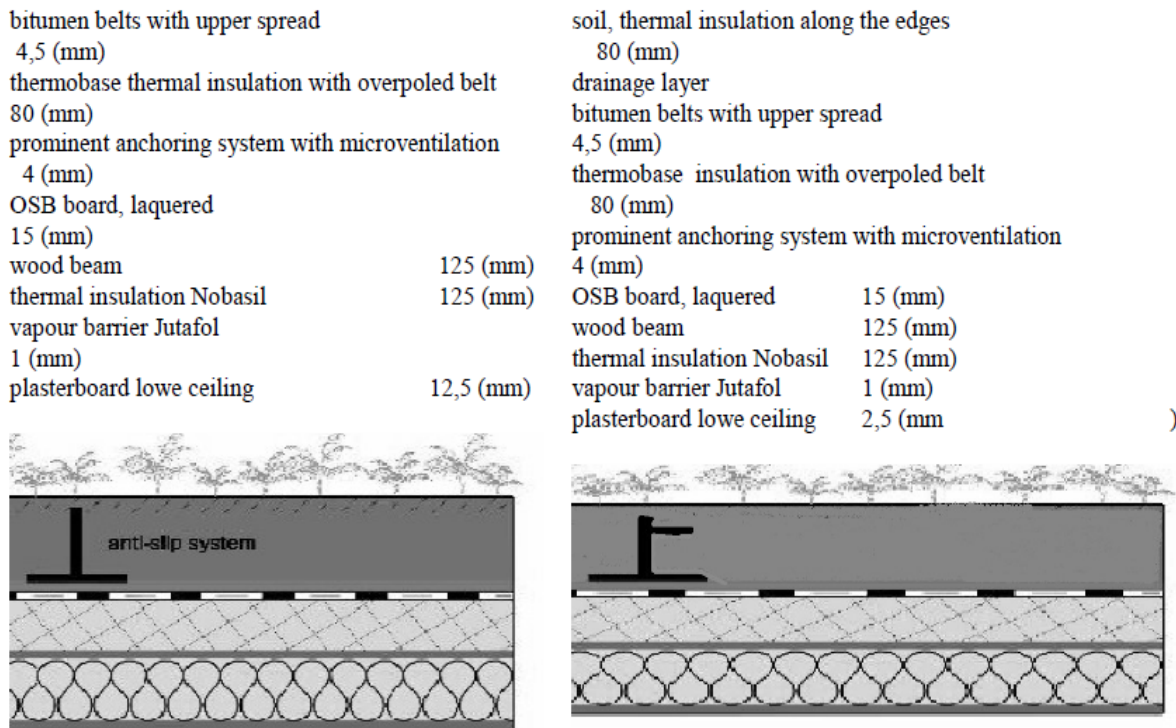


Figure 2: Roof layers' composition    Figure 3: Current roof layers' composition

Distribution and type of sensor in the test sample roof cover.

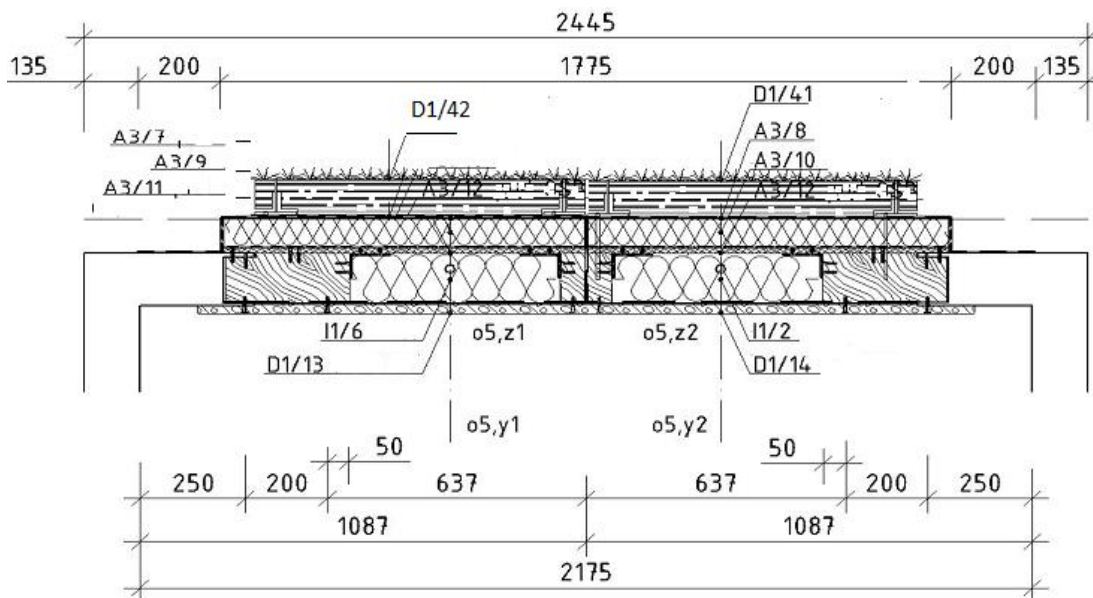


Figure 4: Deployment of sensors

**Measurement of the heat transfer coefficient through the roof construction**

Subject to measurement was continuous implementation of testing measurement of the constructions' thermal parameters and factor during a winter season. The heat transfer coefficient (U-value) measurements were made as the first ones. They were made by the measuring device Testo 635 with a probe for U-value (the heat transfer coefficient) determination and subsequent comparison to calculations **Chyba! Nenašiel sa žiaden zdroj odkazov..** The Testo 635 device measures only in a presumption that the difference between the internal and external temperature is at minimum 20(°C) along with keeping all procedures during the measurement. The emphasis was on the objected measurements. The procedure by itself is not described in the publication. The measurement's results are described in the charts and in the graphs. The measurements of the construction S2 are displayed by a yellow color in the graphs. A single length of the measurements (one-minute interval during 15minutes measurements, two-minute interval during one-hour measurement) is displayed on the X axis and the actually measured values expressed in (W/(m<sup>2</sup>K)) are displayed on the Y axis. **Chyba! Nenašiel sa žiaden zdroj odkazov..**

## 2 Measurement results of the climatic chamber module

The calculated value of the heat transfer coefficient through the construction from the calculating program is referred in the following table 1. **Chyba! Nenašiel sa žiaden zdroj odkazov..**

Table 1: The roof composition from interior side

Number	Name	D [m]	L [W/m.K]	C [J/kg.K]	Ro [kg/m <sup>3</sup> ]	Mi [-]	Ma [kg/m <sup>2</sup> ]
1	Plasterboard	0.0100	0.2200	1060.0	750.0	9.0	0.0000
2	Jutafol N	0.0001	0.3800	1700.0	640.0	65000.0	0.0000
3	Isover	0.1250	0.0390	880.0	50.0	1.4	0.0000
4	OSB boards	0.0120	0.1300	1700.0	650.0	50.0	0.0000
5	MikroventSR	0.0042	0.2100	1470.0	1286.0	17113.0	0.0000
6	Polyurethane	0.0800	0.0320	1500.0	35.0	220.0	0.0000
7	Icopal	0.0042	0.2100	1470.0	1100.0	50000.0	0.0000
8	Draining layer	0.0040	0.5000	1880.0	140.0	3.0	0.0000
9	Volcanic soil	0.0800	0.6000	500.0	1600.0	1.5	0.0000
10	Vegetating grid	0.0400	0.1100	1200.0	2000.0	4.0	0.0000

Boundary conditions are referred in the table 2:

Table 2: Calculation boundary conditions

Thermal resistance during the heat transfer in the interior $R_{si}$ :	0.10 ((m <sup>2</sup> K)/W)
Ditto for calculation of condensation and surface temperatures $R_{si}$ :	0.13 ((m <sup>2</sup> K)/W)
Thermal resistance during the heat transfer in the exterior $R_{se}$ :	0.04 ((m <sup>2</sup> K)/W)
Ditto for calculation of condensation and surface temperatures $R_{se}$ :	0.04 ((m <sup>2</sup> K)/W)

Requirements on the thermal resistance and the heat transfer coefficient, together with the calculated values of the thermal resistance and the heat transfer coefficient through the construction are referred in the table 3. **Chyba! Nenašiel sa žiaden zdroj odkazov..**

Table 3: Requirements on the thermal resistance and the heat transfer coefficient and their calculated values

Requirement: $R_n =$	4.90 ((m <sup>2</sup> K)/W)
Calculated value: $R =$	6.97 ((m <sup>2</sup> K)/W)
Requirement: $U_n =$	0.20 (W/(m <sup>2</sup> K))
<b>Calculated value: <math>U =</math></b>	<b>0.14 (W/m<sup>2</sup>K)</b>

Total comparison of the measurements with the calculated values was made as the measurements of the sample S2. Subsequently, an arithmetical sum of the given partial values was made. These values were arithmetical averaged and compared to the calculated value. The values are referred in the table 4. **Chyba! Nenašiel sa žiaden zdroj odkazov. Chyba! Nenašiel sa žiaden zdroj odkazov. Chyba! Nenašiel sa žiaden zdroj odkazov.**

Table 4: Comparison of the calculated and measured value of the heat transfer coefficient

Measurement		Calculated value
1	0.144 (W/( m <sup>2</sup> K))	0.14 (W/( m <sup>2</sup> K))
2	0.145 (W/( m <sup>2</sup> K))	
3	0.147 (W/( m <sup>2</sup> K))	
4	0.150 (W/( m <sup>2</sup> K))	
5	0.146 (W/( m <sup>2</sup> K))	
6	0.145 (W/( m <sup>2</sup> K))	
$(\bar{x})$	0.146 (W/( m <sup>2</sup> K))	0.14 (W/( m <sup>2</sup> K))

### 3 Conclusion

The measured samples of the roof constructions S1 and S2 in the climate chamber module have no signs of an unprofessional assembly or infringement of working procedures during building phase. All procedures specified by a producer were kept during the single measurement and afterwards, it is possible to state that difference between the measured and

calculated values of the heat transfer coefficient is  $0.0060 \text{ W}/(\text{m}^2\text{K})$ . This difference possibly may be caused by:

- Measuring device Testo 365 with an accuracy  $\pm 0.005 \text{ W}/(\text{m}^2\text{K})$ ,
- Measuring probe for measuring the heat transfer coefficient with an accuracy  $\pm 0.003 \text{ W}/(\text{m}^2\text{K})$ ,
- The values were counted for three decimal places in averaging (0.000).

## Acknowledgements

The paper presents partial research results of project VEGA 1/0674/18 “Theoretical and experimental analysis of architectural-structural shapes and fragments of building envelope structures designed for harsh weather conditions”.

## References

- [1] KATUNSKÝ, [et al.] . (2014). Numerical Analysis and Measurement Results of a Window Sill. *Advanced Materials Research*, 899, p. 147 - 150.
- [2] BALÁŽ, R.: (2016), Technical measurement of the green roof in a winter season , *Advances and Trends in Engineering Sciences and Technologies II - Proceedings of the 2nd International Conference on Engineering Sciences and Technologies, ESaT 2016*.
- [3] FLIMEL M., (2013), Differences  $U_g$  - values of glazing measured in situ with the influence factors of the internal environment, 2013, In: *Advanced Materials research*. Vol. 649, p. 61 - 64 ISBN 978-03785-596-6.
- [4] CHUCHMA, L., KALOUSEK, M., (2014), Electricity storage in passive house in Central Europe region. *Advanced Materials Research*, 2014, roč. 2014, č. 899, p. 213 - 217. ISSN: 1022- 6680.
- [5] KATUNSKÝ, D. [et al.] (2013) Analysis of Thermal Energy Demand and Saving in Industrial Buildings: A Case Study in Slovakia / - 2013. In: *Building and Environment*. Vol. 67, no. 9 (2013), p. 138 - 146. - ISSN 0360-1323.
- [6] BAGOŇA, M. [et al.] (2014), Roof structure evaluation in climatic chamber module, *Advanced Materials Research* Volume 1041, 2014, Pages 239-242 9th International enviBUILD 2014 Conference; Brno; Czech Republic; 18 September 2014 through 19 September 2014;
- [7] KATUNSKÝ, D. a kol.: 2011. Centrum excelentného výskumu progresívnych stavebných konštrukcií a indoor technológií na Ústave budov a prostredia. Ústav budov a prostredia, Stavebná fakulta, Technická univerzita v Košiciach, ISBN 978-80-553-0622-3 s 8-13. 2011.
- [8] KATUNSKÝ, D.: Skúšobné zariadenie pre výskum obalových konštrukcií inteligentných budov, In: *Inovatívny prístup k modelovaniu inteligentných konštrukčných prvkov v stavebníctve*, ZVPVÚIS Košice, XII/2009. ISBN 978-80-89383-04-7, str. 33-42. 2009.
- [9] BALÁŽ, R. – KATUNSKÝ, D. – BAGOŇA, M. – LOPUŠNIAK, M. – VERTAL, M.: Monitorovanie obalových konštrukcií za kvázistacionárneho stavu 2011. In: 35. vedecká medzinárodná konferencia ústavů a kateder pozemních staveb České a Slovenské republiky: Nejnovější poznatky v oboru pozemního stavitelství: Telč 7.- 9. září 2011. Praha. 2011 P. 45-48. ISBN 978-80-01-04959-4.



## Environmental impact analysis of five family houses in Eastern Slovakia through a life cycle assessment

Andrea Moňoková, Silvia Vilčeková

Technical University of Košice, Slovakia  
Civil Engineering Faculty, Institute of Environmental Engineering  
e-mail: andrea.monokova@tuke.sk, silvia.vilcekova@tuke.sk

### Abstract

This study performs a life cycle assessment (LCA) of five new family houses in Eastern Slovakia to compare them in terms of the materials and technologies used. The main goal of the analysis is to investigate and highlight the expectable reduction rate of environmental impact resulting from using green materials and technologies. Their environmental impact is determined by using eToolLCD software. The life cycle impact assessment (LCIA) categories of global warming, ozone depletion, acidification, eutrophication and photochemical ozone creation potential are determined within the cradle-to-grave boundary. The examined family houses are built of conventional materials such as aerated concrete blocks, expanded polystyrene (EPS) for thermal insulation and roofing mineral wool, as well as natural materials such as clay, straw, wood, cellulose and vegetation for the roofs. Family houses built of natural materials are characterized by negative emissions of CO<sub>2eq</sub> in the product phase. Results show that especially the product phase contributes greatly to all environmental impact categories for houses built of conventional materials, such as aerated concrete blocks, mineral wool for thermal insulation, reinforcement concrete and ceramic or concrete tiles.

**Key words:** Life cycle assessment (LCA), Global warming potential (GWP), Family house, Green materials, Green technologies

## 1 Introduction

The construction industry has a significant impact on the consumption of natural resources and energy globally, as well as on greenhouse gas emissions. By applying the life cycle assessment (LCA) methodology in this sector, it is possible to assess and minimize environmental impacts and improve sustainability indicators [1,2]. This method evaluates environmental impact categories related to the production, transport and installation of building materials, as well as building use and end of building life, including recycling or landfill disposal [3]. Weißenberger et al. [4] pointed to the increasing interest of the scientific community in the evaluation of buildings using LCA in recent years. LCA analyses have been performed for residential buildings, both multifamily [5,6] and single-family houses [7-10], as

well as non-residential buildings such as schools [11,12] and office buildings [13-15]. Research in this area has produced interesting results, which are gradually being applied in the design phase. For example, Dahlstrøm et al. [7] conducted LCAs of single-family residences built of conventional materials as well residences built according to the Passive House Standard. An interesting result was that a standard building envelope with an air-to-water heat pump system reduced the environmental impact by approximately 20%, a level comparable with that of a passive house with only electric heating. Comparisons of greenhouse gas emissions have shown that the reduction in a passive design is almost 30%. Lavagna et al. [5] found that single-family houses are responsible for the highest proportion of environmental impact of housing in Europe, and that the same type of building has different impacts in different locations (climatic zones) mainly due to differences in space heating needs. Space heating and electricity use were found to contribute most to the overall impact. Sharma et al. [16] observed that the operational phase required the highest amount of energy (80–85%) and contributed to more than 50% of the overall greenhouse gas emissions. Similarly, Asdrubali et al. [17] performed LCAs of a multi-storey office building, a multi-family residential building and a detached house in Italy and showed that the operational phase had the greatest contribution to the total impact, ranging from 77% (detached house) to 85% (office building), while the impact of the construction phase ranged from 14% (office building) to 21% (detached house). Petroche et al. [18] also found that the operational phase of residential buildings is responsible for the greatest burden in all impact categories except ozone layer depletion, which represents a substantial burden only during the construction phase. On the other hand, an LCA of a two-storey residential building in Canada found that not only the operational but also the construction phase had a significant environmental impact, with the roof and walls accounting for most of the burden [1]. An LCA of a residential building in Turin (demolished by controlled blasting) revealed that waste recycling was sustainable from an energy and environmental point of view, with a recycling potential of 29% in terms of life cycle energy and 18% in terms of greenhouse emissions, compared to the environmental burdens related with the conventional materials embodied in the building shell [19]. In addition to LCA studies on entire buildings, other LCA analyses have focused on specific construction systems, material options or green technologies [20-26]. Kylili et al. [27] performed an LCA of a passive house in the sub-tropical climatic zone and found that concrete was the greatest contributor in all impact categories except abiotic depletion of elements, with the wall systems, floors and foundations significantly contributing to the house's environmental performance. Studies using parametric analysis discovered that utilising insulating materials in the wall systems can have a positive effect in a building's energy efficiency without substantially affecting its total embodied energy. A comparative environmental assessment of reinforced concrete and wood housing constructions confirmed that the steel-reinforced concrete construction had a higher environmental impact compared to the wooden construction [26,28]. This study [28] also revealed that using solar energy for the operation phase reduced the total life cycle carbon emissions by 73%. Asif et al. [29], who studied eight construction materials for a dwelling in Scotland, found concrete to be the material with the highest level of embodied energy, followed by timber and ceramic tiles.

As can be seen from the studies cited above, the LCA method is a widely used tool worldwide. However, very few similar studies have been conducted in Slovakia. The aim of this research, therefore, was to investigate the environmental impact of five family houses from East Slovakia, which use combination of conventional and green materials and

technologies. The first two of selected houses are not typical for Slovak region due to their architecture and as well as from chosen materials point of view. However, they scored best in terms of environmental impact.

The main contribution of this study is that it highlights the feasibility of reducing the environmental impact of building construction through using green materials and technologies as a means of mitigating climate change.

## 2 Aims, scope and methodology

Managing the environmental impact of building construction and operation is a key factor in mitigating the damage caused to the biosphere directly and indirectly. Life cycle assessment (LCA) is the leading industry standard for clearly identifying optimum strategies to reduce buildings' environmental impact. LCA addresses the environmental aspects and potential impact throughout a product's life cycle from raw material acquisition to production, use, end-of-life treatment, recycling and final disposal.

The aim of our analysis was to assess the environmental impact of the global warming potential (GWP), ozone depletion potential (ODP), acidification potential (AP), eutrophication potential (EP) and photochemical ozone creation potential (POCP), expressed as kilograms of  $\text{CO}_{2\text{eq}}$ ,  $\text{CFC}_{11\text{eq}}$ ,  $\text{SO}_{2\text{eq}}$ ,  $\text{PO}_4^{3-\text{eq}}$  and  $\text{C}_2\text{H}_{4\text{eq}}$ , respectively, within the cradle-to-grave boundary. The "kg substance  $s_{\text{eq}}$ " ("kilogram equivalent of a reference substance  $s$ ") expresses the amount of a reference substance  $s$  that equals the impact of the considered pollutant within midpoint category studies. For example, the global warming potential of fossil-based methane on a 100-year scale is 27.75 times higher than  $\text{CO}_2$ , and thus its characterization factor (CF) is 27.75 kg  $\text{CO}_{2\text{eq}}$  [30].

The aim of comparison on environmental impacts is:

- To find out, which phase of family house's life cycle causes the greatest environmental damage.
- To determine, which of the building materials are the biggest contributors to these damages.
- To support a development of technologies and production processes of environmentally friendly products or materials.

The eToolLCD software was used to model the houses' environmental impact, in accordance with EN ISO 14040, EN ISO 14044 and EN 15978. This software is compliant with the CML-IA methodology v4.5 [31]. The software uses third-party background processes aggregated as midpoint indicators, which are stored in a library of software and are coupled with algorithms and user inputs to output the environmental impact assessment. The selected life cycle impact assessment (LCIA) methodology is widely used.

The assessment of the selected houses included all the upstream and downstream processes involved in providing the structures' primary function from the product stage to the construction, use, maintenance, refurbishment, operation and disposal phases. The inventory encompasses all phases from the extraction of raw materials or energy to the release of substances back to the environment or to the point where inventory items exit the system boundary. The functional unit is 1 m<sup>2</sup> of the total floor area. The estimated design life adopted for the LCA study period is 60 years, which is on par with Building Research Establishment

Environmental Assessment Method (BREEAM) certification system. The system boundary, shown in Fig. 1, follows EN 15978 guidelines.

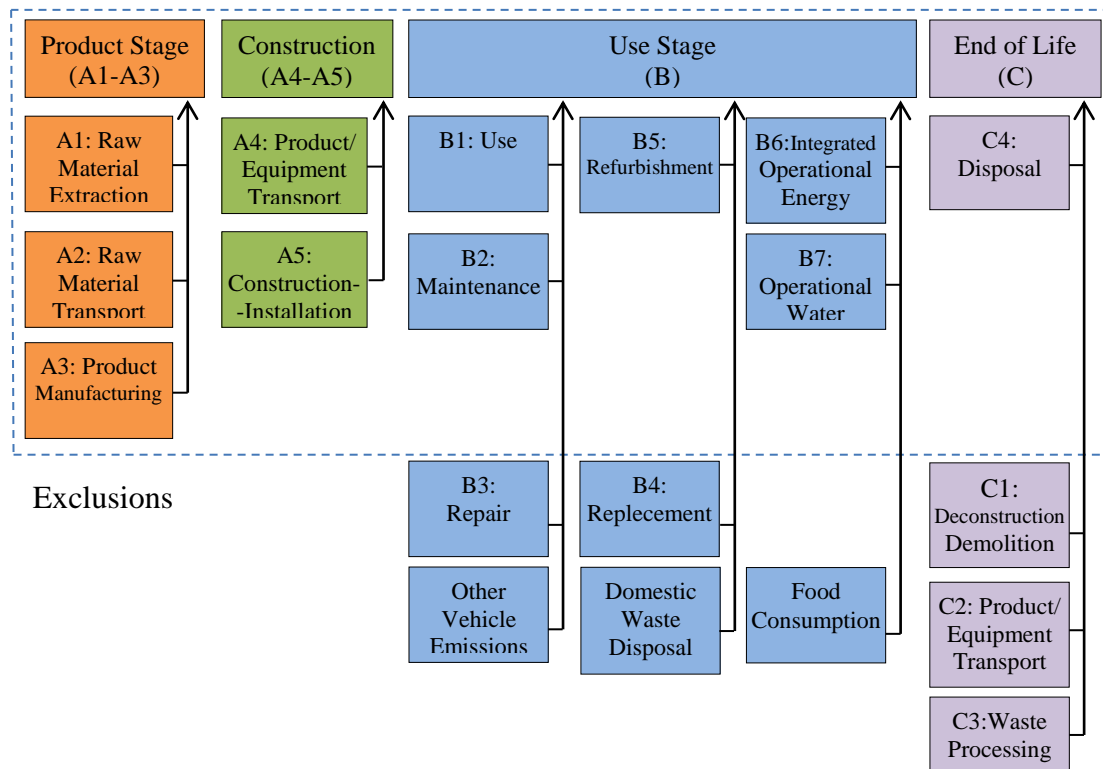


Figure 1: System boundary diagram.

### 3 Inventory analysis: design and technical equipment of the assessed houses

The design was modeled using the available eToolLCD elements, templates and products with Environmental Product Declaration (EPD). The eToolLCD library templates are customizable, and users may submit templates for validation. The template validation process is undertaken by experienced LCA practitioners and involves checking the user inputs and ensuring that the assumptions are adequately referenced.

The selected family houses, presented in Figs. 4–6, are located in villages near the towns of Košice, Bardejov and Gelnica in Eastern Slovakia. The project location is shown in Figs. 2–3.

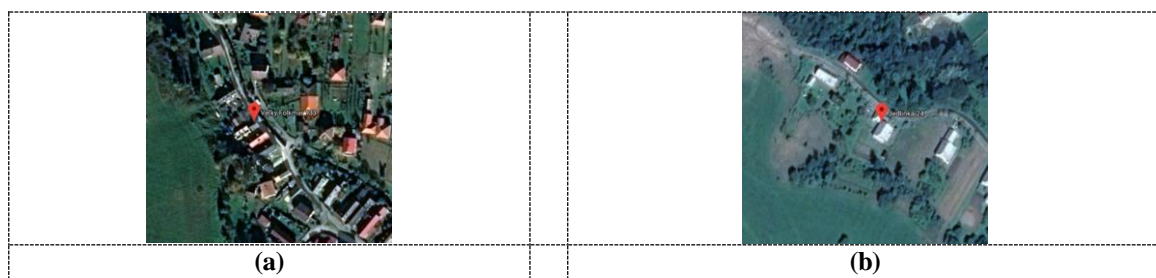


Figure 2: Location of the project – Locality view: (a) Family house 1, (b) Family house 2.



Figure 3: Location of the project – Locality view: (c) Family house 3, (d) Family house 4, (e) Family house 5.

Houses 1 and 2 are located near forest lands with habitats of European importance. Veľký Folkmár is located in the northeast of the Slovenské rudohorie, Jedlinka in the western part of the Low Beskids. Family houses 3, 4 and 5 are situated in flat areas near fertile fields. Unlike the first two houses, they have quick access to the busy metropolis of the East, which also has a major impact on the owners' lifestyle.

Family house 1 is located in the village of Veľký Folkmár and family house 2 in the village of Jedlinka, both in Bardejov district. Their fully built areas are 78 m<sup>2</sup> and 120 m<sup>2</sup>, respectively. Their energy demands for space heating are 76.96 kWh/m<sup>2</sup> per year and 20.7 kWh/m<sup>2</sup> per year, respectively, and for water heating 4,000 kWh per year and 3,580 kWh per year, respectively.

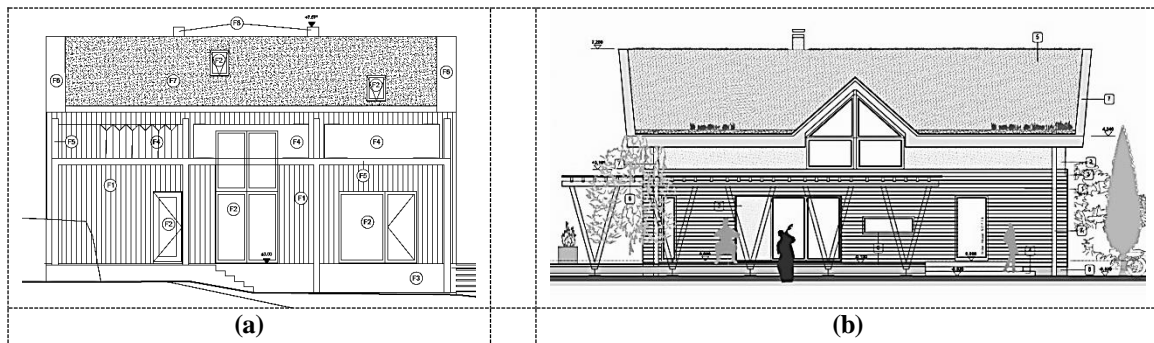


Figure 4: View of evaluated family houses: (a) Family house 1; (b) Family house 2.

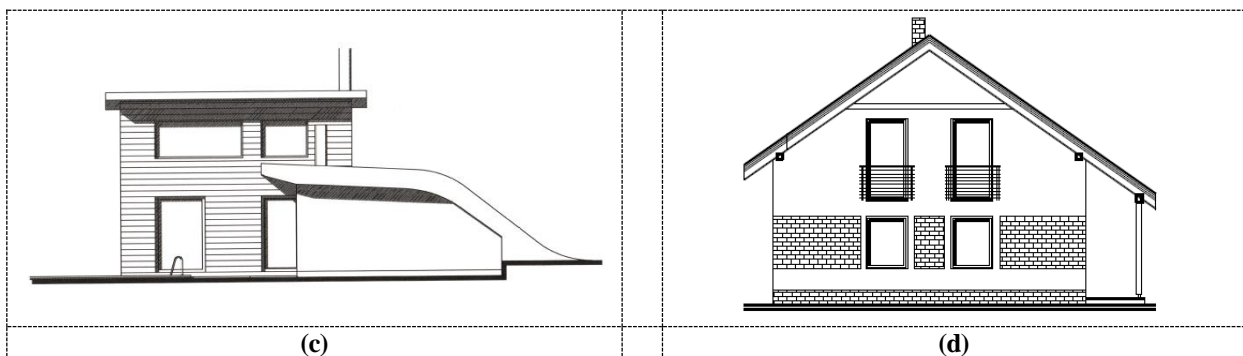


Figure 5: View of evaluated family houses: (c) Family house 3; (d) Family house 4.

Family houses 3 and 4 are located in Rozhanovce in the Košice district. Their fully built areas are 154 m<sup>2</sup> and 122 m<sup>2</sup>, respectively. Their energy demands for space heating are 35.16 kWh/m<sup>2</sup> per year and 26.85 kWh/m<sup>2</sup> per year, respectively, and for water heating 1,500 kWh per year and 1,384 kWh per year, respectively.

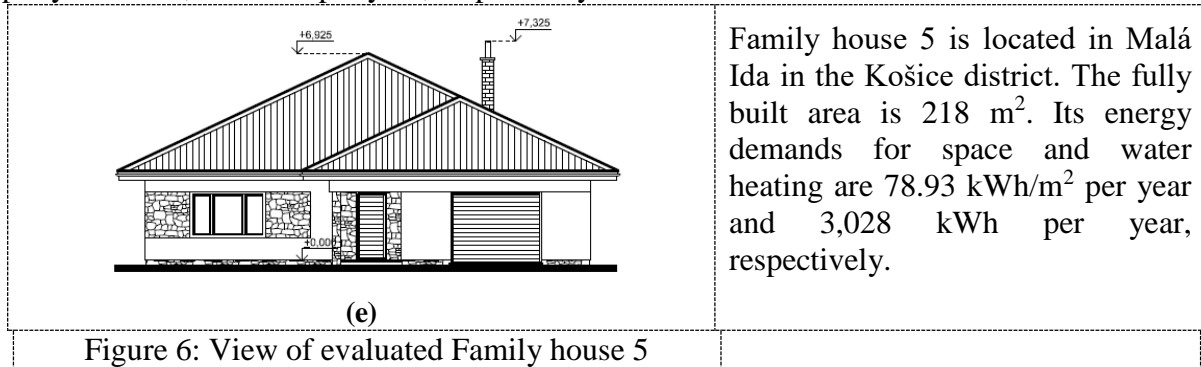


Figure 6: View of evaluated Family house 5

Table 1 provides basic information about the houses, the building materials and their heating, ventilation and air conditioning (HVAC) systems that were evaluated in this study.

Table 1: Description of the family houses

Family house	External walls	Roofs	Floors	Heating
1	clay poured into the shell, timber cladding, clay plaster	extensive vegetation, mineral wool, rafter framework-saddle roof	wood, ceramic tiles, EPS	gas boiler
2	wooden framed structure, straw insulation, clay plaster, timber cladding	extensive vegetation, mineral wool, rafter framework-saddle roof	wood, ceramic tiles, EPS	gas boiler
3	wooden framed structure, wooden insulation, timber cladding, plasterboard	extensive vegetation, cellulose, reinforced concrete	wood, ceramic tiles, EPS	air-to-water heat pump
4	aerated concrete blocks, wooden fibre slabs, silicate plaster	ceramic tiles, cellulose fibres, rafter framework-saddle roof	wood, ceramic tiles, EPS	air-to-water heat pump
5	aerated concrete blocks, wooden fibre slabs, silicate plaster	concrete tiles, cellulose, rafter framework-hip roof	wood, ceramic tiles, EPS	gas boiler

## 4 Results and discussion

The life cycle impact assessment (LCIA) results for each house are shown in Tables 2–6. The colored cells in the tables indicate the rate of each impact category in each life cycle phase (red: **over 50%**; violet: **41–50%**; orange: **31–40%**; green: **21–30%**; yellow: **10–20%**).

The highest contributors to environmental impact are the three phases of the product stage (A1–A3), the integrated operational energy (B6) of the use stage and, to a great extent, the refurbishment phase (B5). Family houses built of natural materials, where wood

predominates, are characterized by negative CO<sub>2eq</sub> emissions in the product stage. Trees absorb carbon dioxide from the atmosphere during photosynthesis and store carbon as their building material. This process – known as terrestrial sequestration – reduces the amount of CO<sub>2</sub> in the atmosphere. Carbon remains bound in the wood even after the plant's death. By burning or decomposition the wood, it returns naturally to the atmosphere. Product phases A1–A3 greatly contribute to the GWP for houses built of conventional materials, such as aerated concrete blocks, reinforced concrete, mineral wool for thermal insulation and ceramic or concrete tiles.

In the integrated operational energy phase, CO<sub>2eq</sub> values are lower for single-family homes with gas boiler space and water heating. House 4 has a CO<sub>2eq</sub> value of 1,000 kg due to the usage of solar collectors, which lower electricity energy consumption significantly for at least 5 months per year.

In the cases of ODP and POCP, house 3 has the highest impact in the product and refurbishment phases. It seems that the materials used in the bearing structure (pre-treated weatherboarding timber clad with plasterboard) contribute the most to this result.

In terms of AP and EP, houses 3 and 4 have the highest impact. This appears to be due to their use of heat pumps, as opposed to gas boilers, used in houses 1, 2 and 5.

Table 2: Environmental impact indicators for each phase – House 1

Impact	Materials and construction			Use stage					End of life stage	Total
	A1–A3	A4	A5	B1	B2	B5	B6	B7	C4	
GWP [kg CO <sub>2eq</sub> ]	270	43	30	-1.2	0.037	20	990	26	22	1400
ODP [kgCFC11 <sub>eq</sub> ]	0.12E <sup>-4</sup>	0.28E <sup>-5</sup>	0.19E <sup>-5</sup>	0	0.19E <sup>-8</sup>	0.38E <sup>-5</sup>	0.16E <sup>-5</sup>	0.13E <sup>-5</sup>	0.48E <sup>-8</sup>	0.24E <sup>-4</sup>
AP [kg SO <sub>2eq</sub> ]	1.5	0.11	0.2	0	0.17E <sup>-3</sup>	0.52	0.28	0.13	0.04	2.8
EP [kg (PO <sub>4</sub> ) <sup>3-</sup> <sub>eq</sub> ]	0.41	0.022	0.056	0	0.4E <sup>-4</sup>	0.12	0.068	0.03	0.19	0.91
POCP [kg C <sub>2</sub> H <sub>4eq</sub> ]	0.26	0.019	0.039	0	0.98E <sup>-5</sup>	0.05	0.037	0.74E <sup>-2</sup>	0.24E <sup>-2</sup>	0.42

Table 3: Environmental impact indicators for each phase – House 2

Impact	Materials and construction			Use stage					End of life stage	Total
	A1–A3	A4	A5	B1	B2	B5	B6	B7	C4	
GWP [kg CO <sub>2eq</sub> ]	-110	29	11	0	0.14	20	360	12	12	330
ODP [kgCFC11 <sub>eq</sub> ]	0.12E <sup>-4</sup>	0.19E <sup>-5</sup>	0.63E <sup>-6</sup>	0	0.7E <sup>-8</sup>	0.5E <sup>-5</sup>	0.6E <sup>-6</sup>	0.61E <sup>-6</sup>	0.78E <sup>-8</sup>	0.21E <sup>-4</sup>
AP [kg SO <sub>2eq</sub> ]	1.4	0.068	0.073	0	0.64E <sup>-3</sup>	0.54	0.1	0.06	0.072	2.3
EP [kg (PO <sub>4</sub> ) <sup>3-</sup> <sub>eq</sub> ]	0.39	0.015	0.045	0	0.15E <sup>-3</sup>	0.13	0.025	0.014	0.58	1.2
POCP [kg C <sub>2</sub> H <sub>4eq</sub> ]	0.21	0.013	0.012	0	0.36E <sup>-4</sup>	0.07	0.014	0.0035	0.52E <sup>-2</sup>	0.33

Table 4: Environmental impact indicators for each phase – House 3

Impact	Materials and construction			Use stage					End of life stage	Total
	A1–A3	A4	A5	B1	B2	B5	B6	B7	C4	
GWP [kg CO <sub>2eq</sub> ]	-150	22	5.9	0	0.065	-230	1400	34	29	1100
ODP [kgCFC11 <sub>eq</sub> ]	0.13E <sup>-3</sup>	0.7E <sup>-5</sup>	0.28E <sup>-6</sup>	0	0.33E <sup>-8</sup>	0.6E <sup>-3</sup>	0.69E <sup>-4</sup>	0.17E <sup>-5</sup>	0.11E <sup>-7</sup>	0.8E <sup>-3</sup>
AP [kg SO <sub>2eq</sub> ]	1.6	0.053	0.042	0	0.31E <sup>-3</sup>	1.4	6.4	0.17	0.13	9.7
EP [kg (PO <sub>4</sub> ) <sup>3-</sup> <sub>eq</sub> ]	0.33	0.012	0.027	0	0.69E <sup>-4</sup>	0.57	1.4	0.039	0.38	2.8
POCP [kg C <sub>2</sub> H <sub>4eq</sub> ]	1.4	0.96E <sup>-2</sup>	0.57E <sup>-2</sup>	0	0.17E <sup>-4</sup>	1.4	0.36	0.98E <sup>-2</sup>	0.66E <sup>-2</sup>	3.2

Table 5: Environmental impact indicators for each phase – House 4

Impact	Materials and construction			Use stage					End of life stage	Total
	A1–A3	A4	A5	B1	B2	B5	B6	B7	C4	
GWP [kg CO <sub>2eq</sub> ]	520	59	25	-12	0.033	92	1000	24	22	1700
ODP [kgCFC11 <sub>eq</sub> ]	0.23E-4	0.39E-5	0.16E-5	0	0.17E-8	0.31E-4	0.52E-4	0.12E-5	0.61E-8	0.11E-3
AP [kg SO <sub>2eq</sub> ]	2	0.14	0.18	0	0.15E-3	0.51	4.8	0.12	0.053	7.7
EP [kg (PO <sub>4</sub> ) <sup>3-</sup> <sub>eq</sub> ]	0.46	0.03	0.045	0	0.35E-4	0.17	1.1	0.027	0.087	1.9
POCP [kg C <sub>2</sub> H <sub>4eq</sub> ]	0.28	0.031	0.034	0	0.87E-5	0.053	0.27	0.68E-2	0.23E-2	0.67

Table 6: Environmental impact indicators for each phase – House 5

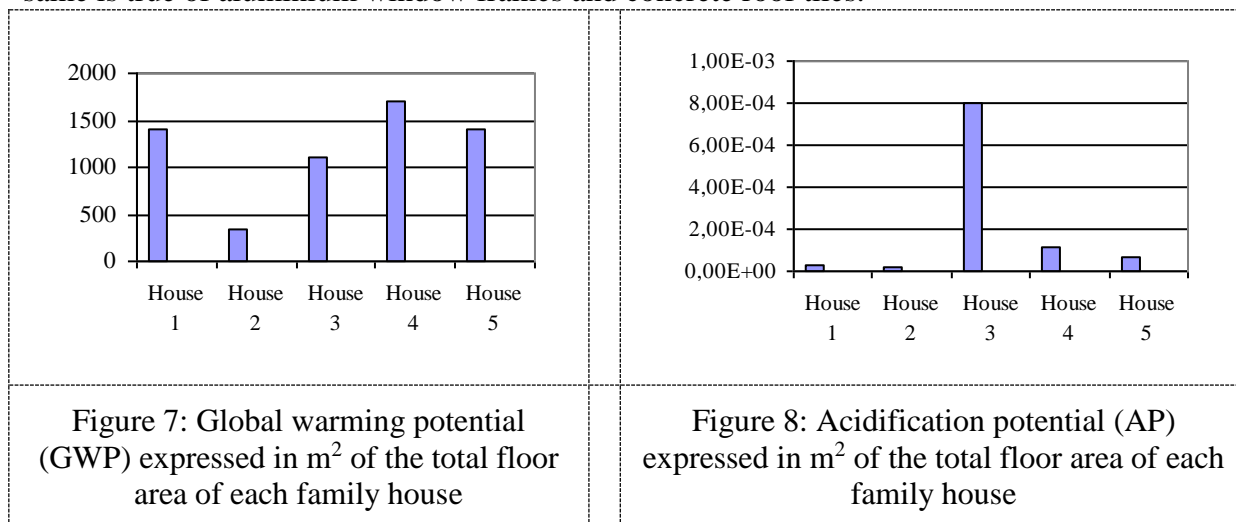
Impact	Materials and construction			Use stage					End of life stage	Total
	A1–A3	A4	A5	B1	B2	B5	B6	B7	C4	
GWP [kg CO <sub>2eq</sub> ]	240	48	7.8	-1.3	0.089	88	1000	24	36	1400
ODP [kgCFC11 <sub>eq</sub> ]	0.23E-4	0.31E-5	0.41E-6	0	0.45E-8	0.35E-4	0.16E-5	0.12E-5	0.29E-8	0.64E-4
AP [kg SO <sub>2eq</sub> ]	1.6	0.12	0.043	0	0.42E-3	0.54	0.29	0.12	0.66E-3	2.7
EP [kg (PO <sub>4</sub> ) <sup>3-</sup> <sub>eq</sub> ]	0.31	0.025	0.014	0	0.94E-4	0.17	0.069	0.028	0.09	0.7
POCP [kg C <sub>2</sub> H <sub>4eq</sub> ]	0.24	0.021	0.8E-2	0	0.23E-5	0.061	0.038	0.69E-2	0.28E-3	0.38

GWP: Global warming potential; ODP: Ozone depletion potential; AP: Acidification potential;

EP: Eutrophication potential; POCP: Photochemical ozone creation potential

Impact key red: over 50%; violet: 41–50%; orange: 31–40%; green: 21–30%; yellow: 10–20%

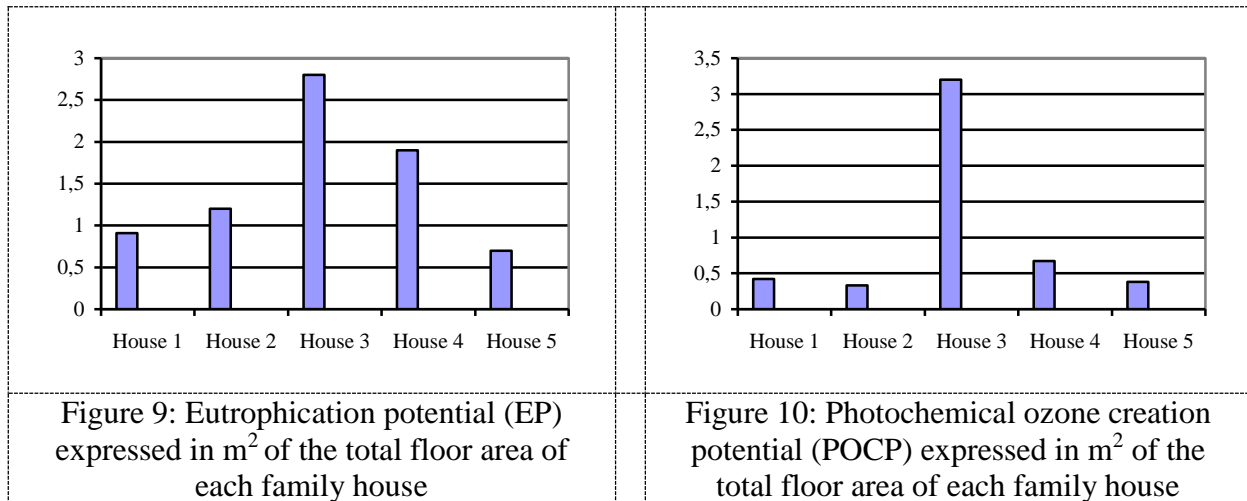
Figs. 7–11 present each environmental impact category expressed in square meters of the total floor area of each house. Fig. 7 shows that house 2, which consists of green materials such as a wooden framed structure, straw for insulation and clay plaster and uses a gas boiler, has the lowest global warming potential: 76% lower than that of houses 1 and 5, 70% lower than that of house 3 and 80.6% lower than that of house 4. In other words, concrete structures, which constitute 18–25% of the entire building, have the highest global warming potential. Materials such as aerated concrete blocks, expanded polystyrene (EPS) thermal insulation boards, polypropylene (PP) and polyvinyl chloride (PVC) also increase the GWP considerably. The same is true of aluminium window frames and concrete roof tiles.





Figs. 7–11 reveal that house 3 has the most adverse overall impact on the environment. This impact was found to be much higher in phases B5 and B6 compared to other the houses, as clearly shown in Tables 2–6. This is likely due to the materials used, which require much more frequent replacement and/or refurbishment.

Fig. 8 shows that house 3 has the highest acidification potential: 20.6% higher than that of house 4, 72% higher than that of houses 1 and 5 and up to 76% higher than that of house 2. This is due to the combination of aerated concrete blocks, concrete structures, waterproofing, aluminium windows, plasterboard tiles and pre-treated weatherboarding timber used in the house.



As far as eutrophication potential is concerned, Fig. 9 shows that house 3 again has the worst score: 32% higher than that of house 4, 57% higher than that of house 2, 67.5% higher than that of house 1 and 75% higher than that of house 5. Materials such as reinforced concrete, oriented strand boards (OSB), aluminium windows, cladding timber panel, pre-treated weatherboarding timber and the proofing insulation used in house 3 are the top contributors to EP.

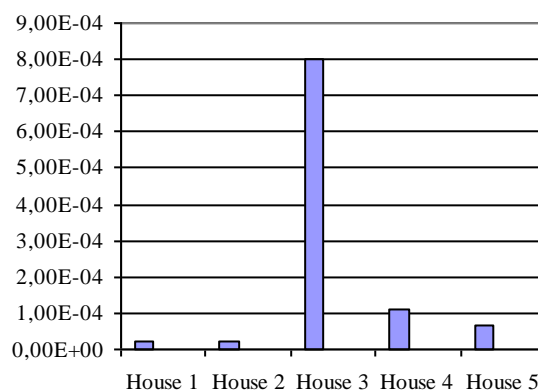


Figure 11: Ozone depletion potential (ODP) expressed in m<sup>2</sup> of the total floor area of each family house

As in the previous cases, house 3 has the highest photochemical ozone creation potential score: 89.7%, 88%, 86.9% and 79% higher than that of houses 2, 5, 1 and 4, respectively (Fig. 10). Its

reinforced concrete structures, impregnated wood materials and aerated concrete blocks combined significantly contribute to the POCP. These materials also have the highest impact on stratospheric ozone depletion.

In terms of ozone depletion potential, house 3 has the highest impact by a wide margin: 97% higher than that of houses 1 and 2, 92% higher than that of house 5 and 86% higher than that of house 4 (Fig. 11).

## 5 Conclusion

The evaluation of five family houses with the LCA method produced significant results in relation to the environmental impact categories of global warming potential, ozone depletion potential, acidification potential, eutrophication potential and photochemical ozone creation potential. Our analysis shows that significant environmental impact of all monitored categories is visible in the product and integrated operational energy phases.

The environmental impact of buildings can be reduced by using green technologies and materials. An important barrier to the implementation of many environmental innovation technologies is the lack of awareness of the real costs of obtaining, using and disposing of materials, especially in Eastern and Central Europe. Therefore, new and cost-effective processes and technologies need to be developed to address environmental externalities and better energy use approaches. Advanced green technology and its penetration into new markets are crucial to meeting society's needs in a way that can continue into the future without exhausting natural resources and devastating the planet. On this basis, it is important to know all the possibilities of obtaining energy from different sources but also to embrace the possibilities of construction with materials and technologies that offer low-cost operation and healthy microclimate buildings and, most importantly, do not leave a large ecological footprint [32]. As assessed in study [33], it is advisable to consider partial production of hot water and/or electricity from solar energy, since the solar thermal potential in Slovakia is five months per year. Moreover, a usage of solar energy significantly reduces CO<sub>2</sub> emissions.

From a sustainability point of view, it is necessary to limit the use of materials with high-energy inputs in production and to exclude substances with an adverse effect on users' health. Consideration should also be given to minimizing transport requirements and reducing the amount of waste from construction by recycling and reusing it. Local, recycled and natural materials such as wood, stone, clay plaster, linoleum, wood flooring, flax, hemp, cork, pulpwood or cellulose should be used more. The environmental impact of the construction alone of conventional building is about as great as the environmental impact of the operation of a passive house over a period of 100 years. Therefore, ecological optimisation of the construction impact is an important part of sustainable architecture. One of the priorities of sustainable construction is to minimize material flows and emissions in building material production, reducing bound energy and individual environmental impact categories.

In the future, we aim to evaluate a significant number of family houses to be able to concentrate attention to the aforementioned impact categories and thus reach more accurate conclusions.

## Acknowledgements

This work was financially supported by Slovak Grants No. 1/0307/16 and 1/0648/17.

Author would like to thank to Ing. arch. Pavol Mészáros and Ing. arch. Viliam Holeva for providing the project documentations of the family houses that have been used in research work presented in this paper.

## References

- [1] Zhang W, Tan S, Lei Y, Wang S (2014) Life cycle assessment of a single-family residential building in Canada: A case study. *Build Simul.* 7: 429–438. <https://doi.org/10.1007/s12273-013-0159-y>.
- [2] Soust-Verdaguer B, Llatas C, García-Martínez A (2016) Simplification in life cycle assessment of single-family houses: A review of recent developments. *Build Environ.* 103:215–227. <http://dx.doi.org/10.1016/j.buildenv.2016.04.014>.
- [3] Rossi B, Marique AF, Glaumann M, Reiter S (2012) Life-cycle assessment of residential buildings in three different European locations, basic tool. *Build Environ.* 51:395–401. <https://doi.org/10.1016/j.buildenv.2011.11.017>.
- [4] Weißenberger M, Jensch W, Lang W (2014) The convergence of life cycle assessment and nearly zero-energy buildings: The case of Germany. *Energ Buildings.* 76:551–557. <https://doi.org/10.1016/j.enbuild.2014.03.028>.
- [5] Lavagna M, Baldassarri C, Campioli A, Giorgi S, Valle AD, Castellani V, Sala S (2018) Benchmarks for environmental impact of housing in Europe: Definition of archetypes and LCA of the residential building stock. *Build Environ.* 145:260–275. <http://doi.org/10.1016/j.buildenv.2018.09.008>.
- [6] Adalberth K, Almgren A, Holleris Petersen E (2001) Life-cycle assessment of four multi-family buildings. *International Journal of Low Energy and Sustainable Buildings.* 2:1–21.
- [7] Dahlstrøm O, Sørnes K, Eriksen ST, Hertwich EG (2012) Life cycle assessment of a single-family residence built to either conventional- or passive house standard. *Energ Buildings.* 54:470–479. <https://doi.org/10.1016/j.enbuild.2012.07.029>.
- [8] Monteiro H, Freire F (2012) Life-cycle assessment of a house with alternative exterior walls: Comparison of three impact assessment methods. *Energ Buildings.* 47:572–583. <https://doi.org/10.1016/j.enbuild.2011.12.032>.
- [9] Shirazi A, Ashuri B (2018) Embodied life cycle assessment comparison of single family residential houses considering the 1970s transition in construction industry: Atlanta case study. *Build Environ.* 140:55–67. <https://doi.org/10.1016/j.buildenv.2018.05.021>.
- [10] Cuéllar-Franca RM, Azapagic A (2012) Environmental impacts of the UK residential sector: Life cycle assessment of houses. *Build Environ.* 54:56–99. <https://doi.org/10.1016/j.buildenv.2012.02.005>.
- [11] Arena AP, de Rosa C (2003) Life cycle assessment of energy and environmental implications of the implementation of conservative technologies in school building in Mendoza-Argentina. *Build Environ.* 38:359–368. [https://doi.org/10.1016/S0360-1323\(02\)00056-2](https://doi.org/10.1016/S0360-1323(02)00056-2).
- [12] Scheuer C, Keoleian GA, Reppe P (2003) Life cycle energy and environmental performance of a new university building: Modeling challenges and design implications. *Energ Buildings.* 35:1049–1064. [http://doi.org/10.1016/S0378-7788\(03\)00066-5](http://doi.org/10.1016/S0378-7788(03)00066-5).
- [13] Junnila S, Horvath A, Guggemos AA (2006) Life-cycle assessment of office buildings in Europe and the United States. *J Infrastruct Syst.* 12:10–17. [https://doi.org/10.1061/\(ASCE\)1076-0342\(2006\)12:1\(10\)](https://doi.org/10.1061/(ASCE)1076-0342(2006)12:1(10)).
- [14] Xing S, Xu Z, Jun G (2008) Inventory analysis of LCA on steel- and concrete-construction office buildings. *Energ Buildings.* 40:1188–1193. <https://doi.org/10.1016/j.enbuild.2007.10.016>.
- [15] Kofoworola OF, Gheewala SH (2008) Environmental life cycle assessment of a commercial office building in Thailand. *Int J Life Cycle Assess.* 13:498. <https://doi.org/10.1007/s11367-008-0012-1>.

- [16] Sharma A, Saxena A, Sethi M, Shree V, Varun (2011) Life cycle assessment of buildings: A review. *Renew Sust Energ Rev.* 15:871–875. <https://doi.org/10.1016/j.rser.2010.09.008>.
- [17] Asdrubali F, Baldassarri C, Fthenakis V (2013) Life cycle analysis in the construction sector: Guiding the optimization of conventional Italian buildings. *Energ Buildings.* 64:73–89. <http://dx.doi.org/10.1016/j.enbuild.2013.04.018>.
- [18] Petroche DM, Ramírez AD, Rodríguez CR, Salas DA, Boero AJ, Duque-Rivera J (2015) Life cycle assessment of residential buildings: A review of methodologies. *WIT Transactions on Ecology and the Environment.* 194:217–225. <http://doi.org/10.2495/SC150201>.
- [19] Blengini GA (2009) Life cycle of buildings, demolition and recycling potential: A case study in Turin, Italy. *Build Environ.* 44:319–330. <https://doi.org/10.1016/j.buildenv.2008.03.007>.
- [20] Estokova A, Porhincak M (2012) Reduction of primary energy and CO2 emissions through selection and environmental evaluation of building materials. *Theoretical foundations of chemical Engineering..* 46(6):704–712. <https://doi.org/10.1007/s10098-014-0758-z>.
- [21] Hanandeh AE (2015) Environmental assessment of popular single-family house construction alternatives in Jordan. *Build Environ.* 92:192–199. <http://dx.doi.org/10.1016/j.buildenv.2015.04.032>.
- [22] Li P, Froese TM (2016) Life-cycle assessment of high performance, low cost homes. *Procedia Eng.* 145:1322–1329. <http://doi.org/10.1016/j.proeng.2016.04.170>.
- [23] Pachrowski G, Noskowiak A, Lewandowska A, Strykowski W (2014) Wood as a building material in the light of environmental assessment of full life cycle of four buildings. *Constr Build Mater.* 52:428–436. <http://dx.doi.org/10.1016/j.conbuildmat.2013.11.066>.
- [24] Häfliger IF, John V, Passer A, Lasvaux S, Hoxha E, Saade MRM, Habert G (2017) Buildings environmental impacts' sensitivity related to LCA modelling choices of construction materials. *J Clean Prod.* 156:805–816. <http://dx.doi.org/10.1016/j.jclepro.2017.04.052>.
- [25] Guggemos AA, Horvath A (2005) Comparison of environmental effects of steel- and concrete-framed buildings. *J Infrastruct Syst.* 11:93–101. [https://doi.org/10.1061/\(ASCE\)1076-0342\(2005\)11:2\(93\)](https://doi.org/10.1061/(ASCE)1076-0342(2005)11:2(93)).
- [26] Gerilla GP, Teknomo K, Hokao K (2007) An environmental assessment of wood and steel reinforced concrete housing construction. *Build Environ.* 42:2778–2784. <http://doi.org/10.1016/j.buildenv.2006.07.021>.
- [27] Kylili A, Ilic M, Fokaides PA (2017) Whole-building Life Cycle Assessment (LCA) of a passive house of the sub-tropical climatic zone. *Resour Conserv Recy.* 116:169–177. <http://dx.doi.org/10.1016/j.resconrec.2016.10.010>.
- [28] Vilčeková S, Čuláková M, Krídlová Burdová E, Katunská J (2015) Energy and environmental evaluation of non-transparent constructions of building envelope for wooden houses. *Energies.* 8(10):11047–11075. <https://doi.org/10.3390/en81011047>.
- [29] Asif M, Munner T, Kelley R (2007) Life cycle assessment: A case study of a dwelling home in Scotland. *Build Environ.* 42:1391–1394. <https://doi.org/10.1016/j.buildenv.2005.11.023>.
- [30] Humbert S, Schryver AD, Bengoa X, Margni M, Jolliet O (2012) IMPACT 2002+: User guide. [https://www.quantis-intl.com/pdf/IMPACT2002\\_UserGuide\\_for\\_vQ2.21.pdf](https://www.quantis-intl.com/pdf/IMPACT2002_UserGuide_for_vQ2.21.pdf).
- [31] Hermon P (2017) eTool. *Life Cycle Assessment*. Office presentation example, isetta square, eToolLCD.
- [32] Jašek M, Česelský J, Vlček P, Černíková M & Berankova EW (2014) Application of BIM process by the evaluation of building energy sustainability. *Advanced Materials Research.* 899:7-10. <https://doi.org/10.4028/www.scientific.net/amr.899.7>.
- [33] Vilčeková S et al. (2018) Interlinked Sustainability Aspects of Low-Rise Residential Family House Development in Slovakia. *Sustainability.* 10:11- 3966.

## Study on utilization of zeolite in concrete precast industry

**Róbert Figmig, Marek Kováč**

Technical University of Košice, Slovakia  
Civil Engineering Faculty, Institute of Environmental Engineering  
e-mail: rober.figmig@tuke.sk, marek.kovac@tuke.sk

### Abstract

Article contains experiment investigating influence of partial cement replacement by zeolite on consistency of fresh concrete, early compressive strength development and temperature development in early stages of curing. Four concrete mixture compositions were tested – containing zeolite in 0%, 5%, 10% and 15% of binder weight. Consistency was tested by flow table test in 5 minutes and 30 minutes after mixing of fresh concrete. Compressive strength and temperature gain were tested after 12, 16, 20 and 24 hours of curing. Results showed significant influence of zeolite on consistency of fresh concrete while compressive strength results were still in the acceptable range.

**Key words:** zeolite, precast concrete, early strength development, flow table test

### 1 Introduction

Trends in environmental protection in every production, transportation and other industry fields lead to minimize the carbon footprint achieving by CO<sub>2</sub> emissions reduction to the lowest values. In the concrete production, cement from portland clinker, as its main component, is considered to be the most demanding from the energy consumption point of view and subsequently from the environmental pollution contribution point of view [1,2,3]. With the aim to reduce the content of pure clinker in the cement, some mineral additives with pozzolanic (like fly ash, metakaolin, zeolite, silica fume) or latent hydraulic (like ground granulated blast furnace slag GGBS) properties are added directly to the cement as supplement or during concrete production as additive [4,5,6,7,8,9]. Considering the complexity of concrete designing issue as a result of technical, economic and environmental requirements, these materials should undergo also detailed assessment before their incorporation into the concrete. Such assessment should take into the consideration parameters like origin (natural or waste, transportation distance), price compared to portland cement, allowed supplement according to technical standard or influence on rheology as well as hardened concrete properties.

It is general known, that commonly used mineral additives used in concrete production either pozzolanic or latent hydraulic are effective in later age of cement hydration. They react with

free  $\text{Ca}(\text{OH})_2$  to form C-S-H crystals and that make the concrete matrix denser and more durable [10]. Another fact is, that specific surface, that are influenced by structure and texture of such additive's grains, is often much higher than in the case of Portland cement, what caused higher water consumption for achieving the same consistency of fresh concrete (with same plasticizer/cement ratio) [11]. Regarding the precast concrete, rapid strength development, but also surfaces without aesthetical defects are unconditionally required [12,13,14]. These properties are most often achieved by low water content in the batch together with optimized dosage of superplasticizer to obtain fresh concrete with required viscosity and consistency in time. Another option is using hardening accelerator; however, this solution makes price of  $1\text{m}^3$  of concrete much more expensive and is not economic effective. Noted requirements are obviously in contrast to above stated properties of mineral additives.

In the experiment described in this paper, we were focuses on utilization of zeolite as mineral additive to precast concrete and in the case of meeting demanding requirement, on the evaluation of optimal replacement of cement. The zeolite was chosen as representative of pozzolanic cement supplement material due to its availability and one of the richest sources around the world located in East Slovakia. Despite the fact that zeolite is natural raw material and primarily used in pharmacy, agriculture or wastewater treatment industry [15,16,17,18,19,20,21], there is a feasible potential for its use into the cement composites due to its pozzolanic property [22,23,24,25,26,27] considering currently limited sources, usable and price of common additives as fly ash, GGBS or silica fume in Slovakia region.

## 2 Materials and methods

In this chapter, materials properties and testing methods used in this experiment will be given and described.

### 2.1 Materials

In the experiment, natural fine and coarse aggregate were used. In terms of increasing of visual surface quality of concrete products in precast industry, 0/2 fraction of aggregate with rounded grains is often used in concrete mix design, so it is also the case of this experiment. Gap graded aggregate composition was chosen in the mix designs. The 4/8 fraction of aggregate was removed completely. Fine sand 0/2 originates from Nieznanowice (PL) locality, 0/4 and 8/16 fractions originate from Geča locality (SK). Gradation of aggregate mixture is given in the Fig. 1. Designed aggregate gradation was assessed by boundaries given in [28].

Cement CEM II/A-S 42.5 R from Považská cementáreň, a.s. Ladce (SK) plant and zeolite ZeoBau 50 - Klinoptilolit from Zeocem, a.s. Bystré (SK) were used in the experiment as cementitious materials.

Polycarboxylate-ether based (superplasticizer SF40 with 34 wt% of solid content from MAPEI company was used in the experiment as a high-water reduction admixture (HWRA).

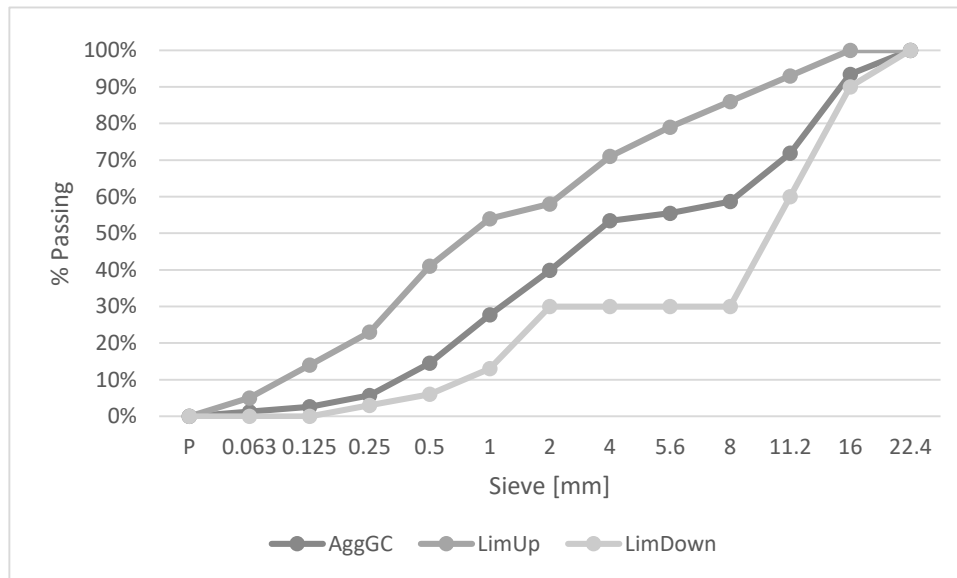


Figure 1: Gradation of aggregate mixture used in mixture designs

Table 1: Chemical composition of binder materials used in the experiment – oxidic form

Material	SiO <sub>2</sub>	Al <sub>2</sub> O <sub>3</sub>	CaO	K <sub>2</sub> O	Fe <sub>2</sub> O <sub>3</sub>	MgO	SO <sub>3</sub>	TiO <sub>2</sub>	LoI
CEM II/A-S 42.5 R	18.6	3.7	62.1	0.9	2.8	2.1	4.4	0.3	na
ZeoBau 50	58.7	9.0	2.8	2.6	1.4	0.7	0.1	0.2	5.1

## 2.2 Methods

Purpose of the experiment is to observe possible usage of zeolite as a supplementary cement material in the concrete precast industry where high early compressive strengths and workability of concrete are essential. Secondary, quality and change of hardened concrete surfaces with changing of zeolite content was observed. Four concrete mixture designs (Table 2) were prepared with ZeoBau 50 content 0%, 5%, 10% and 15% of binder dosage. The temperature of each fresh concrete batch was the same with value 23.8°C, while 50 % of environment humidity and 22.0°C of ambient temperature.

Consistency of fresh concrete was tested by flow table test in 5 min. and 30 min. after mixing. 30 minutes workability time is considered as sufficient in the concrete precast industry. ZeoBau 50 is expected to affect the workability in negative way so all four mix designs are kept with the same amount of mixing water and the same dosage of water reducing admixture to observe and quantify that behavior.

Table 2: Mix design used in the experiment

Mix design		ZB-00	ZB-05	ZB-10	ZB-15
CEM II/A-S 42.5 R	[kg]	405 (100%)	385 (95%)	365 (90%)	345 (85%)
ZeoBau 50	[kg]	0 (0%)	20 (5%)	40 (10%)	60 (15%)
0/2	[%] of total aggregate	5	5	5	5
0/4		50	50	50	50
8/16		45	45	45	45
HWRA	[%] of cementitious	0.75	0.75	0.75	0.75
w/b	[-]	0.40	0.40	0.40	0.40

Because of lower density of ZeoBau 50 compared to used cement, it is also expected the unit weight (in fresh and hardened state) of concrete to be lower with ZeoBau 50 compared to reference mixture without it.

For compressive strength testing, cube samples of 150 mm side were made. As it is important for precast concrete industry, early strength of concrete was tested in the experiment. Concrete made of four different mix designs containing ZeoBau 50 was tested on compressive strength after 12h, 16h, 20h and 24h of curing. Along with the compressive strength, the temperature of concrete samples was measured in respective times to get information on ongoing exothermic chemical reactions thus rate of compressive strength development could be predicted. Specimens were kept in the forms until strength testing. Standard plastic molds with insulating caps were used. The ambient temperature during curing varied from 19.5 up to 22.5 °C.

### 3 Results and discussion

#### 3.1 Consistency

Results of consistency of fresh concretes are given in Fig. 2 and in comparative Fig. 3. As expected, the consistency of fresh concrete was the stiffer the higher percentage of ZeoBau 50 was introduced into the concrete mixture. It could be explained by higher water demand of zeolite and its characteristic mesh which traps molecules of water. Mixture ZB-00 made of 100% cement binder achieved in flow table test 620 mm at the beginning and 625 mm after 30 minutes. Considering initial fresh concrete temperature, this result could be evaluated as greatly satisfactory. The reason for that obviously resides in proper composition and function of cement-water-plasticizer system. Mixture ZB-05 made of 5% ZeoBau 50 as cement replacement achieved 520 mm and 500 mm in flow table test in respective times. Even with small portion of zeolite incorporating, the consistency change is significant but still usable in terms of concrete precast conditions. Mixture ZB-10 made of 10% ZeoBau 50 as cement replacement achieved 405 mm and 360 mm in flow table test in respective times. It can be seen here not only the stiffer consistency at the beginning but also a bigger consistency loss in time. It can be attributed to lower content of “free” water in the fresh concrete but also to sorption abilities of zeolite minerals which could consume the water reducer particles more rapidly. Mixture ZB-15 made of 15% ZeoBau 50 as cement replacement achieved only 330 mm and



280 mm in flow table test in respective times. Mixture ZB-15 flow table test values dropped under 340 mm which is a recommended boundary for using method of flow table test for concrete consistency determination. Experiment proved and quantified the consistency loss due to incorporating zeolite based supplementary cementitious material. Differences are quite significant even at small portions used.

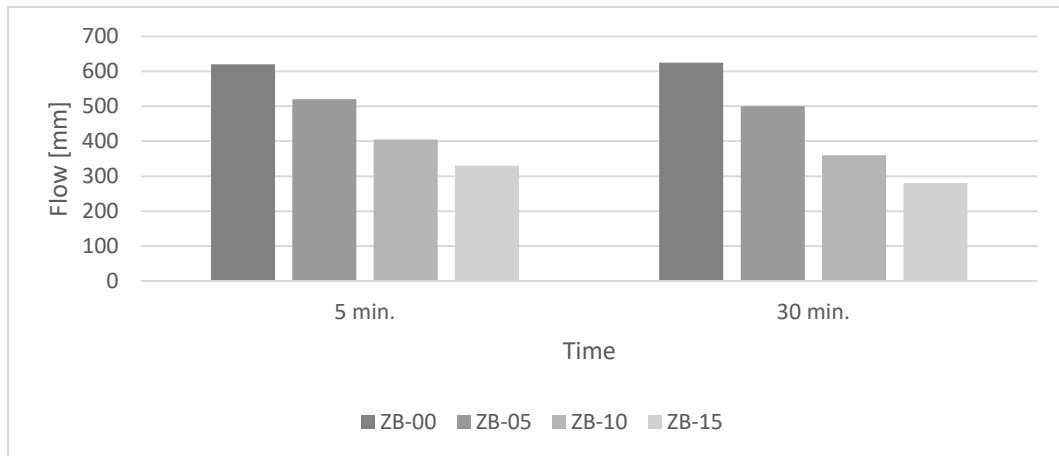


Figure 2: Consistency of concrete with zeolite content

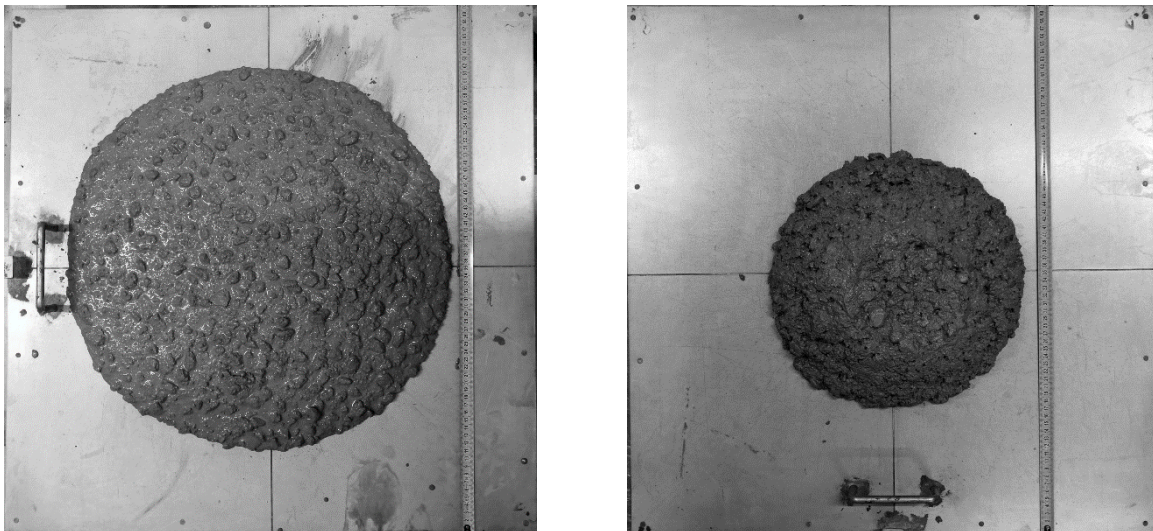


Figure 3: Consistency of concrete after 5 minutes – ZB-05 (left) and ZB-15 (right)

### 3.2 Compressive strength

Results of compressive strength of tested concrete mixtures are given in Figure 4. After 12 hours of curing the highest the portion of zeolite the higher the compressive strength. It ranges from 6.1 MPa (ZB-00) to 8.0 MPa (ZB-15). Fact that zeolite consumes

significant amount of water could actually result in lower w/b than was calculated and assumed in mixture design. This behavior could result in faster development of compressive strength of samples containing zeolite. After 16, 20 and 24 hours of curing, the trend is opposite and the higher the content of zeolite the lower the compressive strength. This behavior could be attributed to ongoing pozzolanic activity which is known to be significantly slower than standard hydration reactions of Portland cement. The difference between the highest and the lowest strength value after 16 hours of curing is 4.0 MPa, after 20 hours of curing it is 6.0 MPa and after 24 hours of curing it is 8.7 MPa.

Temperature development (Fig. 6) of concrete samples were recorded using IR thermometer at respective curing time right before demolding of samples. The temperature development shows the exact same behavior as the strength development. The recorded peak of temperature was recorded after 16 hours of curing in maximum of 36.5°C for ZB-00, 35.5°C for ZB-05, 34.8 for ZB-10 and 33.2 for ZB-15. Again, the lowered w/b ratio caused by presence of zeolite in the mixture could cause faster heat development after 12 hours of curing, but lower dosage of cement is responsible for lower heat development after 16, 20 and 24 hours of curing where even effect of lowered w/b ratio was overcome.

Incorporation of zeolite into concrete mixtures also caused slight decrease in unit weight (Fig. 5). The highest unit weight (2400 kg/m<sup>3</sup>) was achieved by ZB-00 mixture without using zeolite. Mixtures containing zeolite achieved unit weight in range from 2363 kg/m<sup>3</sup> to 2374 kg/m<sup>3</sup>.

In general, 12 MPa is considered (may vary in specific cases) to be sufficient strength to demold and manipulate with precast concrete segment or product. None of tested mixtures achieved that value after 12 hours of curing but all of them achieved it after 16 hours of curing even the ZB-15 with the highest portion of replaced cement.

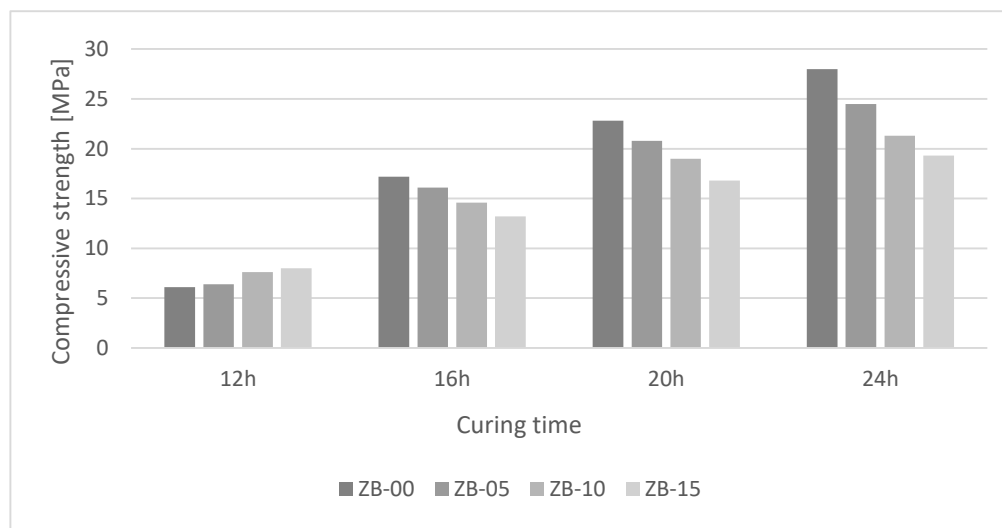


Figure 4: Compressive strength of concrete specimens at respectively curing times

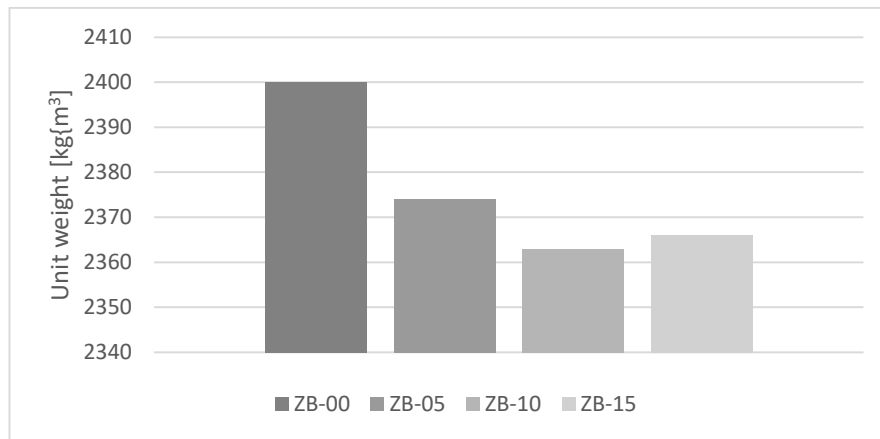


Figure 5: Unit weight of concrete mixtures made of various content of ZeoBau 50

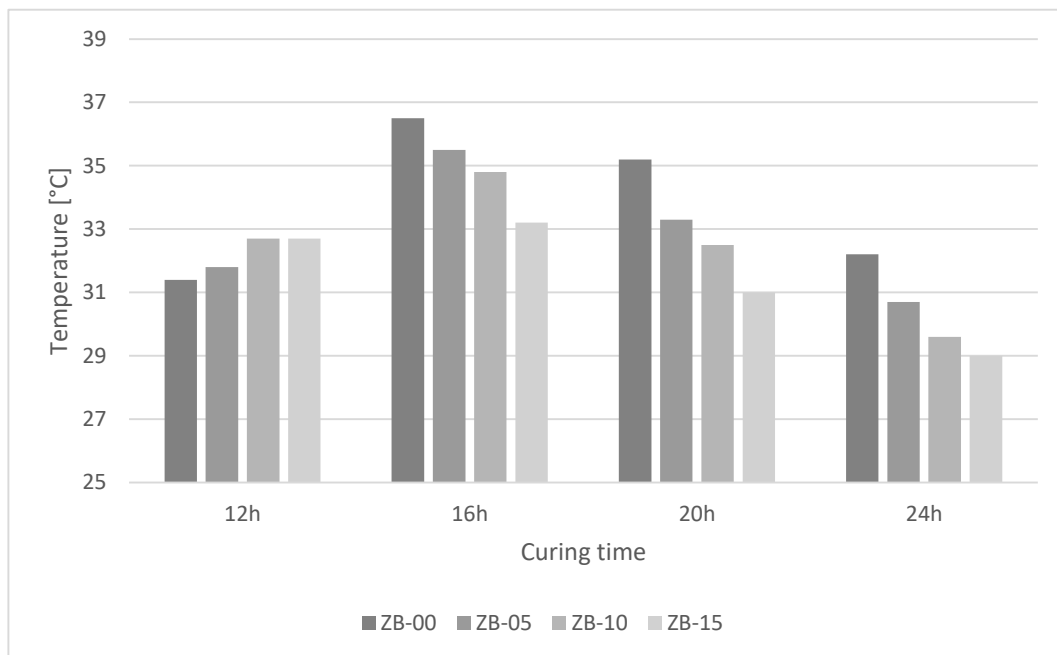


Figure 6: Temperature of concrete specimens at respectively curing times

In the Fig.7 is presented comparison between hardened concrete surface of samples ZB-00 and ZB-05. The samples with no zeolite evinced only flat cavern unlike the samples with zeolite, where bugholes are presented evidently, what could be associated with increasing viscosity with higher zeolite content. Entrapped air then more difficultly squeezed out at a mold wall surface.

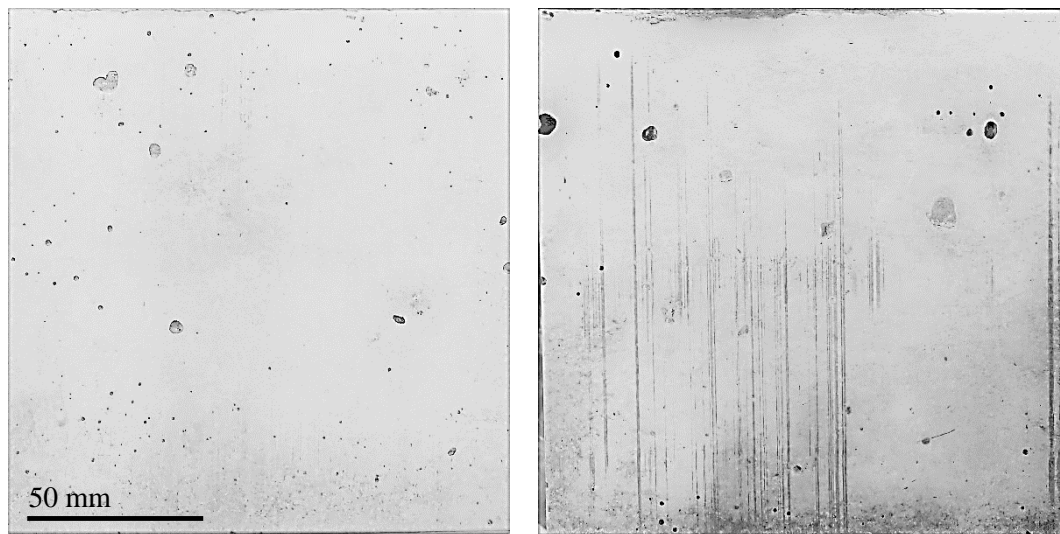


Figure 7: Comparison of hardened concrete surface – ZB-00 (left) and ZB-05 (right)

## 4 Conclusion

Experiment given in the article focused on the possible utilization of zeolite in concrete precast industry. Consistency of fresh concrete, temperature development and early compressive strength development of concrete containing 5%, 10% and 15% of zeolite as cement replacement were investigated. Based on experiment results, following observations could be formulated:

- zeolite significantly affects consistency of fresh concrete in negative way,
- the highest compressive strength and temperature gain after 12 hours of curing were achieved by ZB-15 mixture (the highest portion of zeolite – 15%),
- the highest compressive strength and temperature gain in all other curing times (16, 20 and 24 hours) were achieved by ZB-00 mixture (0% content of zeolite),
- all of tested concrete mixtures achieved 12MPa of compressive strength after 16 hours of curing, 12MPa is considered as sufficient strength to manipulate with precast concrete segment (may vary in specific cases).

Experiment suggests possibility of zeolite utilization in concrete precast industry, but few issues have to be overcome. Mainly consistency and workability of fresh concrete containing zeolite need to be adjusted by combination of added water and/or plasticizer. The effect of this adjustment on compressive strength will be the subject of future research.

## Acknowledgements

This paper has been prepared with a support of the Scientific Grant Agency of the Ministry of Education, Science, Research and Sport of the Slovak Republic and the Slovak Academy of Sciences (VEGA Grant No. 1/0648/17).

## References

- [1] Machado I. L et al. (2018). Improvement of the Environmental Energy Sustainability in the Production of Cement Portland with Addition of Thermally Activated Clays. In Martirena F., Favier A., Scrivener K. (eds) *Calcined Clays for Sustainable Concrete*. RILEM Bookseries, vol 16. Springer, Dordrecht.
- [2] Singh, G. B. & Subramaniam, K. V. (2019). Production and characterization of low-energy Portland composite cement from post-industrial waste. *Journal of Cleaner Production*. 239, 118024.
- [3] Oliveira, F. C. et al. (2019). Portland cement clinker production using concentrated solar energy—A proof-of-concept approach. *Solar Energy*. 183, 677-688.
- [4] Kupwade-Patil, K. et al. (2018). Impact of Embodied Energy on materials/buildings with partial replacement of ordinary Portland Cement (OPC) by natural Pozzolanic Volcanic Ash. *Journal of cleaner production*. 177, 547-554.
- [5] Carvalho, S. Z. et al. (2018). Reducing environmental impacts: The use of basic oxygen furnace slag in portland cement. *Journal of cleaner production*. 172, 385-390.
- [6] Ustabaş, İ. & Kaya, A. (2018). Comparing the pozzolanic activity properties of obsidian to those of fly ash and blast furnace slag. *Construction and Building Materials*. 164, 297-307.
- [7] Cavalcante, D. G. et al. (2018). Influence of the levels of replacement of portland cement by metakaolin and silica extracted from rice husk ash in the physical and mechanical characteristics of cement pastes. *Cement and Concrete Composites*. 94, 296-306.
- [8] Liu, Y. et al. (2018). Alkali-treated incineration bottom ash as supplementary cementitious materials. *Construction and Building Materials*. 179, 371-378.
- [9] Yakubu, Y. et al. (2018). Potential application of pre-treated municipal solid waste incineration fly ash as cement supplement. *Environmental Science and Pollution Research*. 25 (16), 16167-16176.
- [10] Tokyay, M. (2016). *Cement and concrete mineral admixtures*. Boca Raton: CRC Press.
- [11] Khan, S. U. et al. (2014). Effects of different mineral admixtures on the properties of fresh concrete. *The Scientific World Journal*. 2014, 1-11.
- [12] Elliott, K. S. (2016). *Precast concrete structures*. Boca Raton: CRC Press.
- [13] Bachmann, H. & Steinle, A. (2011). *Precast concrete structures*. Berlin: Ernst & Sohn.
- [14] Levitt, M. (1982). *Precast concrete: materials, manufacture, properties and usage*. Boca Racon: CRC Press.
- [15] Auerbach, S. M., Carrado, K. A. & Dutta, P. K. (2003). *Handbook of zeolite science and technology*. Boca Raton: CRC press.
- [16] Moshoeshoe, M., Nadiye-Tabbiruka, M.S. & Obuseng, V. (2017). A review of the chemistry, structure, properties and applications of zeolites. *American Journal of Materials Science*. 7 (5), 196-221.
- [17] Muir, B. & Bajda, T. (2016). Organically modified zeolites in petroleum compounds spill cleanup—Production, efficiency, utilization. *Fuel processing technology*, 149, 153-162.
- [18] Karakurt, C., Kurama, H. & Topcu, I. B. (2010). Utilization of natural zeolite in aerated concrete production. *Cement and Concrete Composites*. 32 (1), 1-8.

- [19] Koshy, N. & Singh, D. N. (2016). Fly ash zeolites for water treatment applications. *Journal of Environmental Chemical Engineering*. 4 (2), 1460-1472.
- [20] Rashed, M. N., & Palanisamy, P. N. (2018). Introductory Chapter: Adsorption and Ion Exchange Properties of Zeolites for Treatment of Polluted Water. *Zeolites and Their Applications*, 1.
- [21] Jakkula, V. S. & Wani, S. P. (2018). Zeolites: Potential soil amendments for improving nutrient and water use efficiency and agriculture productivity. *Scientific Reviews & Chemical Communications*. 8 (1), 1-15.
- [22] Lv, Y., Ye, G. & De Schutter, G. (2019). Investigation on the potential utilization of zeolite as an internal curing agent for autogenous shrinkage mitigation and the effect of modification. *Construction and Building Materials*. 198, 669-676.
- [23] Hajforoush, M., Madandoust, R. & Kazemi, M. (2019). Effects of simultaneous utilization of natural zeolite and magnetic water on engineering properties of self-compacting concrete. *Asian Journal of Civil Engineering*. 20 (2), 289-300.
- [24] Tran, Y. T., et al. (2018). Natural zeolite and its application in concrete composite production. *Composites Part B: Engineering*. 165, 354-364.
- [25] Zhang, J. et al. (2018) Effective solution for low shrinkage and low permeability of normal strength concrete using calcined zeolite particles. *Construction and Building Materials*. 160, 57-65.
- [26] Nagrockiene, D. & Girskas, G. (2016). Research into the properties of concrete modified with natural zeolite addition. *Construction and Building Materials*. 113, 964-969.
- [27] Ahmadi, B. & Shekarchi, M. (2010). Use of natural zeolite as a supplementary cementitious material. *Cement and Concrete Composites*. 32, 134-141.
- [28] SUTN. (2015). STN EN 206/NA. Concrete. Specification, performance, production and conformity – National Annex. Slovakia.

## Inlet device with double exponential profile distributor for indoor air dispensation

Florin Domnita<sup>1</sup>, Peter Kapalo<sup>2</sup>

<sup>1</sup> Technical University of Cluj-Napoca, Romania  
Building Services Faculty, Department of Building Services Engineering  
e-mail: florin.domnita@insta.utcluj.ro

<sup>2</sup> Technical University of Košice  
Faculty of Civil Engineering, Institute of Architectural Engineering  
e-mail: peter.kapalo@tuke.sk

### Abstract

This paper presents a device for introducing air inside a room with the novelty of double-exponential profile of the distributor. This allows entering the rooms of large quantities of blow-in air with low velocities, with the result of possible use in locations with a high required air exchange. In the Laboratory of Ventilation and Air Conditioning of the Technical University of Cluj-Napoca, it was designed and built an experimental stand in order to investigate the velocity field of a double-equal strength (double exponential profile) inlet device for spatial air-distribution. There are presented the measurements that were performed in the laboratory in order to establish the velocity field and the spatial distribution of air. The proposed solution can be used in many applications to provide high rates of air through the ventilation systems.

**Key words:** inlet device, air velocity, jet, distribution, movement, double exponential, spatial.

## 1 Introduction

The main purpose of the inlet devices is to achieve ventilation effect by obtaining a proper distribution of the introduced air jet. Therefore, is necessary to use inlet devices that allow the introduction of a maximum rate of air into a room without exceeding admissible indoor air velocities in the occupied zone [1]. Several studies [2, 3, 4, 5, 6 and 7] are also focused with relevant results on similar issues, such as: air velocities in the occupied zone, indoor airflow shape and impact on indoor air quality of indoor air distribution.

This paper presents a device for introducing air with the novelty of double-exponential profile of the distributor. This allows entering the rooms of large quantities of blow-in air with low velocities, with the result of possible use in locations with a high required air exchange.

Since the air distribution in mechanically ventilated rooms is determined for the most part (about 90%) of air jets, it means that the current lines generated by air jets must provide appropriate ventilation effect primarily in the occupied zone [1]. A number of clean rooms ventilation solutions (e.g. operating theaters) recommended the use of large inlet air devices to enable the introduction of high rates of airflow with low primary air velocities values [8]. In this way it increases also the phenomenon of indoor air induction into the main stream of the inlet air jet.

In real situations, the current lines of the air jets are more or less influenced by other fields of air pressure created in natural or mechanical way by infiltrated or accidentally appeared air currents, by the presence of natural obstacles which are due to the presence of machinery, furniture, building components or the occupants themselves. Compare with this, both in theoretical studies and researches on experimental stands, it creates the conditions for free airflow evolution. It is considered that the air jet current lines are arising from the pole of the jet. Also, it must be taken measures to stabilize the airflow in the ventilation duct in the upstream section from the inlet device.

## 2 Experimental stand and measurement apparatus

The solution presented in this paper refers to a double exponential discharge device distributor, in order to ensure a flow of the inlet air jet as close as possible to the theoretical model of free isothermal jet [1].

For this purpose, in the Laboratory of Ventilation and Air Conditioning of the Technical University of Cluj-Napoca, is designed and built an experimental stand (see Figure 1 and Figure 2) for the measurement of the air velocity field of a double-equal strength (double exponential profile) inlet device for spatial air-distribution.



Figure 1: Stand for studying the air velocity field of the double-equal strength inlet device (double-exponential profile) for spatial air-distribution.



The airflow measurement apparatus is a digital thermo-anemometer (TA 35 type AIRFLOW) with high accuracy class ( $\pm 0.01$  m/s) and measurement range for air velocity from 0.05 m/s to 25 m/s.

The stand is made of the following components (see Figure 2):

- A – simple-equal strength (simple exponential profile) inlet device, size: 900x1,800 mm, fitted with adjustable blades to produce a uniform air distribution throughout the discharge plane;
- B – rectangular connecting duct with internal airflow stabilization blades, size: 300x1,800 mm, to achieve a plane-parallel airflow;
- C - distributor of simple-equal strength of the inlet device, size: 300x1,800 mm, to assure stationary plane-parallel airflow in the upstream section;
- D –rectangular bend (90°) with internal airflow stabilization blades;
- E - reducer from rectangular to circular section;
- V - mono-aspirant centrifugal fan with airflow rate  $D = 4,375$  m<sup>3</sup>/h.

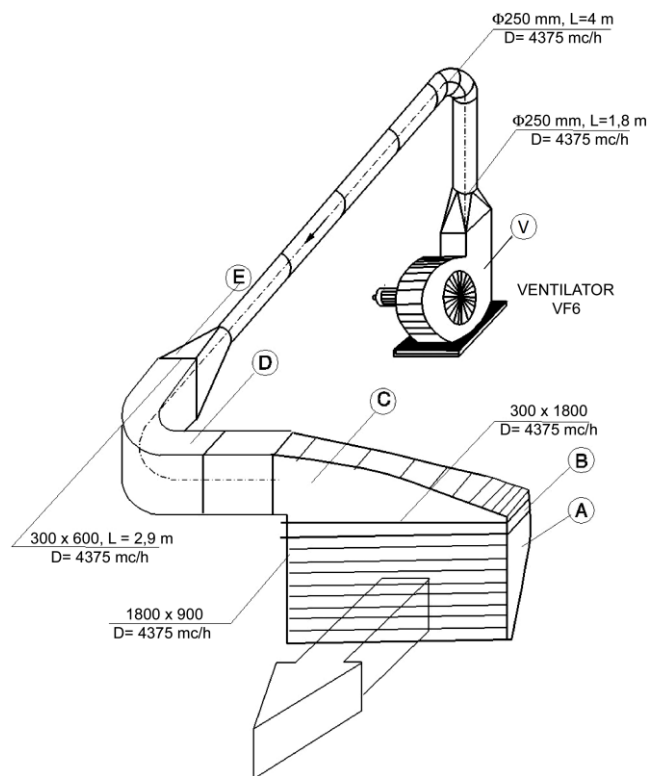


Figure 2: Stand for studying the air velocity field of the double-equal strength inlet device (double-exponential profile) – Isometric drawing.

The whole inlet device is made of three main components: A, B and C.

The double-equal strength (double exponential profile) inlet device for spatial air-distribution was designed by applying twice (for horizontal and for vertical distribution) the equations which allow to calculate the dimensions of the two distributors with variable section [9],

represented in Figure 2 by parts A and C.

All inlet devices intend to supply air in the occupied area at values for velocity, temperature, humidity, concentrations of different pollutants that correspond to the comfort conditions in the room. These considerations lead to the value of the initial velocity in the discharge plane, noted with  $v_0$ . To ensure the uniformity of ventilation, the air velocity is advisable to be as close to a constant value all over the discharge plane.

In this way, the initial velocity  $v_0$  in the discharge plan of the device will be constantly around 0,75 m/s, a value which corresponds to an easy physical activity. Due to the large size of the inlet device, it was necessary to provide airflow stabilization and control blades.

The air jet develops into a free space, which is not influenced by any disturbance surfaces or objects, so the measurements will not be at all affected.

### 3 Measurements and processing results

The investigation of the air velocity field of the double-equal strength inlet device (double-exponential profile) involves measuring the values of air velocity with an apparatus that does not influence the course of the current lines through both specialized transducer dimensions and the manner of making measurements [10].

There were performed a sufficient number of measurements, with enough equipment accuracy, to provide accurate values of air velocity into the air jet streams [10].

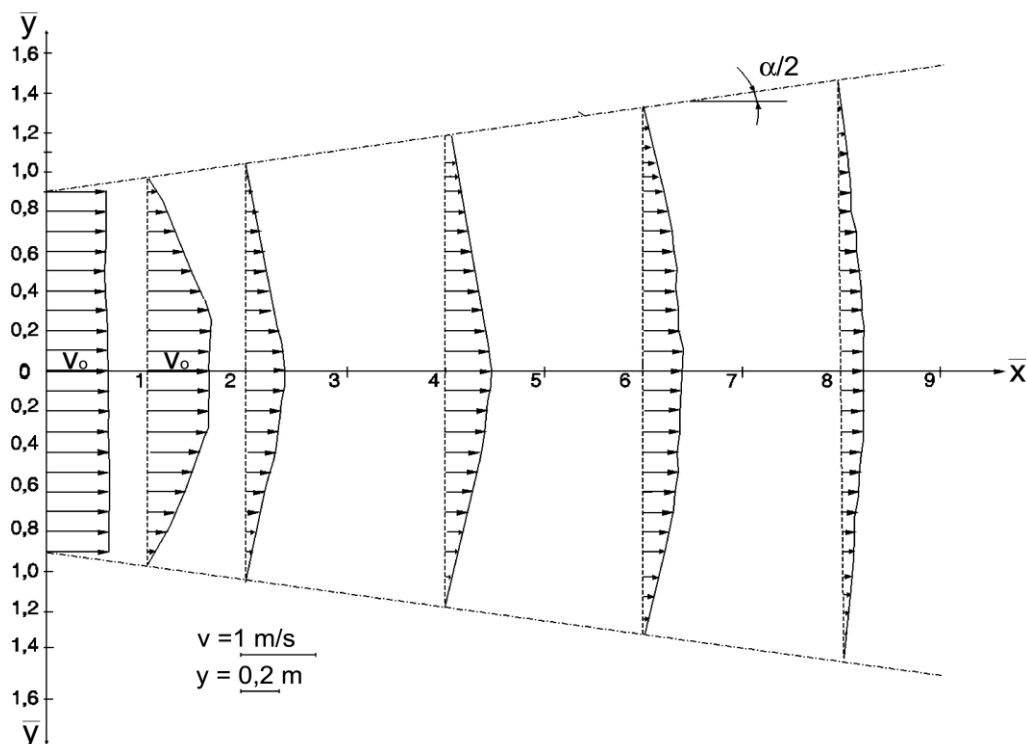


Figure 3: Air velocity hodographs measured in horizontal plane.

To measure the air velocities along the jet, in perpendicular planes to the jet axis, at different

distances (noted with  $x$ ) from the discharge plane, is using a classical method that uses, for keeping the same measurement points along the jet, a roller grid with square mesh [10]. Measuring transverse planes of the air velocity field have been predetermined by the rectangular roller grid with dimensions of 3000 x 1500 mm and with 100 x 100 mm square mesh. The measuring grid was placed successively at predetermined distances from the plane of discharge, beginning with the distance  $x = 0$  m (discharge plane) and finishing at the distance where axial air velocity is 0.25 m/s. Measured velocities were noted in all the nodes of the grid [10], resulting the air velocity hodographs in two perpendicular planes: one, horizontal and the other one, vertical (see Figure 3 and Figure 4) [8], [10].

In preparation for developing the mathematical model of the spatial air jet, it was chosen the dimensionless mode of expression of geometric and kinematic quantities. Thus, the measurements were made at dimensionless distances:  $\bar{x} = 0$ ,  $\bar{x} = 1$ ,  $\bar{x} = 2$ ,  $\bar{x} = 4$ ,  $\bar{x} = 6$  and  $\bar{x} = 8$ , resulting the hodographs of air velocities in two perpendicular planes (see Figure 3

and Figure 4). The expression of dimensionless distances is:  $\bar{x} = \frac{x}{d_0}$  ( $d_0 = \frac{2 \cdot a \cdot b}{a + b}$  – equivalent diameter of the rectangular inlet device with dimensions  $a$  and  $b$ ).

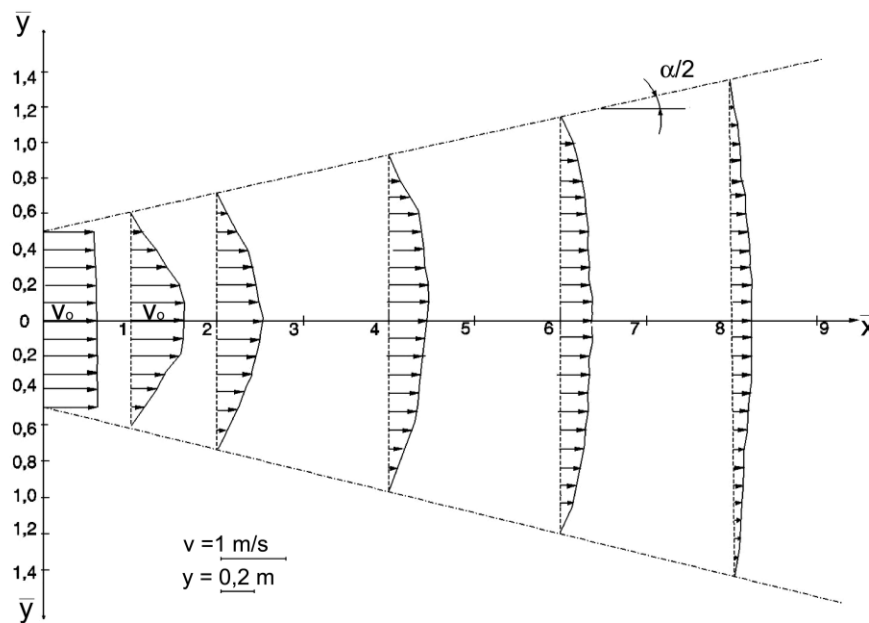


Figure 4: Air velocity hodographs measured in vertical plane.

After the air comes out the discharge device, enter into a stagnant air environment. As the air jet moving mass advances, due to induction, an amount of increasingly higher of stagnant air join to the moving air. In this way, the initial air jet kinetic energy is gradually consumed, decreasing the speed of air movement.

The hodographs of air velocities have changed from rectangle (in the discharge plane) to curvilinear trapezoid, respectively curvilinear triangle with the growth of distance [8]. The configuration of the isokinetic curves highlights the shape of the air jet. This represents a greater approach to the free, round, isotherm air jet [1]. This is also explained by the ratio 1:2 between the sides of the discharge device.

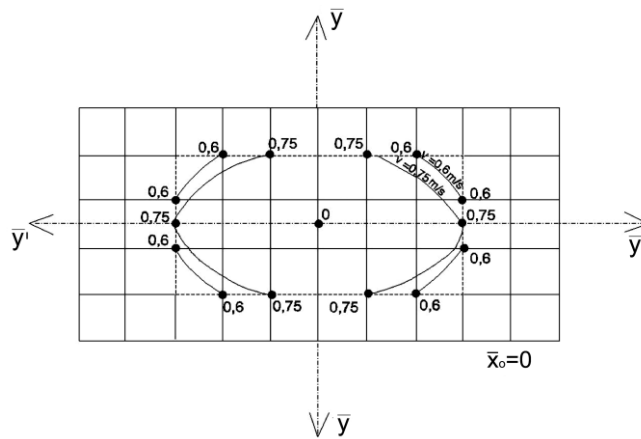


Figure 5: Isokinetic curves for  $\bar{X} = 0$ .

Based on the measured air velocities in the grid nodes, isokinetic curves were drawn (see Figure 5, Figure 6, Figure 7, Figure 8, Figure 9 and Figure 10).

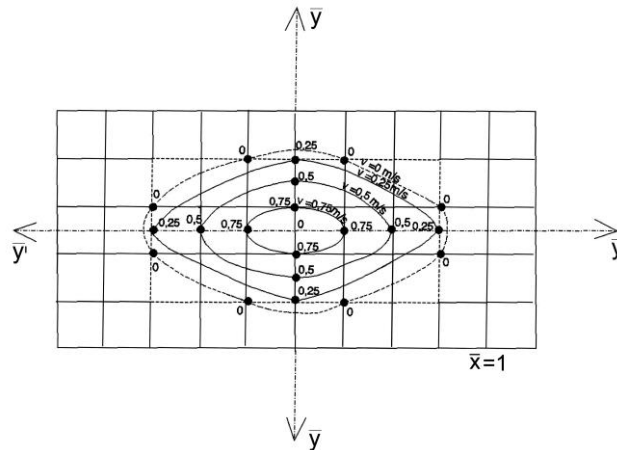


Figure 6: Isokinetic curves for  $\bar{X} = 1$ .

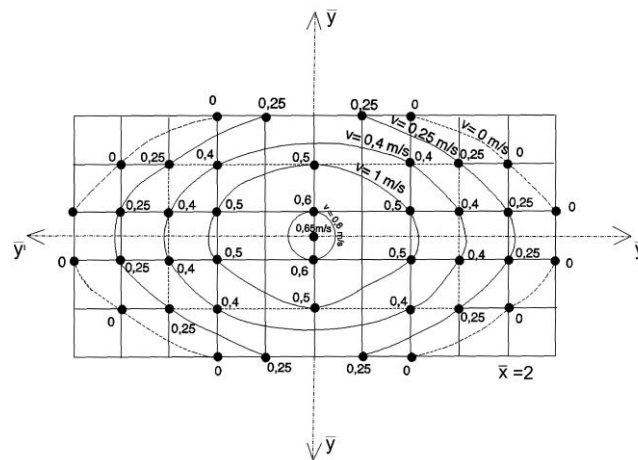


Figure 7: Isokinetic curves for  $\bar{X} = 2$ .

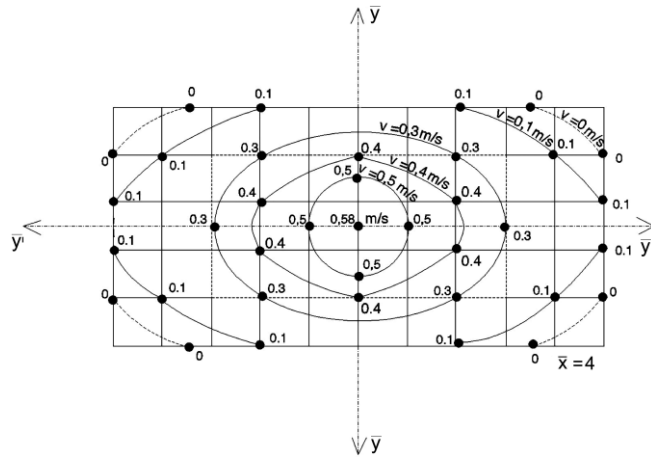


Figure 8. Isokinetic curves for  $\bar{X} = 4$ .

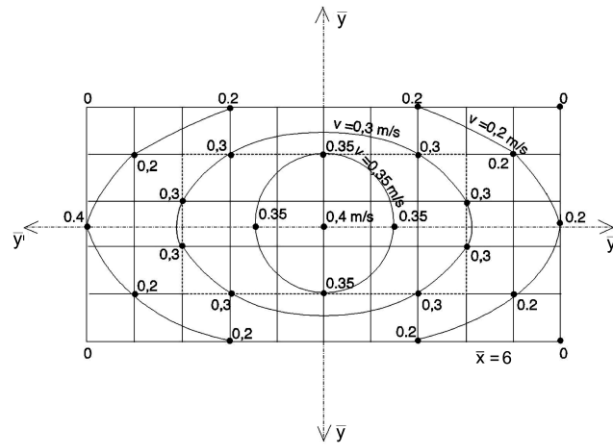


Figure 9: Isokinetic curves for  $\bar{X} = 6$ .

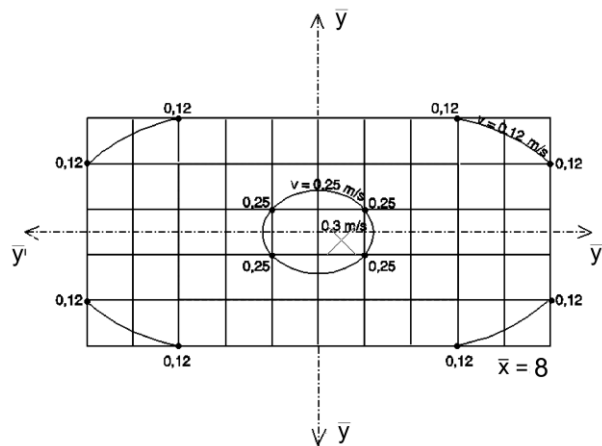


Figure 10: Isokinetic curves for  $\bar{X} = 8$ .

The air velocities hodographs form revealed the air jet envelope and angle of divergence, which depends on the initial airflow rate. The result is a divergence angle of the air jet  $\alpha$  of about  $32^\circ$  and a dimensionless air jet throw equal with 9.

These curves also highlighted the three areas of this type of air jet, with the following lengths:

- initial sector  $X_1 = 1.4 \times d_0$ ;
- transition sector  $X_2 = 1.2 \times d_0$ ;
- main sector  $X_3 = 6.4 \times d_0$ .

The air velocity hodographs confirmed the increase of airflow rate in the air jet with the distance to the discharge plane [11]. Accepting the theory of similarity, the measurements that were made will allow establishing a mathematical model of these air supply system through a large inlet area [11]. In this order, we will apply the classical method of calculation the jets characteristic elements that use the dividing the variable elements along the jet to the constant elements from the device discharge plan, resulting dimensionless variables [1]. The results will be presented as dimensionless variables in order to ensure that this can be generalized and easily applied to other values of airflow rates or other dimensions of inlet devices.

## 4 Conclusion

This type of air jet presents a compact enlargement with a divergence angle of  $32^\circ$ , a dimensionless air jet throws equal with 9 and an induction factor appropriate for a satisfactory ventilation effect [12].

The double-equal strength inlet device (double-exponential profile) provides relatively uniform air velocities in any perpendicular measurement planes of the air jet stream. Thus, the proposed solution can be used to provide ventilated air in many applications. Also, the large range obtained for air velocities lead to a great flexibility in operations for this kind of devices.

Following the evolutionary stage of inlet air devices, able to achieve enhanced ventilation effects, the designed and executed stand has some advantages:

- Provides a controlled airflow, close to laminar airflow conditions;
- Provides to the ventilated room an approximately constant air quality, appropriate for indoor environment demanded comfort;
- Ensures investment, execution and exploitation costs at reasonable values;
- Assures a good opportunity of harmonization with interior design elements;

Provides the possibility of directing the air jet, where it requires, towards certain areas that require greater conditioned air airflow.

## Acknowledgements

This article was elaborated in the framework of the project VEGA 1/0697/17.

## References

- [1] Popovici, T. *Instalații de ventilare și condiționare – în Romanian (Ventilation and air conditioning systems)*, Volume 1, Cluj-Napoca, U.T.PRESS, 2010.
- [2] Janbakhsh, S., Moshfegh, B. - *Experimental investigation of a ventilation system based on wall confluent jets*, Building and Environment, Volume 80, 2014, p. 18-31, ISSN 0360-1323,

- <https://doi.org/10.1016/j.buildenv.2014.05.011>.  
(<http://www.sciencedirect.com/science/article/pii/S0360132314001474>)
- [3] Ansari, A., Chen, K.K., Burrell, R.R. *et al.* Effects of confinement, geometry, inlet velocity profile, and Reynolds number on the asymmetry of opposed-jet flows. *Theor. Comput. Fluid Dyn.* 32, p. 349–369 (2018) doi:10.1007/s00162-018-0457-1
- [4] Cao, X., Li, J., Liu, J., Yang, W. *2D-PIV measurement of isothermal air jets from a multi-slot diffuser in aircraft cabin environment*, Building and Environment, Volume 99, 2016, p. 44-58, ISSN 0360-1323, <https://doi.org/10.1016/j.buildenv.2016.01.018>.  
(<http://www.sciencedirect.com/science/article/pii/S0360132316300191>)
- [5] Hurnik, M., Blaszcok, M., Popiolek, Z. - Air distribution measurement in a room with a sidewall jet: A 3D benchmark test for CFD validation, Building and Environment, Volume 93, Part 2, 2015, p. 319-330, ISSN 0360-1323, <https://doi.org/10.1016/j.buildenv.2015.07.004>.  
(<http://www.sciencedirect.com/science/article/pii/S0360132315300524>)
- [6] Voznyak, O., Korbut, V., Davydenko, B., Sukholova, I. *Air distribution efficiency in a room by a two-flow device* (2020). doi:10.1007/978-3-030-27011-7\_67 Retrieved from [www.scopus.com](http://www.scopus.com)
- [7] Voznyak, O., Sukholova, I., Myroniuk, K. *Research of device for air distribution with swirl and spread air jets at variable mode*. Eastern-European Journal of Enterprise Technologies, 6(7), p. 15-23. (2015). doi:10.15587/1729-4061.2015.56235
- [8] Domnița, F. V. *Contribuții privind decontaminarea și condiționarea aerului în spitale – în Romanian (Contributions regarding ventilation and air decontamination in hospitals)*, Pd. D. Thesis, Cluj-Napoca, 2003, p. 26-80
- [9] Niculescu, N., Stoenescu, P., Duță, G., Colda, I. *Instalații de ventilare și climatizare. în Romanian (Ventilation and air conditioning systems)*, EDP Bucharest, 1982
- [10] Sandberg, M. Measurement technics in room airflow. *ROOMVENT Proceedings*. Warsaw, 1994, p.345-349
- [11] Chen, Q. Prediction of room air motion by Reynolds-Stress models. *Buiding and Environment*, Vol. 31, 1996, p.278-285
- [12] Hanzawa, H., Melikow, A. K. *Airflow characteristics in the occupied zone of ventilated spaces*. ASHRAE Transactions 102/2007, p.411-417

## Deflection of concrete slabs with GFRP reinforcement caused by shrinkage

**Darina Kušnírová, Sergej Priganc**

Technical University of Košice, Slovakia  
Civil Engineering Faculty, Institute of Structural Engineering  
e-mail: darina.kusnirova@tuke.sk, sergej.priganc@tuke.sk

### Abstract

The use of new reinforcing materials and products in the construction industry requires their thorough assessment for a variety of design situations. One of the significant effects is the shrinkage of the concrete, which in the case of asymmetrically reinforced elements can cause the element to be deformed. The research was focused on slabs asymmetrically reinforced by composite reinforcement (GFRP) and by three reinforcement stages. To eliminate the effect of concrete non-homogeneity, a concrete slab of the same dimensions was made of the same concrete. The results show a significant effect of shrinkage on reinforced slabs.

**Key words:** concrete shrinkage, slabs, deflection, steel and GFRP reinforcement

## 1 Introduction

In construction practice, new materials are constantly emerging and used, or other, unconventional uses of already known materials are being sought. At present, the design of concrete structures is heading towards the replacement of conventional steel reinforcement bars for non-metallic materials - fiber reinforced polymers (FRP). These modern trends of reinforcing in concrete load-bearing structures bring many areas that are not yet sufficiently explored. These also include the effect of concrete shrinkage on the deformation of concrete elements reinforced with composite FRP reinforcement.

At the Faculty of Civil Engineering of the Technical University in Košice, the influence of temperature on the behavior of elements reinforced with GFRP reinforcement has already been investigated [1]. Now we focus on the research of the effect of shrinkage on deformation and stress in elements reinforced by GFRP reinforcement (glass FRP). These are long-term tests aimed at measuring deformations and deflections of elements.



## 2 Long-term tests

To research the deformations of concrete elements caused by shrinkage, specimens of thin slabs reinforced at one surface were used. In the cross-section of thin slabs, there is minimal occurrence of stresses from uneven distribution of moisture across cross-sectional height [2]. Hydrating heat is uniformly lost from the cross-section, the temperature of the element is uniform [3]. The shrinkage deformations should also be uniform in cross-section. Due to the low ratio of concrete volume to surface exposed to drying in slabs, drying shrinkage can take significant value [3]. Due to the reduction of reinforcement shrinkage on only one side of the slab, uneven shortening of the surfaces results, resulting in a deflection caused by concrete shrinkage. At the same time, tensile stresses occur in the concrete which, if exceed the tensile strength of the concrete, can cause cracks formation [4].

### 2.1 Design of test elements

In order to compare the impact of the reinforcement on the stress of the concrete elements, it is desirable to examine elements with different reinforcement ratio (at least two levels). For the experiment, 3 reinforcement ratios ( $\mu = A_r / A_c$ ) 0.3% (4 $\phi$ 8mm), 0.5% (7 $\phi$ 8mm) and 0.8% (7 $\phi$ 10mm) were selected (Table 1 - mechanical reinforcement ratio  $\mu_m = A_r E_r / A_c E_c$ ) and two types of reinforcement: steel B500 (with modulus of elasticity 200GPa) and GFRP (with modulus of elasticity 50GPa). Six reinforced slabs and 1 reference non-reinforced slab with dimensions of 1800x600mm and thickness 120mm were made. There was used concrete with properties determined at 28<sup>th</sup> day: compressive strength on cubes 46MPa, cylindrical compressive strength 43MPa, flexural tensile strength 6.8MPa, splitting tensile strength 4.7MPa and modulus of elasticity 30.7GPa. The reinforcement cover was 10mm, transverse reinforcement  $\phi$ 6mm at a distance of 200mm (Fig. 1).

Table 2: Amount and type of produced test specimens

Mark	Specimen (dimension)	Reinforcement	Amount of reinforcement	Reinforcement Area	Ratio $\mu = A_r / A_c$	Ratio $\mu_m = A_r E_r / A_c E_c$	Count
S1	slab (1800 x 600 x 120 mm)	Steel	4 $\phi$ 8mm	201mm <sup>2</sup>	0,3%	1,8%	1
S2			7 $\phi$ 8mm	352mm <sup>2</sup>	0,5%	3,2%	1
S3			7 $\phi$ 10mm	550mm <sup>2</sup>	0,8%	5,0%	1
G1		GFRP	4 $\phi$ 8mm	201mm <sup>2</sup>	0,3%	0,5%	1
G2			7 $\phi$ 8mm	352mm <sup>2</sup>	0,5%	0,8%	1
G3			7 $\phi$ 10mm	550mm <sup>2</sup>	0,8%	1,2%	1
UN		unreinforc	-	-	-	-	1

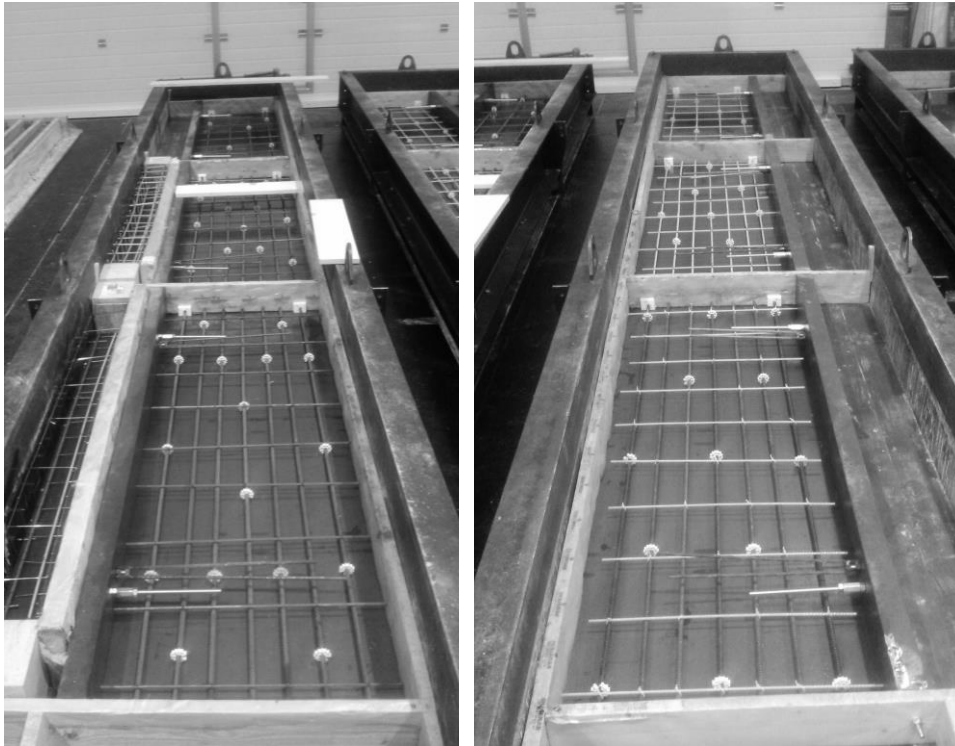


Figure 1: Forms with reinforcement ready to concreting

## 2.2 Methodology of long-term tests

On the seventh day after concreting, the specimens were removed and placed in a “chamber” to prevent sudden fluctuations in humidity and temperature during working in the laboratory. In order to eliminate as much as possible the influence of self-weight on the deformations and deflections of the slabs, the placement of the slabs in the vertical position (Fig. 2) [5] [6] was chosen. In this case, the self-weight of the slabs acts in the center plane of the slab and a very high cross-section resists acting moments. This results in very low stress (of the order of 0.02MPa) and deformations which can be neglected. With such a bearing, the deflection of the slab in the direction perpendicular to the center plane of the slab does not arise from the influence of the self-weight. In this way it was possible to observe the almost plain effect of concrete shrinkage on the deformation of the elements.

The layout of the points for measuring the deflection is shown in Fig. 3. The camber of the curved specimen, i. a. deflection in the center of the longitudinal sides that relates to their ends, was measured at the given points. All these deformations were measured using a steel frame equipped with dial gauges for direct deflection measurement [5]. Deflections were measured for 371 days (1 year after concreting) at intervals ranging from 3 days at the beginning to 2 months at the end of the reporting period.

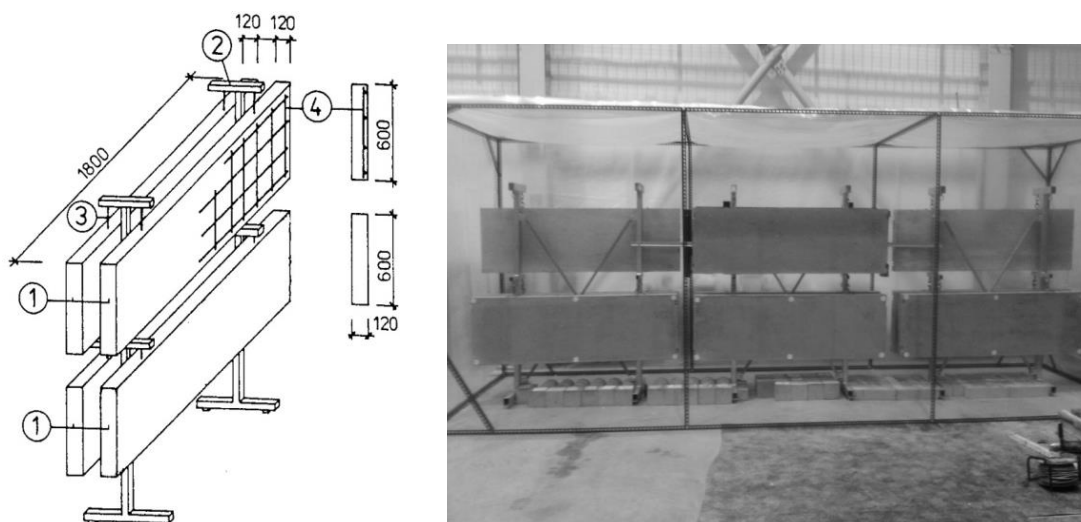


Figure 2: Storage of specimens: 1- concrete slabs, 2- stand, 3- hang up, 4- slab reinforcement

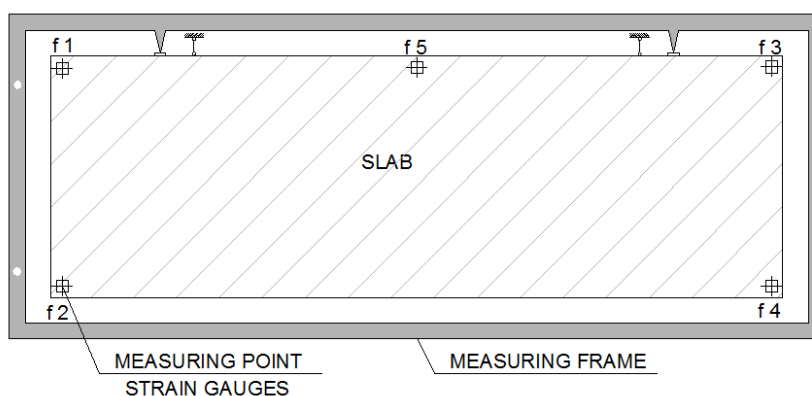


Figure 3: The disposition of the points for measuring the deflection

### 3 Results

From the measured values of the displacements of the measuring points, the deflections of the slabs were identified, which are shown in Figure 4. Their development over time corresponds to the changes in the relative humidity of the environment at the place where the slabs are stored (Fig. 5). The slabs reinforced with steel reinforcement (with the largest amount of reinforcement) have the largest, slabs reinforced with GFRP reinforcement Armastek, respectively unreinforced slab have the smallest deflection. That corresponds to the mechanical degree of reinforcement ( $A_r E_r / A_c E_c$ ) (Fig. 6).

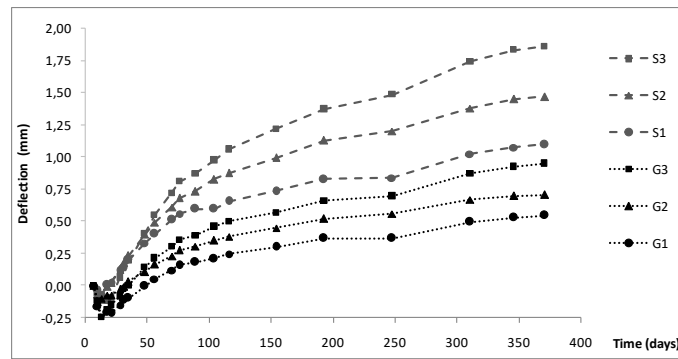


Figure 4: Deflection in the middle of slabs

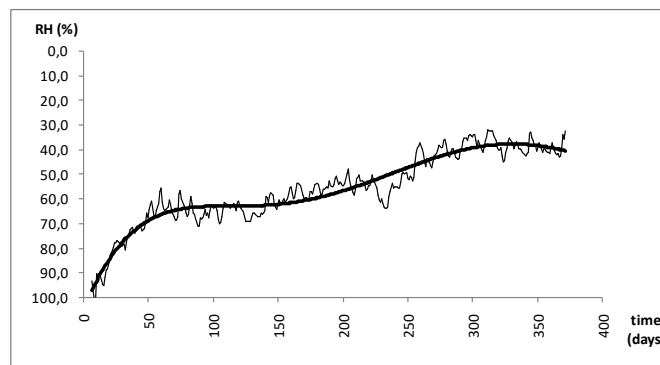


Figure 5: Relative humidity

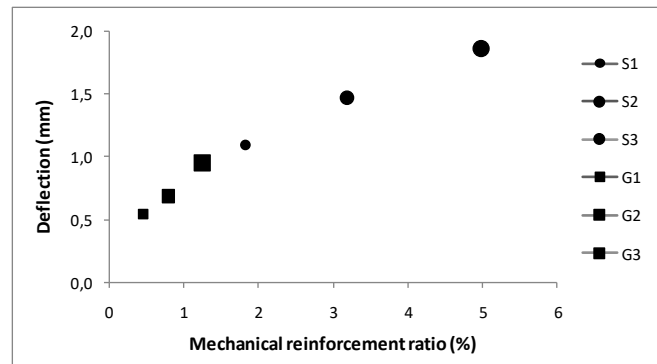


Figure 6: Slabs deflection according to mechanical reinforcement ratio

Fig. 7 shows the deflection ratio of slabs reinforced by different types of reinforcement (same degree of reinforcement). At higher degrees of reinforcement, the deflection ratio is relatively comparable. GFRP reinforcement is active in preventing shrinkage all the time. However, at low levels of reinforcement, it seems that GFRP reinforcement initially does not prevent free shrinkage of the concrete at all. The influence of reinforcement (i.e. deflection) appears later, increases suddenly and gradually stabilizes (at the end of the period under review). Stabilization occurs at a value of approximately 2, so that the resulting deflection of steel reinforced slabs is 2 times greater than that of slabs reinforced with the same reinforcement ratio of GFRP reinforcement.

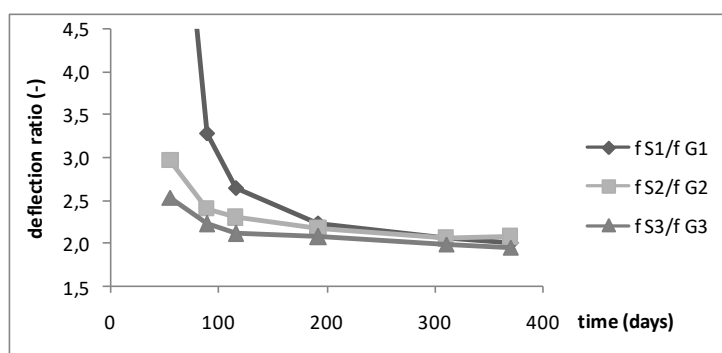


Figure 7: Deflection ratio of slabs reinforced by different types of reinforcement

## 4 Conclusion

The results of the experiment confirm the assumption of the influence of a different modulus of elasticity on the resulting deformations and deflections of slabs reinforced at one surface. It was found that the deflections of the steel-reinforced slabs are 2 times greater than the deflections of the GFRP-reinforced slabs at the same area of the reinforcement used at the end of the period under review. The deflection value from the shrinkage itself, e.g. for S3 (reinforced with  $7\phi 10\text{mm}$  steel reinforcement), it constitutes up to 26% of the limit deflection (for ceilings), which is not a negligible value when assessing structures to the ultimate serviceability. In conclusion, the shrinkage of concrete has a significant effect on the resulting deformation of the structure.

## Acknowledgements

The article was supported by the scientific grant agency of the MŠVVaŠ SR and SAV project VEGA 1/0661/16 The behavior of load bearing elements from ordinary and lightweight concrete influenced by temperature.

## References

- [1] Kušníř, Š. & Priganc, S. (2016). Strain of Elements Reinforced by GFRP at Elevated Temperatures. In *Advances and Trends in Engineering Sciences and Technologies 2*, (pp. 177-182). Leiden: CRC Press/Balkema.
- [2] ACI Committee 224. (2001). *Control of cracking in concrete structures*. American Concrete Institute
- [3] Aitcin, P.C., Neville & A.M., Acker, P. (1997). Integrated view of shrinkage deformation. *Concrete international*. Vol. 19/9, 35-41.
- [4] Samra, R.M. (1995). New analysis for creep behavior in concrete columns. *Journal of structural engineering*. Vol. 121 (Is. 3), 399-407.
- [5] Fecko, L. (1986). Monitoring of deformation of reinforced concrete slabs due to shrinkage (in Slovak). *Stavebnický časopis*. Vol.34 (Is.8), 615-630.
- [6] Hájek, J., Fecko, L. & Nürbergerová, T. (1983). Long-term deformation of reinforced concrete slabs at different load levels (in Slovak). *Stavebnický časopis*. Vol. 31 (Is.6), 517-531.